Localization and Tracking of Agents for Close Range Applications

by

Sanvidha Charaka Kumara Herath
(BSc in Engineering)

Submitted in fulfilment of the requirements for the degree of

Doctor of Philosophy

Deakin University

July, 2012

DEAKIN UNIVERSITY

ACCESS TO THESIS – A

I am the author of the thesis entitled Localization and Tracking of Agents for Close Range Applications

submitted for the degree of Doctor of Philosophy

This thesis may be made available for consultation, loan and limited copying in accordance with the Copyright Act 1968.

'I certify that I am the student named below and that the information provided in the form is correct'

Full Name Herath Mudiyanselage Sanvidha Charaka Kumara Herath

Signed Signature Redacted by Library

Date 22/09/2012

DEAKIN UNIVERSITY

CANDIDATE DECLARATION

I certify that the thesis entitled Localization and Tracking of Agents for Close Range Applications

submitted for the degree of Doctor of Philosophy

is the result of my own work and that where reference is made to the work of others, due acknowledgment is given.

I also certify that any material in the thesis which has been accepted for a degree or diploma by any university or institution is identified in the text.

'I certify that I am the student named below and that the information provided in the form is correct'

Full Name: Herath Mudiyanselage Sanvidha Charaka Kumara Herath

Signed Signature Redacted by Library

Date 22/09/2012

To my loving parents and wife

Table of Contents

Abstract

This thesis mainly investigates the state estimation problem in close-range involving multiple targets using the phase di erence and frequency shift of the returned Doppler modulated signals. The linear sensor array with minimal con guration that addresses the data association and missing information problem is provided for multiple mobile targets. A recently developed robust state estimation approach is employed to obtain an accurate estimate of the target dynamics progressively in a linear framework using non-linearly modeled Doppler radar measurements. Furthermore, the strength of our approach is experimentally veri ed.

Tracking mobile targets using a Doppler radar system mounted on a moving vehicle is also considered in this thesis. Dopplers modulated from mobile targets due to the relative motion with the sensor array is analyzed in order to estimate their states. Maximum likelihood based approach is provided in order to enhance the localization accuracy.

As the main theme is based on measurements with linear sensor arrays, optimal sensor arrangements in such arrays are studied for two most popular measurement technologies: Angle-of-Arrival(AoA) and range based localization systems. Cramer-Rao lower bound and the corresponding Fisher Information Matrix(FIM) are utilized for the analysis.

Unique localization with elimination of data association problem is explored for Time-Delay-of-Arrival(TDoA) and Time-of-Arrival measurement technologies. A comprehensive analysis on the unique solution area is provided for the TDoA based systems.

Publication List

P.N. Pathirana, S.C.K. Herath and A.V.Savkin, \Multi-target tracking via space transformations using a single frequency continuous wave radar" Transactions on Signal Processing, vol.60 , no.10 ,pp.5217-5229 , Oct. 2012.

S.C.K. Herath and P.N. Pathirana, \Optimal sensor placement in linear arrays: Part I - AoA based localization," in ISSNIP 2011 : Proceedings of the 7th International Conference on Intelligent Sensors, Sensor Networks and Information Processing, pp. 277-281, IEEE, Adelaide, S. Australia.

S.C.K. Herath and P.N. Pathirana, \Optimal sensor separation for AoA based localization via linear sensor array," in ISSNIP 2010 : Proceedings of the 6th International Conference on Intelligent Sensors, Sensor Networks and Information Processing, pp. 187-192, IEEE, United States.

S.C.K. Herath and P.N. Pathirana, \Maximum likelihood approach for tracking multiple mobile agents with a moving Doppler radar system," in ISSNIP 2010 : Proceedings of the 6th International Conference on Intelligent Sensors, Sensor Networks and Information Processing, pp. 193-198, IEEE, United States.

S.C.K. Herath, C.V.D Nagahawatte and P.N. Pathirana, \Tracking multiple mobile agents with single frequency continuous wave radar," in ISSNIP 2009 : Proceedings of the 5th International Conference on Intelligent Sensors, Sensor

Networks and Information Processing, pp. 163-167, IEEE, New York, N. Y.

P.N. Pathirana, S.C.K. Herath, and A.V. Savkin, \Mobile agent tracking with single frequency continuous wave radar: A linear robust ltering based approach," IFAC 2011 : Proceedings of the 18th IFAC World Congress, pp. 9990-9995, International Federation of Automatic Control, Milano, Italy.

S.C.K. Herath, P.N. Pathirana, B.T Champion and and S.W. Ekanayake, \Localization with Ghost Elimination of Emitters Via Time-Delay-of-Arrival Measurements," Accepted for publication in IEEE 6th International Conference on Information and Automation for Sustainability (ICIAFS 2012).

C.V.D Nagahawatte, S.C.K. Herath and P.N. Pathirana, \Localization of an Object in Motion in 3D Space Via Angle Only Measurements," Accepted for publication in IEEE 6th International Conference on Information and Automation for Sustainability (ICIAFS 2012).

Articles under review

S.C.K. Herath, P.N. Pathirana, G.L. Williams, \Optimal Sensor Arrangements in Angle of Arrival (AoA) and Range Based Localization with Linear Sensor Arrays," under review in International Journal of Distributed Sensor Networks.

Chapter 1

Introduction

Target localization and tracking has a rich history dating back to several centuries. In ancient history visual and auditory information were used to localize or track an object of interest such as prey or enemies. With the development of science and technology, numerous techniques have emerged for the same task, improving the accuracy and reliability of information. The concept of target localization and tracking involves estimating the location or any other dynamic parameters of a target of interest using typically noisy and possibly nonlinear measurements of the target measured from a number of sensor positions.

The science of localization and tracking gathered an immense momentum specially during World War II [1, 2]. Since then, numerous problems and techniques have evolved in this domain. The well known measurement techniques include the angle-of-arrival(AoA), target range, time-of-arrival(ToA), or the Dopller frequency modulated by the target. In some applications, two or more aforementioned techniques are combined together for higher accuracy.

The Radio Detection And Ranging (RADAR) technology which is very similar to ultrasonic sonar was developed during World War II to track the enemy ships and aeroplanes. Nowadays it has many applications in numerous elds such as aerospace, naval and weather forecast. Most of the implementations of Radar is for the far range applications such as locating an aircraft or a ship hundreds of

kilometers away. Close range localization and tracking such as indoor monitoring using Radar is an emerging field of interest. There are many other techniques such as AoA, target range and ToA for close range localization and tracking and the improvement of the accuracy and reliability is an interesting field of research. Currently, the research on these particular areas provides a constructive impact on safety and wellbeing of humans.

1.1 Background

Radar is widely used in different applications with different measurement technologies; Continuous Wave Radar, Pulsed Radar and Doppler Radar are some of them. Doppler Radar systems can be used to extract the dynamic information of a moving target. Most of these applications are for long range localization and tracking of non-cooperative targets.

It is well known that if there is a relative motion between the source and the observer, an apparent shift in frequency will occur, which is known as **Doppler shift**. A particular approach for close range localization and tracking is discussed in [3, 4] in which a low-complexity Doppler radar is used with a two-element receiver array. Multiple moving targets were first resolved based on their Doppler returns which are related to the radial velocities toward the receiving elements. The Angle-of-arrival (AoA) of each target was then estimated utilizing the phase difference of the scattered Doppler modulated signal at the two receiver elements. The complexity of this approach is less and it is based on the assumption that no two targets have the same Doppler returns toward any receiving element. When the targets of interest are not well resolved in Doppler dimension, the estimation error of AoA increases significantly. This problem is particularly severe for human tracking, since micro Doppler returns modulated from human limbs have a broad Doppler spread. Four- element radar array that combines Doppler signal processing with software

beam forming is used to resolve targets in both Doppler and the AoA space in [5]. This particular approach enables the detection of targets with overlapping Doppler signals. However, in an array of limited dimensions, the side lobes due to strong targets can prevent the localization of weaker targets when the targets are not resolvable in the Doppler domain. The CLEAN algorithm [6] is implemented in the beam-former to iteratively remove the side lobe features of the strong target to make it possible to detect weaker targets. An enhancement of CLEAN, which is known as RELAX algorithm [7], is also implemented to further improve the accuracy of the target-parameter estimation.

The performance of any particular localization algorithm is a strong function of the relative sensor-target geometry [8, 9]. A characterization of the geometry of the sensors and targets with various matrices related to Cramer-Rao inequality or the corresponding Fisher information matrix has been studied in [10]. Since the Cramer-Rao lower bound is a function of the relative sensor-target geometry, a number of approaches have been explored to identify underlying geometrical con gurations which minimize some measure of this variance lower bound [8, 10{17].

Most of the existing literature is concerned on the placement of AoA/ range sensors around the target for optimal localization [11, 13] but linear sensor arrays play a crucial role in some real world applications such as radar [9,18{25]. This study considers the localization problem involving a single target and multiple adjustable AoA/ range sensors located as a linear array(uniform and non-uniform). In this case, Cramer-Rao lower bound with the corresponding Fisher information determinant is used to investigate the optimality of the relative sensor-target geometry, exploring the intrinsic relation with the spacial diversity and the underling measurement model.

Time-Delay-of-Arrival(TDoA) is another important technique to localize and track a target of interest. These systems, generally localize an emitter by processing

signal arrival-time measurements at three or more sensors in R^2 and four or more sensors in R^3. In the absence of noise and interference, the ToA measurements at two sensors are utilized to produce a relative arrival time that, restricts the possible emitter location to a hyperbola in R^2 and a hyperboloid in R^3, with the two sensors as foci. Emitter location is estimated from the intersections of two or more independently generated hyperbolas in R^2 and the intersections of three or more independently generated hyperboloids in R^3 [26].

1.2 Overview of the study and contributions

The study in this dissertation is mainly three fold. In the first section, it concentrates on sensor placement for optimal localization using different localization techniques and then in the second section it discusses about the unique localization of targets using Time-Delay-of-Arrival(TDoA) and Time-of-Arrival (ToA) techniques. In the final section, the discussion is based on the close range localization and tracking, using Doppler radar.

An analysis on the linear sensor arrays for optimal localization

The study for the optimal sensor placement has two main aspects;

1. Developing techniques using Cramer-Rao lower bound with the corresponding Fisher information determinant to investigate the optimality of the relative sensor-target geometry, exploring the intrinsic relation with the geometrical diversity and the underling measurement model.

2. Optimality analysis for a single target and multiple adjustable AoA and range sensors located as a linear array(uniform and non-uniform).

An analysis on the unique localization of targets using ToA and TDoA systems

The study for the unique localization of targets using ToA and TDoA techniques has two main aspects;

1. Analysis on the unique solution region with measurements errors for a target using the minimum number of TDoA measurements.
2. Study of the data association problem for multiple targets in both ToA and TDoA techniques.

A novel approach in Doppler radar for close range localization

The study for the Doppler radar based localization has following aspects;

1. Development of techniques to localize close range multiple targets using Continuous Wave Single Frequency(CWSF) radar. These techniques are relatively simpler than other techniques such as pulsed-Doppler and frequency-modulated radar,
2. Application of a linear sensor array with minimal con guration that addresses the data association and missing information problem.
3. Employment of recently developed robust state estimation approach to obtain an accurate estimate of the target dynamics progressively in a linear framework using non-linearly modeled Doppler radar measurements.
4. Evaluate the assertions with simulations and a hardware system.

1.3 Thesis outline

This thesis is structured as follows. Chapter 2 provides a comprehensive analysis of the literature in the elds related to this study. Moreover, the theoretical background of the techniques used in the remaining chapters are introduced.

Chapter 3 provides the study of optimal sensor placement for linear arrays. The theoretical analysis is carried out on Angle-of-Arrival and range based localization systems with Gaussian error assumption and the computer simulations are presented to verify the results.

Chapter 4 presents the analysis on the unique localization with TDoA and ToA measurement techniques. First, the unique localization of an emitter with minimum number of TDoA measurements is analysed and then the elimination of the data association problem in both TDoA and ToA techniques is discussed with computer simulations.

Chapter 5 introduces the Doppler radar based close range localization and tracking technique for multiple mobile targets. A linear robust filtering based approach is used for stationary sensors and a maximum likelihood approach is employed for moving sensor platform. Computer simulation case studies are also presented to verify the theoretical assertions. This chapter presents a close range radar experimental setup which is developed for real world applications.

Chapter 6 presents conclusions on close range tracking and localization and directions for further work in the field. Here, an overview of the research is provided with the connectivity between different topics presented in the study.

Chapter 2

Localization and Tracking: An Introduction

2.1 Radar

A blind person makes his way along a busy street, maintaining a fixed distance from the wall of a building and also a safe distance form the vehicles whizzing by on his other side, just by tapping the sidewalk repeatedly with his cane as he walks. A bat deftly avoids the obstacles on its path and finds small insects that are its prey in a very dark cave just by emitting a train of shrill beeps. Just as unerringly, a fighter aircraft closes in on a possible enemy trespasser, hidden behind a cloud bank a hundreds of kilometers away.

Underlying each of these impressive feats is a very old and fundamental principle: detecting objects range from the echoes they reflect. The main difference in the techniques is that, the blind person and the bat utilize the echoes from the sound waves, whereas in the case of fighter aircraft, it detects the echoes from the radio waves.

RADAR is the acronym of the words Radio Detection And Ranging, which reflects the emphasis placed by early scientists and experimenters on a device to detect the presence of a target and estimate its location. It was initially developed as a long range detection device to warn of the approach of hostile aeroplanes and for directing antiaircraft weapons such as missiles [1,2]. Sophisticated modern

radar systems can usually extract more information from the signal of the target of interest with higher accuracies.

History of radar

The code word Radar was o cially introduced by the US Navy in late 1940s, as the name what had previously been called, among other jargons, radio echo equipment [1]. Another group in US Army Signal Corps, who also did pioneer work in radar development, used the term radio position nding until they adopted the name radar in 1942. The British in 1943 substituted their own term RDF with radar. The DF is the abbreviated form of direction nding and the origin of the R is obscure, which was purposely selected to enclose the fact that the range measuring equipment was under development [1]. In France, radar was called as DEM(detection electromagnetique), and Funkmessgerat was the name in Germany.

Even though the advancement of radar as a fully- edge technology occurred during the World War II, the fundamental principle of radar is almost as old as the eld of electromagnetism itself. The similarity between the radio and the light waves was demonstrated by Heinrich Hertz, in 1886 by experimentally testing the Maxwell's theories. In his experiment, he showed that the radio waves could be re ected by dielectric and metallic bodies. Although the Hertz's experiments were carried out with relatively short wavelengths radiation(0.66m), subsequent work in radio engineering was almost entirely at longer wavelengths. Until late thirties, the shorter wavelengths were not prominent in use [1].

In 1903, Hulsmeyer (a German engineer) experimented with the observation of the radio waves returned from ships. Even though his innovation generated little interest, Marconi identi ed the potentialities of short waves in radio detection and strongly urged their use in 1922 for such applications [1]. Although Marconi successfully demonstrated radio communication between continents, he was not successful in obtaining support for some of his other theories related to very short

waves. One was the suggestion that very short waves could propagate well beyond the optical line of sight-a phenomenon currently known as tropospheric scatter.

Continuous Wave (CW) was used in the first radar systems and they worked on the principle that the interference produced between the signal received from the transmitter and the Doppler-modulated signal reflected by a moving target. This particular type of radar was originally known as **CW wave-interference radar**. **Bistatic CW radar** is the current name for such systems [1]. The initial experimental detection of aircrafts utilized this principle rather than a monostatic(single-site) pulse radar as the CW hardware were readily available. The development of the successful pulse radar was halted until the suitable components, such as high-peak-power tubes, and a thorough understanding of the pulse receivers. The early evolutions of pulse radar systems were basically concerned with military applications. The first commercial application of this particular radar principle was probably the aircraft altimeter [1].

In the thirties, the development of radar was constrained to frequencies at Ultra High Frequency(UHF) or lower. A significant advancement in microwave region was apparent during the forties. However, in fifties, there was a backpedaling of the upward frequency trend, and a considerable amount of radar development was again implemented in the UHF region, specially for long-range detection.

Radar in nature

Even though the radar technology is novel to the humans, it can be found in nature. The bats and porpoise are both known to utilize ultrasonic echo-locating principle which is very similar to radio frequency echo location or ultrasonic sonar used in modern technology. The built-in ultrasonic \radar"of a bat enables it to fly through dark environments with impunity and locate and catch flying insects. The bat usually emits a series of ultrasonic pulses at a repetition frequency of the order of 10 to 20 cycles per second under normal circumstances with a width about

2ms [1]. The shape of the transmitted pulse is not exactly rectangular, but reaches a maximum and then falls. Even more signi cant is the fact that this transmission is not a simple pulse. It is similar to a frequency-modulated pulse or a frequency-modulated pulse compression. Bats are capable of detecting obstacles as close as 5cm [1]. Another exciting observation is that the thousands of bats y in dark caves very close to each other without apparent di culty from mutual interference.

Applications of radar

Radar technology has been utilized on ground, in air, and at sea. Ground-based radar has been used mainly in detection and localization of aircrafts or space targets. Shipboard radar is used to detect other ships or aircrafts, or it can be used as a navigation aid to locate shore lines or obstacles. Airborne radar systems are used to detect other aircrafts, ships or vehicles, or it can be utilized for storm avoidance and navigation. The design of a radar system depends on the environment in which it operates and the nature of the vehicle that carries it [1].

Civilian applications: Currently, the main use of radar apart from the military applications is for navigation. The most common civilian application of radar is in air-tra c-control. These radar systems monitors the air tra c in the vicinity of airports and en route between air terminals. In hostile weather, radar is used with ground-control-of-approach systems for safe landing. Nowadays, commercial aircrafts are equipped with radar altimeters to determine their height above the ground and weather-avoidance radar to navigate around dangerous weather conditions.

Radar is used for safe navigation in ships, especially in poor visibility or in hostile weather. Another application of radar can be found in surveying over large distances. One of the most important application of radar in civilian domain is the detection and tracking of weather changes, especially tornadoes and hurricanes.

Military applications: Most of the civilian applications of radar mentioned above

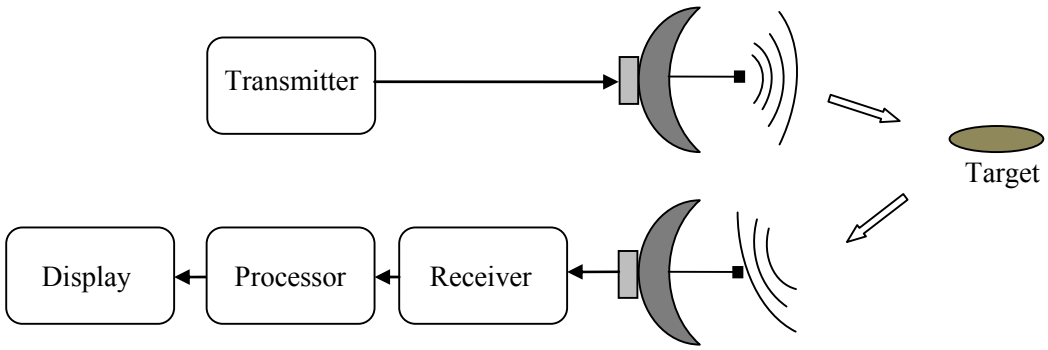

Figure 2.1: Radar system

are also applied in the military domain, specially in radar navigation. Moreover, military employ radars for surveillance and for the control of weapons. Surveillance radar is used to localize and track hostile targets in order to take proper military actions. The examples for such radar systems are DEW(Distance Early Warning) radars, BMEWS(Ballistic Missile Early Warning System) and shipboard surveillance radars and AEW(Airborne Early Warning) radars. In the domain of control of weapons, the examples are homing radars on guided missiles, airborne-interception radar which is used to help a ghter aircraft to nd its target, and bombing radars [1].

Scienti c applications: The radar is used by research scientists to enhance the knowledge of meteorology, aurora, meteors and other objects in the universe. Space vehicles and satellites can be guided by radar and it can also be utilized in exploration of interplanetary space. The radar techniques can also be utilized in microwave spectroscopy, radio astronomy, and radar astronomy.

Radar technology in brief

As depicted in Figure 2.1, common radar systems in their most rudimentary form, consist of six elements: a radio signal transmitter, signal receiver, two antennas for transmitting and receiving(in some cases, the same antenna is used in common for transmitting and receiving), signal processing unit and the display. Depending on

the application, the radio signal can be sent as a Continuous Wave(CW), Frequency Modulated Continuous Wave(FMCW) and in pulses. In the world of radar the term target is mainly used to refer to anything the system wishes to detect during its scan: a vehicle, a ship, an aircraft, a human, rain, or even free electrons. The most important factors which in uence the range at which the target can be detected are

The power of the transmitted radio waves

Fraction of time the power is transmitted

Dimensions of the antennas

Radio wave re ection characteristics of the target

Time span the target is in the antenna beam during the scan

Wave length of the radio waves

Strength of background noise or clutter

A radar identi es the presence of objects and determines their location in space by emitting the electromagnetic energy and processing the re ected echo. In pulse radar, the receiver is turned on after a relatively short burst of electromagnetic energy is transmitted on the area of interest. The distance of the target form the radar system is measured by utilizing the time that elapses between the transmission of the pulse and the receipt of the echo. On the basis of time, the transmitted signal and the echo can be di erentiated.

If the weak echo can be extracted among the strong transmitted signal, the radar can be operated continuously. Usually, the received echo signal power is signi cantly smaller than the transmitted power. The isolation of weak echo from strong transmitted signal is practically not su cient even if two antennas are used for transmission and reception.

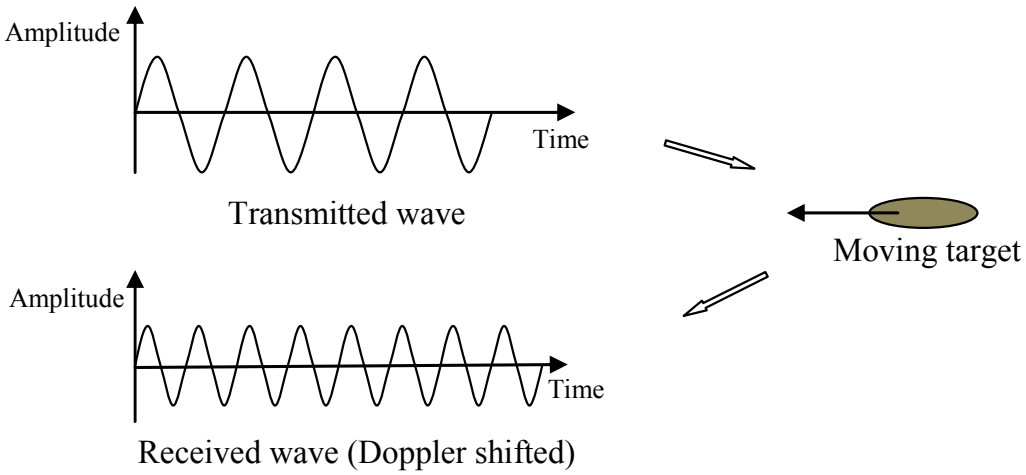

Figure 2.2: Doppler e ect

Doppler Radar

One e ective way of separating the weak received signal from the transmitted signal is to measure the change in the echo-signal frequency due to the phenomenon known as **Doppler e ect** [1, 27]. For this Doppler e ect to take place, there should be a relative motion between the target and the receiver. When the Doppler shift is used for the detection of targets, a part of the transmitted signal that falls on the receiver is not, in principle, problematic. In most of the cases it is a requirement for detecting the Doppler shift in the received signal.

In the areas of acoustics and optics, it is well known that if there is a relative motion between the source and the observer, an apparent shift in frequency will occur. This is the basis of Continuous Wave radar and known as the **Doppler e ect**(Figure 2.2).

Consider a radar system and a target R distance apart. Then the total number of wavelengths ( ) that can be accommodated between the two-way path between the radar and the target is $2R=$ (assume that the distance and the wavelength are measured in the same units). Then the total angular excursions taken by the signal during its journey is $4 R=$. If there is a relative motion between the

receiver and the target, R and the phase are constantly changing. The change in with respect to time is the Doppler angular frequency $!_d$ given by

$$!_d = 2 \quad f_d = \frac{d}{dt} = \frac{4}{} \frac{dR}{dt} = \frac{4 \quad v_r}{};$$

where f_d is the Doppler frequency shift and v_r is the relative frequency of the target with respect to the receiver. Then the Doppler frequency shift is

$$f_d = \frac{2v_r}{} = \frac{2v_r f_o}{c}; \tag{2.1.1}$$

where f_o is the transmitted frequency and c is the velocity of propagation which is approximately $3 \quad 10^8 ms^{-1}$ for electromagnetic waves.

There are numerous applications of CW radar and the the study of CW radar serves as a means for better understanding the characteristics and use of the Doppler radar information encapsulated in the received signal, whether in a CW or a pulse radar applications. It not only allows the separation of the received signal from the transmitted signal, but also provides a measurement of radial velocity of the target toward the receiver which can be utilized to distinguish between the moving targets from the stationary objects or clutter [1].

Future directions in close-range radar

Through wall tracking of human activities is a growing eld of interest due to the increasing demand in many defense and commercial applications ranging from urban warfare to rescue operations [28{34]. For an example, when a person is trapped in a collapsed building, nding the location promptly is vital for search and rescue operations. In defense applications, tracking of human movements inside an enclosed are or a building increases the chances of successful law enforcements or military operations minimizing casualties.

Robust estimation of the target state in real time is essential in such real world

applications. Ultra wide band (UWB) radar popular in this domain with resolution of the order of centimetres have been reported in [28{34]. Studies in [29{31] use impulse wave form for tracking while frequency modulated continuous wave (FMCW) is employed in [28]. In [33] stepped frequency is used and the noise wave form is analysed in [34] to realize a high range resolution. The major drawback of these systems is the degradation of the accuracy in measurements due to the dispersion and signal loss as the waves are penetrating through some wall materials such as concrete.

Micro-Doppler e ects can be used to recognize the human activities [35]. Non-rigid-body motions of human limbs modulate Micro-Dopplers and they contain valuable information related to human gait recognition. Since it was presented in [35], a number of studies have explored micro-Dopplers for human motion analysis. A simple classi er is designed by Otero [36]to recognize walking humans using spectral analysis. Various time frequency analysis are used to extract micro-Doppler features of radar target returns in [37]and [38]. In another study, micro-Doppler modulations are explored to distinguish among humans, animals and vehicles in [39{41]. Micro-Doppler signatures are used to classify di erent human activities in [42] and this is done by training a support vector machine (SVM) using the measurement features of the activities.

Localization and tracking

The target tracking problem is the next step of the target localization problem. Several techniques can be employed to nd the target, and the particular algorithmic related approach is based on nding solution to the nonlinear estimation problem. The widely used approaches in these scenarios are the batch of recursive solutions which are usually considered with recursive ltering algorithms. In this particular domain, the Extended Kalman Filter (EKF) is the most common solution to the recursive tracking problem. The EKF has no optimality properties and

the linearization a ects the performance [43]. In many practical situations, nonlinearities associate with the measurements and the system dynamics which makes the EKF less favorable for some target tracking problems [44,45]. Compared to the EKF, unscented Kalman lter and particle lters have shown better performance in target tracking.

In typical radar based tracking, the target's range and the angle-of-arrival are measured. Commonly, linear target dynamic models are considered in the Cartesian coordinate system and hence the measurements are nonlinear functions of the target's state [44,45]. In these type of tracking problems, nonlinear lters are usually required [44]. On the other hand, measurement conversion methods have been studied for target tracking based on range and angle-of-arrival measurements [44,46{48]. The fundamental theory in this method is to rstly transform the nonlinear measurements in to a linear combination of Cartesian coordinates and secondly estimate the bias and the covariance of the converted measurement noise and nally use a standard linear Kalman lter [49]. In radar based tracking problems, these particular measurement conversion methods perform better than the EKF [44,46{48]. The absence of any mathematically rigorous proof on the boundness of the ltering error is a major drawback of the EKF and the measurement conversion method. Moreover, in many practical problems, the EKF can diverge quickly from the actual state [50,51]. Even though the particle lters and unscented Kalman lters perform well in tracking applications [50,52], results related to the convergence are not easily obtainable [50,51,53,54].

Localization and tracking of multiple mobile targets is useful in many defense and commercial applications such as security surveillance, disaster search, rescue missions and urban warfare [3,55{58]. Radar systems in the past were mainly used for long range localization and tracking and those systems were very expensive and bulky in the design. Due to the rapid development in electronic engineering in recent

decades the cost and the physical dimensions of Radio Frequency(RF) components have reduced signi cantly. Hence, many useful radar systems can now be realized with a reasonable cost; specially for indoor and commercial applications which were less prominent in the past. Through-the-Wall Radar Imaging(TWRI) which has very useful applications in numerous situations is a recent research interest [59{61]. This shows the interest in applying the radar technology in close-range applications such as counter terrorism engagements and rescue operations.

Among the other radar systems Continuous Wave (CW) radar systems have attracted extensive attention due to its design and implementation simplicity [3, 55]. Single frequency CW radar can measure Doppler frequency shifts due to the relative motion of the targets to a higher accuracy. However, in target range measurements, more sophisticated systems derived from CW radar are currently being used. These systems are costly, and require complex hardware systems to implement. For example, Frequency Modulated CW (FMCW) radar and pulsed Doppler radar both evolved from the CW radar technique and they are capable of detecting range but poor in clutter mitigation. Comparatively, CW radar is excellent in clutter suppression; therefore, it can be used to localize moving targets as the Doppler shift in frequency provides a natural exclusion of clutter in the ltering [1, 27].

Furthermore, by measuring the phase di erence of CW waves arriving at closely separated(less than the half-wave length) two antenna elements, the angle-of-arrival of a target can be measured [3, 62]. In [63{65] only the location information of the targets were found using the phase di erence of the Doppler-shifted signal, while Doppler-shift is only utilized to distinguish between the targets rather than deducing their velocity components. [66, 67]consider more complex pulsed radar system where correction of the received Doppler modulated signal under Gaussian assumptions is studied in [68]. Multi-target tracking through range and angle measurements are studied in [67, 68] providing comprehensive descriptions based on static optimization

techniques.

The time derivatives of displacement is typically used in systems which require velocity information of moving targets. This results in a time lag in velocity estimation. The accumulation of errors can be signi cant as the location estimation errors are directly translated into velocity estimations specially for more dynamic targets. Therefore, the location and the velocity of the target can be estimated simultaneously when using CW radar with a dynamic system model for state estimation. Another advantage of this approach is that it is also robust to system uncertainties and measurement errors. Contrastingly, the Doppler frequency shift due to the target motion is utilized in [69] to estimate the target velocity independently allowing a better estimate due to additional measurements and increased dimension of the measurement space. Indeed, this measurement modeling introduces additional non-linearities. For the position measurement only case discussed in [69], converted measurement approach [70] has been used to obtain a better linear formulation. Here, the non-linear measurement equation is linearized with a rst order approximation equivalent to EKF in the estimation process. This type of linearizations, specially in systems with large uncertainties, are known for accumulation of errors and in certain instances divergence can occur in the state estimation.

In our study, Doppler radar based target tracking is considered and a linear state estimator is derived with provable performance limits . Here, nonlinear Doppler frequency modulation and corresponding angle of arrivals from the mobile targets are used as measurements. A completely linear algorithm is given using a novel measurement conversion technique that does not depend on Taylor-series type approximations. Mathematically rigorous proof of the boundedness of the ltering error is a signi cant contribution of this method. Such results are not obtainable from EKF.

The linear sensor array with minimal con guration(two sensors) that addresses

the data association and missing information problem is considered for tracking multiple mobile targets as an alternative to increasing the number of sensors in the array.

Di erent measurement techniques

Radar is mainly utilized for localization and tracking of targets. The fundamental techniques used for this purpose are common for other systems which are designed to localize and track the targets of interest. These fundamental techniques are range measurements, angle-of-arrival (bearing) measurements and time-of-arrival measurements.

When it comes to localization and tracking, there are preliminary problems to be addressed. They can be mainly categorized in to several sections: errors due to measurements, sensor location uncertainties, data association , missing information and false alarms. Where ever possible, these problems are considered separately to disentangle and simplify the localization or tracking result. As an example, consider a multiple target localization problem where the measurements are noisy. This can be analyzed as a single target localization problem if the measurements can be allocated to a particular target. If the origin of the measurements are unknown, obviously, there are two major problems to be analyzed in this case: measurement errors and the data association problem [71{77]. Clutter and electronic counter-measures give rise to the missing measurements and false alarms.

The nature of the localization and/ or tracking problems is highly dependent on the measurement technology that has been employed. Angle-of-arrival, range, time-of-arrival and Doppler measurements provide di erent information for the localization and/ or tracking. In each case, the type of the available information inherent to the measurement technology de nes the problem statement and the problem solution. As an example, target tracking problem involving both angle-of-arrival and range based technologies are easier to handle than the angle-of-arrival-only based

technologies.

2.2 Optimal localization in angle-of-arrival and range based linear arrays

In this dissertation, the problem of localization using the angle-of-arrival only and range only measurements are considered for the optimal localization in linear arrays. Angle-of-arrival sensors measure the bearing of a target with respect to a local or global coordinate system [78{84] and allow passive localization by analyzing the characteristics of the received signal, for example, the phase di erence between two adjacent waves. The angle-of-arrival based localization has a long history [85] and gathered a signi cant interest during World War II [2, 86]. A closed form error approximation of the maximum likelihood estimator was obtained by Stans eld in 1947 [86] and it is considered as one of the rst localization methods. It is a weighted least-squares (LS) estimator which assumes small independent bearing noise with Gaussian distribution and no sensor location error. A closed form solution to the problem is feasible under these assumptions as shown in [86] and thoroughly analyzed in [87]. In this study, it is shown that the Stans eld estimator is asymptotically biased. The pseudolinear estimator (PLE) provided in [8] relaxed the prior knowledge requirement of the emitter range by the Stans eld estimator. A novel sensitivity discussion is provided in [2] after rigorously analyzing the angle-of-arrival-only localization systems. For Gaussian distributed bearing noise, the passive emitter localization problem can be translated into a nonlinear least-squares estimation problem by engaging the maximum likelihood approach. In [64] the non-linear least-squares problem was linearized by Taylor series expansion resulting an iterative Gauss-Newton algorithm. A linearized least-square approach is given also in [43]. The maximum likelihood estimator is approximated in this method but this can lead to large errors if the measurement noise is large or the

sensor-target geometry is unfavorable for accurate localization. Under the normal density assumption, the maximum likelihood cost function is actually a weighted nonlinear least-square cost function. An initial estimate of the target position is required in linearized and iterative algorithms as closed-form solutions do not exist in nding the global minimum in such cost functions [8, 43, 64, 87]. A bias and variance analysis of the maximum likelihood estimation is studied in [87]. In [8, 88, 89] di erent study is carried out where the convergence of the iterative least-square algorithm for angle-of-arrival-only localization is explored.

Range based localization is a common passive measurement technique where the location of an emitter is obtained by triangulation of range information collected at a number of sensors. Range from a source to a sensor can be measured in several ways including the time of arrival of signal or signal strength. These techniques have numerous potential applications in mobile positioning in wireless telecommunication systems, radar and unmanned aerial vehicles (UAVs) [90{98].

Source localization using range measurements is challenging because the source location is related to the measurements in a highly nonlinear manner. An unconstrained least squares solution named as Quadratic-term Elimination (QE) is used to localize the source in [99, 100]. This approach is known to perform better than some previous localization methods such as Spherical Interpolation (SI) and Spherical intersection (SX) [101]. A di erent approach can be found in [102], where probabilistic sampling is used to obtain the localization. Localization of multiple emitting acoustic sources for wireless sensor networks has been examined using the Maximum Likelihood (ML) method in [103]. The Projection Onto Convex Sets (POCS) together with iteration to localize the source has been discussed in [104].

The potential performance of any particular localization algorithm is a strong function of the relative sensor-target geometry [9, 105]. As an example, the convergence of iterative estimation algorithm can be a ected by the relative sensor-target

geometry. A partial characterization of the sensor-target geometry with di er-ent matrices related to Cramer-Rao inequality or the resulting Fisher information matrix has been explored in [10]. Since the Cramer-Rao lower bound is a function of the relative sensor-target geometry, several studies have been carried out to identify underlying geometrical con gurations which minimize some measure of this variance lower bound [8, 10{16, 26, 106]. The target of these studies is to nd the geometric con gurations which are likely to result in more accurate localizations. In general, an optimization is carried out on the Cramer-Rao lower bound for those relative sensor-target geometries which minimize the selected measure. Any particular sensor-target positions which minimize some measure of variance lower bound is considered to be optimal with respect to this measure. It is obvious that the measurement technology employed by the sensors is related to the particular sensor-target positions which optimizes the chosen measure of the localization performance. In [12] the case of moving the sensors in order to localize and track moving targets while maintaining an optimal localization geometry is studied. Indeed, for mobile sensor-based localization problems, a similar measure of localization performance can be utilized to identify optimal sensor trajectories, hence derive control laws for navigating sensors along such optimal trajectories [8, 12, 14, 15, 107{110]. The problem of determining the optimal trajectory for a single moving platform with an angle-of-arrival sensor is explored in [111] and the optimal trajectory is determined by maximizing the determinant of the Fisher Information Matrix (FIM), which minimizes the uncertainty of the overall estimation problem. Deriving and dealing with actual Mean Squared Error (MSE) expressions for angle-of-arrival and range based localization methods can be mathematically challenging due to the nonlinear nature of the estimation problem. Hence Fisher information matrix can be employed to simplify the analysis to a greater extent [11, 13, 43].

Linear sensor arrays play a crucial role in some real world applications such

as radar [9, 20, 21, 23{25]. But most of the existing literature concern more on positioning the sensors around the target for optimal localization [11, 13]. In this study, we provide a characterization of the relative sensor-target geometry for linear sensor arrays based on AoA-only and range-only localizations. To the best of our knowledge, no such analysis exists in the existing literature.

2.3 Time-of-arrival and time-delay-of-arrival systems

Another important measurement technique is to utilize the time-of-arrival measurements of a signal transmitted by a target to several sensor positions to nd the location of a target. If the originated time of the signal at the target is not known, time-di erence-of-arrival between the sensors can be utilized to localize the target. Localization based on TDoA technology is currently applicable in numerous applications including intelligent transport system (ITS), resource management and performance enhancement in mobile cellular networks, electromagnetic radar and acoustic-based systems. TDoA-based systems may be used to estimate the location of a wireless emitter or audio source, where a considerable amount of work exists, [112{115].

TDoA systems, generally localize an emitter by processing signal arrival-time measurements at three or more sensors in R^2 space and four or more sensors in R^3 space. Essentially, the time-di erence-of-arrival measurements give the range di erence between two sensors with respect to the target. In the absence of noise and interference, the arrival-time measurements at two sensors are combined to produce a relative arrival time that, con nes the possible emitter location to a hyperbola in R^2 and a hyperboloid in 3D, with the two sensors as foci. As depicted in Figure 2.3, emitter location is estimated from the intersections of two or more independently generated hyperbolas in 2D and the intersections of three or more independently

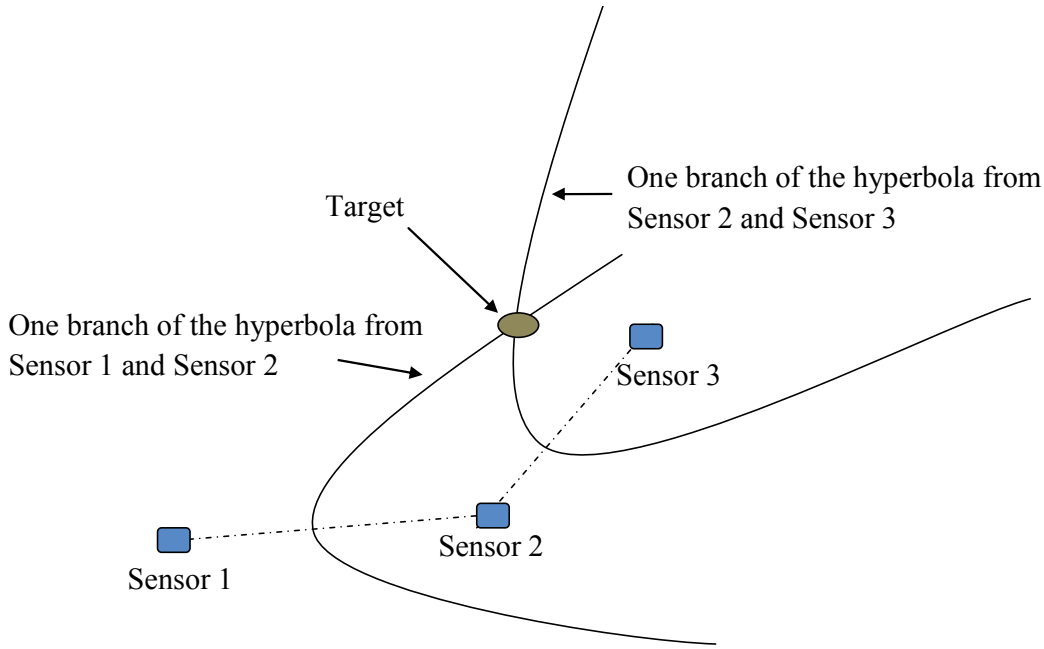

Figure 2.3: Time-Delay-of-Arrival measurement technique

generated hyperboloids in R^3 [26]. If two hyperbolas or three hyperboloids are considered, they can have either one or two points of intersection. The location ambiguity occurred by two points of intersection may be resolved by using a priori information about the location or an additional sensor to construct an additional hyperbola/ hyperboloid.

TDoA based localization inherently allows passive localization which is very useful in modern electronic warfare as the target can be localized without its knowledge [116, 117]. This localization technology has been known even before World War II [118]. Mainly the studies on TDoA has been on maximum likelihood estimations and the development of closed-form solutions [101, 119, 120], hence a relatively small number of calculations are required in localizing a target. In some other studies [26, 64, 121] the examination is carried out from purely statistical point of view by making assumptions on the probability density of the measurement errors. In this case, for the localization, an initial estimate of the target position is needed and which is not necessarily trivial to obtain. The convergence properties of the

iterative localization algorithm is highly dependent on the accuracy of the initial estimate.

Unique localization of multiple emitters using TDoA or ToA measurements which addresses the data association problem and an analysis on unique localization of an emitter using minimum number of TDoA measurements with bounded error are provided in our study.

Chapter 3

Optimal Sensor Placement for Linear Sensor Arrays

In the classical problem of target localization, the target position is estimated by multiple sensor measurements. In practice, these measurements are typically noisy. In some situations the geometry of the sensor array is pre xed, for example linear sensor arrays [9,18{25] which are common in practice. There is a limited freedom to place the sensors in order to get optimal performance in these particular geometries. In this chapter we analyze the optimal sensor-target geometries for common passive measurement techniques known as AoA-only and range-only technologies. In our approach, we consider the localization problem involving a single target and multiple adjustable AoA/ range sensors located in a linear array(uniform and non-uniform linear arrays).

The potential performance of any particular localization algorithm is highly dependent on the relative sensor-target geometry [8,9]. For example, the convergence of iterative estimation algorithm can be a ected by the relative sensor-target geometry. Lets consider a problem where the location of a single target is to be found using two angle-of-arrival sensors with noisy measurements. In this matter, hypothesis about the characteristics of the measurement error is not required. Two angle-of-arrival sensors independently take two measurements and the intersection of the those bearing lines provides an estimation for the target position. Even for

the noisy measurements the equations have a unique solution. In fact, if the measurements are noisy, the two bearing lines corrupted with noise do not intersect on the exact target location. Hence, the localization performance is dependent on the sensor-target geometry [8]. The distance between the intersection of two bearing lines and the true target location is a measure of performance of the localization. Obviously, this distance is inversely proportional to the performance. In this chapter, mathematical characterization is carried out for the localization geometries in linear sensor arrays utilizing AoA-only and range-only technologies.

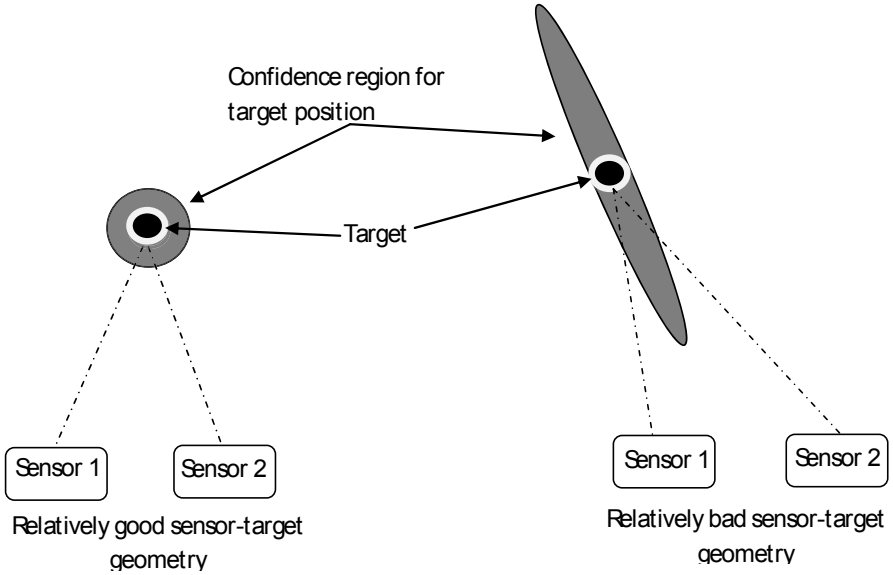

Figure 3.1: Sensor-target geometry and error

Before embarking on to the mathematical analysis which is chosen to represent this characterization, it is very important to understand how the sensor-target geometry in uence the potential localization performance. Figure 3.1 illustrates two di erent geometrical localization scenarios for AoA-only localization technique. The relative performance of a given localization geometry can be measured by the amount a xed error in a angle measurement translates into a corresponding error in target position. Localization performance can be regarded as less if a small error

in the measurement translates into a higher error in the localization. In fact, the relative performance of the sensor-target geometry should be considered as a relative measure. Hence, in a good performing geometry, a similarly constant error in the angle measurement should be translated into a relatively smaller error in the target position estimate. In some scenarios, the sensitivity of the target localization, as a function of the magnitude of the measurement error can be used to characterize the sensor-target geometry. It is obvious that a measure of the localization performance can be derived as a function of the particular sensor-target geometry.

Several studies have been carried out to identify underlying geometrical configurations which minimize some measure of the variance of the Cramer-Rao lower bound [8,10{16,26,106], as it is a function of the sensor-target geometry. The objective of these studies is to find the geometric configurations which are likely to result in localizations with good performance. Generally, an optimization is considered on the Cramer-Rao lower bound for those relative sensor-target geometries which minimize the selected measure. Such a sensor-target position which minimize some measure of variance lower bound can be regarded as optimal with respect to this measure. An incomplete characterization of the sensor-target geometry with different matrices related to Cramer-Rao inequality or the resulting Fisher information matrix has been studied in [8, 10]

In this chapter we provide a more rigorous characterization of the relative sensor-target geometry for linear sensor arrays based on AoA-only and range-only localization. We consider only one target for static localization problem. Here, an uncertainty ellipse which depicts the geometrical variance distribution of an efficient target estimate can be generated by utilizing the Cramer-Rao lower bound. This particular uncertainty ellipse is affected by the sensor-target geometry and the corresponding measurement technology. Hence, the objective of this chapter is to find the sensor-target geometry/ geometries which minimizes the area/ volume of

the corresponding uncertainty ellipse.

When the Cramer-Rao lower bound is obtained, the variance is the reciprocal of the Fisher information [43]. Hence, the determinant of the Fisher information can be used to assess the are of the uncertainty ellipse. Hence, the sensor-target geometries are analysed with respect to the determinant of the Fisher information matrix, and the geometries which maximize this particular determinant are considered optimal in this sense.

The analysis of the optimal geometry is subjected to the following constraints:

1. Fixed Uniform Linear Arrays(FULA): One sensor of the linear array is xed and the distance between the consecutive sensors are equal.

2. Uniform Linear Arrays(ULA): The distance between the consecutive sensors are equal.

3. Fixed Non-Uniform Linear Arrays(FNULA): One sensor of the linear array is xed and the distance between the consecutive sensors may not be equal.

4. Non-Uniform Linear Arrays(NULA): The distance between the consecutive sensors may not be equal.

In fact, the results presented in this paper provide fundamental information about how the localization performance is a ected by the sensor-target geometry for linear sensor arrays[1]. This information is of signi cant value to users of multiple sensor(linear arrays) based localization systems.

[1]Please note that the material presented in this chapter was published as conference papers: S.C.K. Herath and P.N.Pathirana , Optimal sensor placement in linear arrays: Part I - AoA based localization, in ISSNIP 2011 : Proceedings of the 7th International Conference on Intelligent Sensors, Sensor Networks and Information Processing, pp. 277-281, IEEE, Adelaide, South Australia and in S.C.K. Herath and P.N.Pathirana , Optimal sensor separation for AoA based localization via linear sensor array, in ISSNIP 2010 : Proceedings of the 6th International Conference on Intelligent Sensors, Sensor Networks and Information Processing, pp. 187-192, IEEE, United States.

3.1 Conventions and notation

Consider the i^{th} sensor of a multiple AoA/range sensors located in a linear array which is positioned to localize a single stationary target(Figure 3.2) in R^2. The unknown location of the target is given by $p = [x_p \; y_p]^T$. The AoA/range sensors are marked as $i \; 2 \; f1;2;::::;Ng$ and $N \quad 2$ with the position of the i^{th} sensor given by $S_i = [x_{si} \; y_{si}]^T$. The distance between the sensor S_i and the target P is given by $r_i = kp \quad S_i k$. The bearing $_i$ from sensor S_i to the target is measured clockwise from x-axis such that $_i(p) \; 2 \; [0;2 \;)$.

3.2 Cramer-Rao lower bound and Fisher information matrix

In general, the set of measurements from N sensors can be written as $\hat{z} = z(p) + n$, where $z(p) = [z_1(p) : : : z_N(p)]^T$ and $n = [n_1 : : : n_N]^T$. It is assumed that the measurement errors of distinct sensors are independent of each other. Also, for simplicity, it is assumed that the error variances of multiple distinct sensors are equal and is given by ^2_z. The covariance matrix for N number of sensors is then given by $R_z = \; ^2_z I_N$, where I_N is an N-dimensional identity matrix. The general measurement vector $\hat{z}$ can thus be considered as an observable normally distributed random vector and can be described by $\hat{z} \quad N \; (z(p); R_z)$.

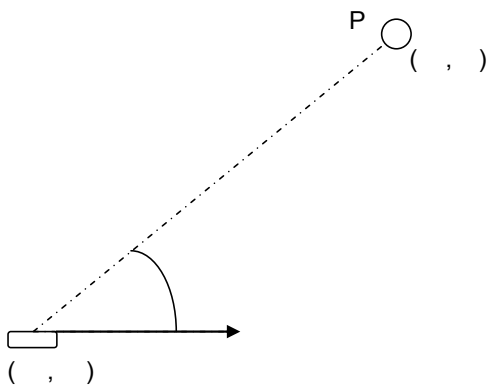

Figure 3.2: Measurement from a sensor.

Under the Gaussian measurement error assumption, the likelihood function of p given the measurement vector $\hat{z} \sim N(z(p); R_z)$ is given by

$$f_z(\hat{z}; p) = \frac{1}{(2\pi)^{N/2} |R_z|^{1/2}} \exp\left[-\frac{1}{2}(\hat{z} - z(p))^T R_z^{-1} \frac{1}{2}(\hat{z} - z(p))\right] \tag{3.2.1}$$

where $|R_z|$ is the determinant of R_z and $z(p)$ is the mean value of $\hat{z}$. The natural logarithm of $f_z(\hat{z}; p)$ can be written as

$$\ln f_z(\hat{z}; p) = \frac{1}{2}(\hat{z} - z(p))^T R_z^{-1} \frac{1}{2}(\hat{z} - z(p)) + c; \tag{3.2.2}$$

where c is a constant independent of p.

The Cramer-Rao inequality lower bounds the covariance achievable by an unbiased estimator under two mild regularity conditions [43, 122, 123]. Considering the unbiased estimate $\hat{p}$ for p, the Cramer-Rao bound states that

$$E[(\hat{p} - p)(\hat{p} - p)^T] - I^{-1}(p) \geq C(p); \tag{3.2.3}$$

where $I(p)$ is the Fisher information matrix. In general if I is singular then no unbiased estimator for p exists with a finite variance. If I is nonsingular then the existence of an unbiased estimator of p with finite variance is theoretically possible [124,125]. If (3.2.3) holds with equality then the estimator is called efficient and the parameter estimate $\hat{p}$ is unique.

Consider the set of measurements from N sensors $\hat{z} \sim N(z(p); R_z)$. The Fisher information matrix, in this case, quantifies the amount of information that the observable random vector $\hat{z}$ carries about the unobservable parameter p. It can be stated that the Fisher information characterizes the nature of the likelihood function(3.2.1). If the likelihood function is sharply peaked then the true value of p is easy to estimate from the measurements. The $(i,j)^{th}$ element of I is given by

$$(I(p))_{i;j} = E\left[\frac{@}{@p_i}\ln(f_z(\hat{z};p))\ \frac{@}{@p_j}\ln(f_z(\hat{z};p))\right]; \tag{3.2.4}$$

In the general case, under the Gaussian noise assumption, $(i;j)^{th}$ element of I is given by

$$(I(p))_{i;j} = \frac{@\hat{z}(p)^T}{@p_i}R_z^{-1}\frac{@\hat{z}(p)}{@p_j} + \frac{1}{2}tr\left[R_z^{-1}\frac{@R_z}{@p_i}R_z^{-1}\frac{@R_z}{@p_j}\right]; \tag{3.2.5}$$

where $tr(:)$ is the trace of the square matrix. This particular term accounts for the cases when covariance R_z is a function of the true parameter state p. But, in this study it is assumed that R_z is independent of the parameter p to be estimated. Then the above (3.2.5) simplifies to

$$(I(p))_{i;j} = \frac{@\hat{z}(p)^T}{@p_i}R_z^{-1}\frac{@\hat{z}(p)}{@p_j} \tag{3.2.6}$$

If $(I(p))_{i;j} = 0$, then p_i and p_j are orthogonal and their maximum likelihood estimates are independent. Then the general Fisher information matrix is given by

$$I(p) = r_p z(p)^T R_z^{-1} r_p z(p): \tag{3.2.7}$$

where $r_p z(p)$ is the Jacobian of the measurement vector with respect to p.

As long as $I(p)$ is invertible the matrix $I^{-1}(p) , C(p)$ is symmetric positive definite and defines the uncertainty ellipsoid. The eigenvalues of $C(p)$ are arranged according to $_1 \quad _2 \quad ::: \quad _M$. Note that $\sqrt{_i};8\ 2\ f1;:::;Ng$ is the length of the i^{th} axis of the ellipsoid and also that the axes of the ellipsoid lie along the relevant eigenvectors of $C(p)$.

The potential performance of an unbiased estimator can be assessed by the scalar functional measure of the shape and size of the uncertainty ellipse. The estimated uncertainty can be measured by several different scalar functions of $C(p)$. As an example, the mean squared error of the unbiased and efficient estimate is directly

related to the trace of the $C(p)$ given by $tr(C(p)) = \sum_{i\ i}$. The volume of the uncertainty ellipsoid given by $det(C(p)) = \prod_{i\ i}$ is another important measure of the performance.

In this study, the volume of the uncertainty ellipsoid is utilized as the measure of the total uncertainty in an estimate $\hat{p}$ of p. In our analysis, we use the determinant of the Fisher information matrix ($I(p)$) as an inverse measure of the uncertainty ellipsoid volume as it is mathematically easier to deal with the determinant rather than the inverse Fisher information matrix for the analysis.

3.3 AoA based localization

Consider the i^{th} sensor of a multiple AoA sensors located in a linear array which are positioned to localize a single stationary target in R^2. The measured value of angle ($_i$) is given by,

$$\hat{}_i = {}_i(p) + n_i = \arctan\left(\frac{y_p - y_{si}}{x_p - x_{si}}\right) + n_i; \tag{3.3.1}$$

where the $\arctan$ is defined such that ${}_i(p) \in [0; 2\ )$. The measurement error n_i is assumed to be normally distributed with zero mean and variance ^{2}, i.e. $n_i \sim N(0; {}^2)$.

Then using (3.2.7), Fisher information matrix ($I(p)$) for N number of sensors can be written as,

$$I(p) = \frac{1}{{}^2}\sum_{i=1}^{N}\frac{1}{r_i^2}\begin{bmatrix}\sin^2{}_i & \sin{}_i\cos{}_i\\ \sin{}_i\cos{}_i & \cos^2{}_i\end{bmatrix} \tag{3.3.2}$$

Then the Fisher information determinant for AoA-only localization can be given as,

$$det(I(p)) = \frac{1}{4}\sum_{S}\frac{\sin^2({}_j - {}_i)}{r_j^2 r_i^2}; \tag{3.3.3}$$

and

$$\det(I(p)) = \frac{1}{4^4}\left[\sum_{i=1}^{N}\frac{1}{r_i^2}\sum_{i=1}^{N}\frac{\cos 2\theta_i}{r_i^2}\right]^2 + \left[\sum_{i=1}^{N}\frac{\sin 2\theta_i}{r_i^2}\right]^2;$$

where $S = \{\{i,j\}\}$ is defined as the set of all combinations of i and j with $i,j \in \{1,\ldots,N\}$ and $j>i$, implying $|S| = \binom{N}{2}$. The number of combinations is indicated by the $|\cdot|$.

3.4 Range based localization

Consider the i^{th} sensor of a multiple range sensors located in a linear array which are positioned to localize a single stationary target in R^2. The measured value of angle (r_i) is given by,

$$\hat{r}_i = r_i(p) + e_i; \tag{3.4.1}$$

where the e_i is the measurement error and it is assumed to be normally distributed with zero mean and a variance σ_r^2, i.e. $e_i \sim N(0, \sigma_r^2)$.

Then using (3.2.7), the Fisher Information Matrix ($I_r(p)$) for N number of sensors around the target can be written as,

$$I_r(p) = \frac{1}{\sigma_r^2}\sum_{i=1}^{N}\begin{bmatrix}\cos^2\theta_i & \sin\theta_i\cos\theta_i \\ \sin\theta_i\cos\theta_i & \sin^2\theta_i\end{bmatrix} \tag{3.4.2}$$

The Fisher information determinant for range-only localization can be given as,

$$\det(I_r(p)) = \frac{1}{\sigma_r^4}\sum_{S}\sin^2(\theta_j - \theta_i); \tag{3.4.3}$$

and

$$\det(I_r(p)) = \frac{1}{4\sigma_r^4}\left[4N^2 - \left(\sum_{i=1}^{N}\cos 2\theta_i\right)^2 - \left(\sum_{i=1}^{N}\sin 2\theta_i\right)^2\right];$$

where $S = \{\{i,j\}\}$ is defined as the set of all combinations of i and j with $i,j \in \{1,\ldots,N\}$ and $j > i$, implying $|S| = \binom{N}{2}$.

These relationships for AoA and range are used in accessing the optimal geometries in following sections.

3.5 Optimal geometries for inline AoA sensors

3.5.1 Fixed Uniform Linear Arrays(FULA)

Theorem 3.5.1. Consider a target at $P(x_p, y_p) \in R^2$. N number of linear AoA sensors (one fixed at the origin), separated by x distance from each other (Figure 3.3) are b distance away from the target. The Fisher information determinant for this case is,

$$\det(I_x(p)) = \frac{1}{\sigma^4}\sum_{j=2}^{N}\sum_{i=0}^{j-2}\left[\frac{b[j-(i+1)]x}{[(a-ix)^2+b^2][(a-[j-1]x)^2+b^2]}\right]^2; \tag{3.5.1}$$

where $(a,b) = (x_p, y_p)$.

Proof. Transforming (3.3.2) into Cartesian co-ordinates and rearranging leads to (3.5.1). □

Corollary 3.5.2. Consider that the target location is $P(x_p, y_p)$ and the position of the fixed sensor(S_1) and the line on which the second sensor to be placed is known. Then the optimal distance between these two sensors is equal to the distance between the fixed sensor and the target (ie. $\|S_1 - S_2\| = \|S_1 - P\|$).

Proof. With no loss of generality consider two sensors, one fixed at the origin ($S_1 = [0\ 0]^T$), the other one on the x-axis ($S_2 = [x_{s2}\ 0]^T$) as shown in the Figure 3.4. The Fisher information determinant for this case is,

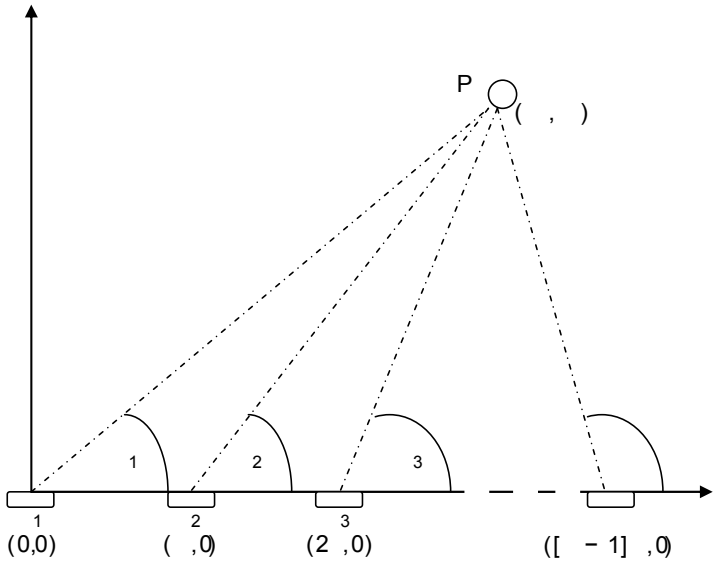

Figure 3.3: Localization with ULA of N number of sensors(AoA/ Range) with one sensor xed at the origin.

$$\det(I_x(p)) = \frac{1}{4}\left[\frac{y_p x_{s2}}{(x_p^2 + y_p^2)[(x_p - x_{s2})^2 + y_p^2]}\right]^2 : \tag{3.5.2}$$

By maximizing (3.5.2) with respect to x_{s2}, it can be shown that, $\det(I_x(p))$ maximizes when,

$$x_{s2} = \sqrt{x_p^2 + y_p^2}:$$

Hence, $kS_1 - S_2k = kS_1 - Pk$. □

3.5.2 Uniform Linear Arrays(ULA)

Theorem 3.5.3. Consider N sensors on a given straight line b distance away from a target in R^2. When x is the distance between consecutive sensors (Figure 3.5), the optimal localization of the target occurs for the x, which maximize the following Fisher information determinant,

$$\det(I_x(p)) = \frac{1}{4}\sum_{j=2}^{N}\sum_{i=0}^{j-2}\left[\frac{(b[c-d]x)}{[(cx)^2 + b^2][(dx)^2 + b^2]}\right]^2; \tag{3.5.3}$$

where

$$c = \frac{N-1}{2} - i;$$

and

$$d = \frac{N-1}{2} - [j-1]:$$

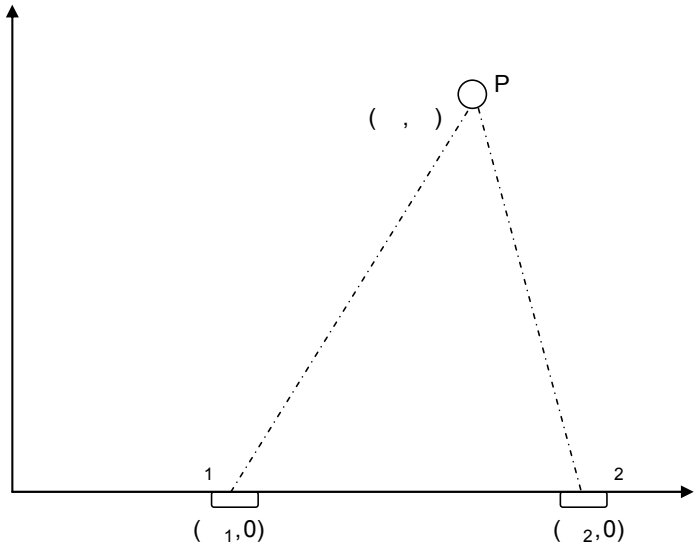

Figure 3.4: Localization with two sensors(AoA/ Range) on x-axis.

Proof. Transforming (3.3.2) into Cartesian co-ordinates and rearranging leads to (3.5.3). □

Corollary 3.5.4. **For two AoA sensors, the optimal sensor separation occurs when** $kS_1 \quad S_2k = kS_1 \quad Pk = kS_2 \quad Pk$.

Proof. Consider the sensor-target geometry shown in Figure 3.4. Using (3.3.2), the Fisher information determinant for this case is,

$$\det(I_x(p)) = \frac{(\qquad\qquad\qquad\qquad\qquad\qquad)_2}{(x_p \quad x_{s1})^2 + x_p^2 \quad (x_p \quad x_{s2})^2 + x_p^2} : \qquad (3.5.4)$$

It can be shown that the maximum of (3.5.4) occurs when

$$x_{s1} = x_p \quad y_p = \frac{p}{3};$$

and

$$x_{s2} = x_p + y_p = \frac{p}{3}:$$

When this relationship holds for the optimal sensor separation, $kS_1 \quad S_2k = kS_1 \quad Pk = kS_2 \quad Pk$. □

3.5.3 Fixed Non-Uniform Linear Arrays(FNULA)

Suppose that a target $(P)\ 2\ R^2$ is to be localized using N number of linear array of sensors $(S_1; S_2; \ ; \ : \ : \ : \ ; S_N)$. transforming (3.3.2) in to Cartesian co-ordinates, it can be shown that the Fisher information determinant for this case is,

$$\det(I(p)) = \frac{1}{4}\sum_{S}\left(\frac{bkS_j - S_ik}{kS_j - Pk^2 kS_i - Pk^2}\right)^2; \quad (3.5.5)$$

where b is the distance between the target and the linear array and $S = \{\{i,j\}\}$ is defined as the set of all combinations of i and j with $i,j \in \{1,\dots,N\}$ and $j>i$, implying $|S| = \binom{N}{2}$.

Finding the optimal sensor separations becomes an $(N-1)$-dimensional optimization problem. Finding the solutions is mathematically challenging when $n>3$ and the solutions for the $n=3$ case have been found in [126] which is a two-dimensional optimization problem.

Non-Uniform Linear Arrays(NULA)

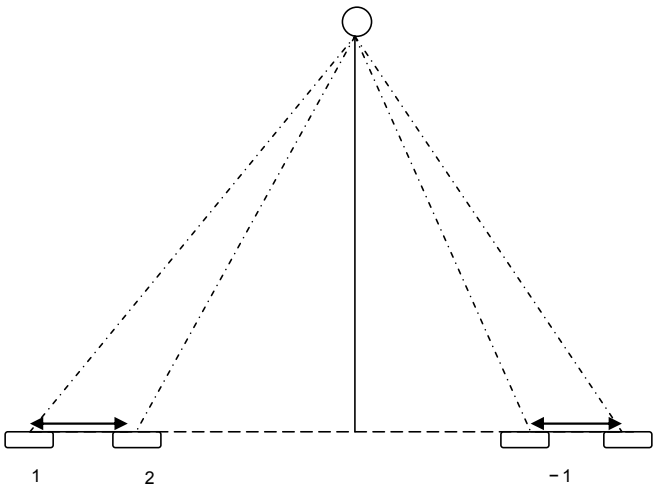

Figure 3.5: AoA/Range localization with N number of sensors.

Theorem 3.5.5. Consider N number of AoA sensors on a given line b distance away from a target in R^2. At the optimal geometry, sensors form an equilateral triangle with the target.

1. N is even; $N/2$ sensors overlap at each corner of the triangle located on the line.
2. N is odd; $(N-1)/2$ and $(N+1)/2$ sensors overlap at each corner of the triangle located on the line respectively.

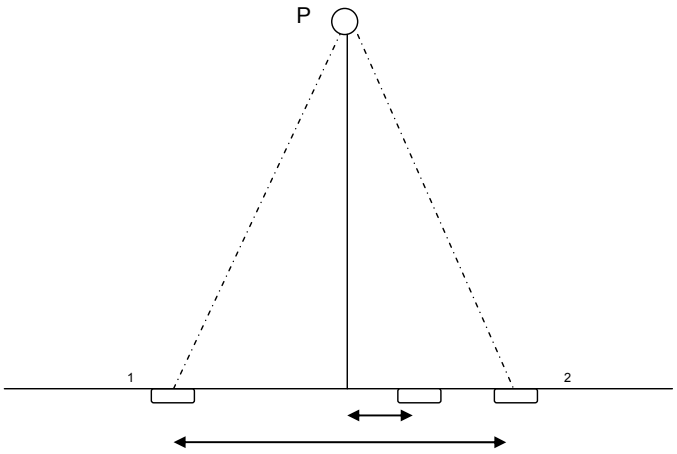

Figure 3.6: Localization with N number of AoA sensors.

Proof. Consider the sensor-target geometry shown in Figure 3.6. When the total number of sensors used for localization is odd ($N \in \{3,5,7,\ldots\}$); assume that $(N-1)/2$ number of sensors are overlapping at each corner of the triangle (S_{k_1} and S_{k_2}), which are y distance apart and the remaining sensor is x distance away from the symmetric axis. Using (3.3.2) the Fisher information determinant for this case can be written as,

$$\begin{aligned}\det(I_{x;y}(p)) = & \frac{N-1}{2}\frac{b^2(y+x)^2}{[(y^2+b^2)(x^2+b^2]^2} \\ & + \frac{N-1}{2}\frac{b^2(y-x)^2}{[(y^2+b^2)(x^2+b^2]^2} \\ & + \left(\frac{N-1}{2}\right)^2\frac{b^2(2y)^2}{(y^2+b^2)^4}. \end{aligned} \tag{3.5.6}$$

It can be shown that (3.5.6) is at maximum when $x = b/\sqrt{3}$ and $y = b/\sqrt{3}$ $\forall N \in \{3,5,7,\ldots\}$.

When the total number of sensors used for localization is even ($N \in \{2,4,6,\ldots\}$); assume that $N/2$ and $N/2-1$ number of sensors are overlapping at each corner of the triangle (S_{k_1} and S_{k_2}), which are y distance apart and the remaining sensor is x distance away from the symmetric axis. Using (3.3.2) the Fisher information determinant for this case can be written as,

$$\begin{aligned}\det(I_{x;y}(p)) = & \frac{N}{2}\frac{b^2(y+x)^2}{[(y^2+b^2)(x^2+b^2]^2} \\ & + \frac{N}{2}\frac{b^2(y-x)^2}{[(y^2+b^2)(x^2+b^2]^2} \\ & + \frac{N}{2}\left(\frac{N}{2}-1\right)\frac{b^2(2y)^2}{(y^2+b^2)^4}. \end{aligned} \tag{3.5.7}$$

It can be shown that (3.5.7) reaches it's maximum when $x = b/\sqrt{3}$ and $y = b/\sqrt{3}$ $8 N 2 f 2; 4; 6; : : :g$.

Then it is clear that for any $N \quad 2$, $x = b/\sqrt{3}$ and $y = b/\sqrt{3}$ provide the optimal geometry for AoA based localization which is an equilateral triangle. □

3.6 Optimal geometries for inline range sensors

3.6.1 Fixed Uniform Linear Arrays(FULA)

Theorem 3.6.1. Consider that a target is at $P(x_p; y_p) 2 R^2$. N number of linear range sensors (one xed at the origin), separated by x distance from each other (Figure 3.3) are b distance away from the target. The Fisher information determinant for this case is,

$$\det(I_x(p)) = \frac{1}{4r} \sum_{j=2}^{N} \sum_{i=0}^{j-2} \frac{(b[j \quad (i+1)]x)^2}{[(a \quad ix)^2 + b^2][(a \quad [j \quad 1]x)^2 + b^2]} ; \tag{3.6.1}$$

where $(a; b) = (x_p; y_p)$.

Proof. Transforming (3.4.3) into Cartesian co-ordinates and rearranging leads to (3.6.1). □

Corollary 3.6.2. Consider that the target is at $P(x_p; y_p)$ and the position of one sensor(xed) and the line on which the second sensor to be placed is known. The optimal geometry occurs when the angle subtended by the sensors at the target is $=2$ (ie. $S_1\hat{P}S_2 = \quad =2$).

Proof. With no loss of generality consider two sensors, one xed at the origin ($S_1 = [0\ 0]^T$)and the other on the x-axis ($S_2 = [x_{s2}\ 0]^T$). The target is at $P(x_p; y_p)$ as shown in Figure 3.4. The Fisher information determinant for this case is,

$$\det(I_x(p)) = \frac{1}{4r} \quad \frac{(\ y_p x_{s2})^2}{(x_p^2 + y_p^2)[(x_p \quad x_{s2})^2 + y_p^2]} : \tag{3.6.2}$$

By maximizing the (3.6.2) with respect to x_{s2}, it can be shown that, $\det(I_x(p))$ maximizes when,

$$x_{s2} = \frac{x_p^2 + y_p^2}{x_p}: \tag{3.6.3}$$

This proves that the optimal geometry occurs when the angle subtended by the sensors at the target is $=2$. □

3.6.2 Uniform Linear Arrays(ULA)

Theorem 3.6.3. Consider N sensors on a given line that are b distance away from the target in R^2. With equal distance between consecutive sensors (Figure 3.5), the optimal localization of the target occurs for the x, which maximizes the following Fisher information determinant,

$$\det(I_x(p)) = \frac{1}{4} \sum_{j=2}^{N} \sum_{i=0}^{j-2} \frac{(b[c-d]x)^2}{[(cx)^2+b^2][(dx)^2+b^2]} \quad ; \tag{3.6.4}$$

where

$$c = \frac{N-1}{2} - i;$$

and

$$d = \frac{N-1}{2} - [j-1]:$$

Proof. Transforming (3.4.3) into Cartesian co-ordinates and rearranging leads to (3.6.3). □

Corollary 3.6.4. For two range sensors, the optimal sensor target geometry occurs when the angle subtended by the sensors at the target is $\pi/2$ (ie. $S_1\hat{P}S_2 = \pi/2$).

Proof. Consider the sensor-target geometry shown in Figure 3.4. Using (3.4.3), the Fisher information determinant for this case is,

$$\det(I_x(p)) = \frac{[y_p(x_{s2}-x_{s1})]^2}{(x_p-x_{s1})^2+x_p^2 \quad (x_p-x_{s2})^2+x_p^2}: \tag{3.6.5}$$

It can be shown that the maximum of (3.6.4) occurs when

$$x_{s2} = \frac{x_p^2+y_p^2-x_p x_{s1}}{x_p-x_{s1}}:$$

When this relationship holds for the optimal sensor target geometry, the angle subtended by the sensors at the target is $\pi/2$. □

This result agrees with the geometrical relationships obtained in [11], where they prove that, for two range sensors, the optimal sensor-target geometry is unique and occurs when the angle subtended by the sensors at the target is $\pi/2$. This result agrees with [106].

3.6.3 Fixed Non-Uniform Linear Arrays(FNULA)

Consider N number of linear sensors $(S_1; S_2; \ldots; S_N)$ are employed to localize a target $(P) \in R^2$. One sensor is fixed at the origin. Transforming (3.4.3) into Cartesian co-ordinates, it can be shown that the Fisher information determinant for this case is,

$$\det(I_r(p)) = \frac{1}{r^4} \sum_{S} \left(\frac{\|bkS_j - S_ik\|}{\|kS_j - Pk\|\|kS_i - Pk\|} \right)^2; \tag{3.6.6}$$

where b is the distance between the target and the linear array whilst $S = \{\{i; j\}\}$ is defined as the set of all combinations of i and j with $i; j \in \{1; \ldots; N\}$ and $j > i$, implying $|S| = \binom{N}{2}$.

Finding the optimal sensor separation becomes an $(N-1)$-dimensional optimization problem and further studies can be carried out.

3.6.4 Non-Uniform Linear Arrays(NULA)

Suppose that a target $(P) \in R^2$ is to be localized using N number of inline sensors $(S_1; S_2; \ldots; S_N)$. transforming (3.4.3) into Cartesian co-ordinates, it can be shown that the Fisher information determinant for this case is,

$$\det(I_r(p)) = \frac{1}{r^4} \sum_{S} \left(\frac{\|bkS_j - S_ik\|}{\|kS_j - Pk\|\|kS_i - Pk\|} \right)^2; \tag{3.6.7}$$

where b and S carries the same meaning in the above section. Here in this case too finding the optimal sensor separation leads to an N-dimensional optimization problem which requires further studies.

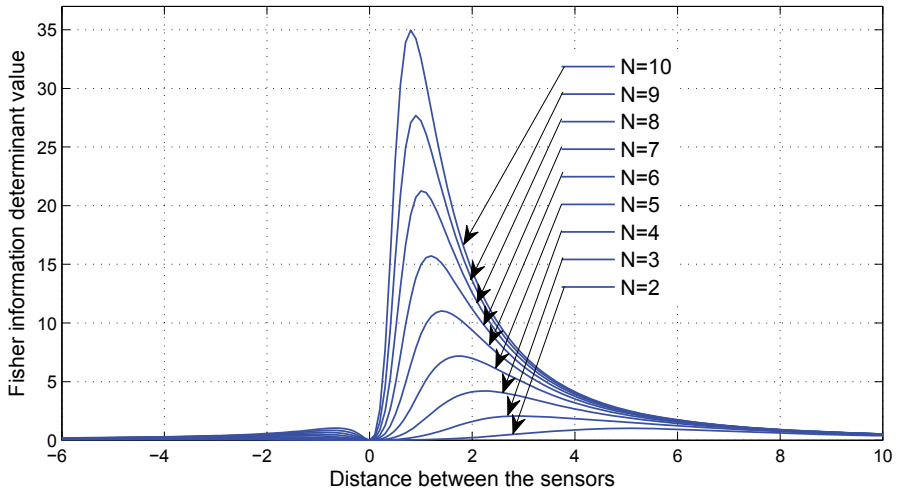

Figure 3.7: Variation of Fisher information determinant value with the distance between two adjacent sensors of ULA for di erent number of AoA sensors (one sensor xed).

3.7 Simulations

3.7.1 AoA-only linear sensor arrays

Consider a sensor-target geometry as depicted in Figure 3.3, where sensor S_1 is xed at the origin and the other sensors (S_2,S_3, ... S_N) are free to be located on the x-axis with equal distance from each other. The target is at $P = [3\ 4]^T$. Figure 3.7 shows the variation of the Fisher information determinant value with the distance between the sensors for di erent numbers of sensors.

It can be seen from the Figure3.7, that when the number of sensors are increased, the Fisher information determinant value increases and the inter-sensor distance decreases for optimal localization which is unique for a given number of sensors.

Two adjustable sensors

Consider sensors S_1 and S_2 are located anywhere on the x-axis (Figure 3.4). The target is at $P = [3\ 4]^T$. The variation of the Fisher information determinant value with the positions of the two sensors is depicted in Figure 3.8 and the corresponding contour plot in Figure 3.9. It can be seen that the Fisher information value is

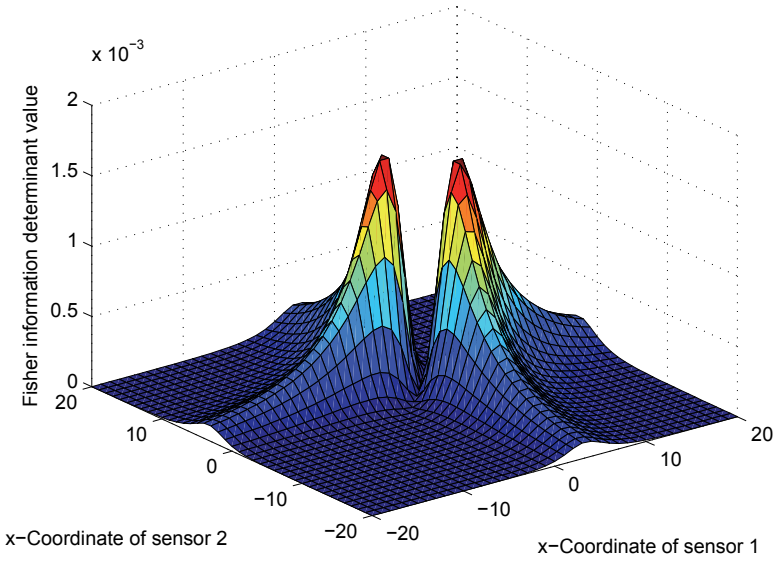

Figure 3.8: Variation of Fisher information determinant value with the AoA sensors positions.

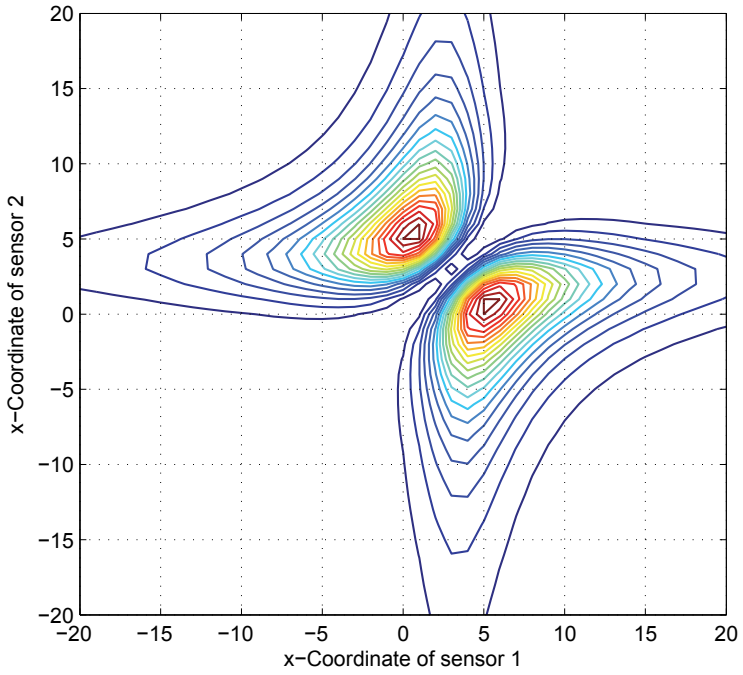

Figure 3.9: Variation of Fisher information determinant value with the AoA sensors positions(Contour plot).

maximized when $x_{s1} = \frac{9 - 4\sqrt{3}}{3}$ and $x_{s2} = \frac{9+4\sqrt{3}}{3}$(Corollary 3.5.4). When x_{s1} and x_{s2} attain these values, the geometry of the sensor-target con guration is an equilateral triangle. (ie. $kS_1 \quad S_2k = kS_1 \quad Pk = kS_2 \quad Pk$).

ULA with multiple adjustable sensors

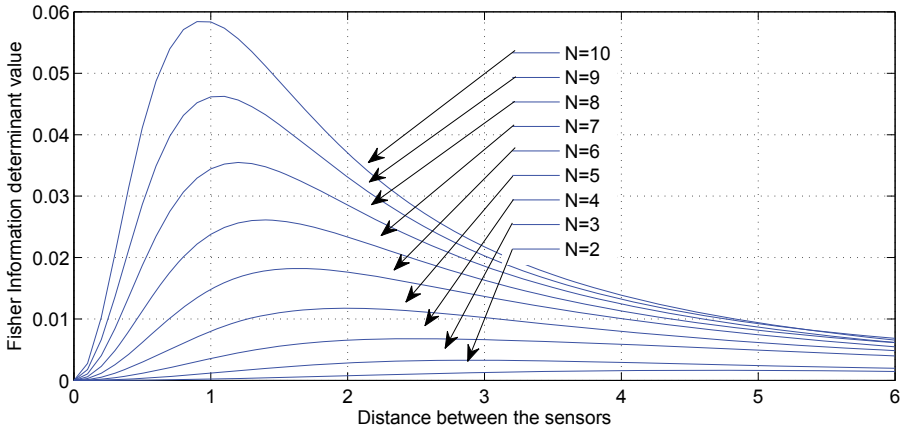

Figure 3.10: Variation of Fisher information determinant value with the distance between two adjacent sensors of ULA for di erent number of AoA sensors (All adjustable).

As illustrated in Figure 3.5, all the sensors are equally separated by x distance and the distance to the target from the line on which the sensors are placed is 4. The variation of Fisher information determinant value with respect to x is depicted in Figure 3.10 for di erent numbers of sensors.

It can be seen from the gure that when the number of sensors are increased, the Fisher Information determinant value increases and the distance between the sensors decreases for optimal localization while it is unique for a given number of sensors.

3.7.2 Range-only linear sensor arrays

Consider a sensor-target geometry as depicted in Figure 3.3, where sensor S_1 is xed at the origin and the other sensors (S_2,S_3, ... S_N) are located anywhere on the x-axis keeping the same distance from each other. The target is at $P = [3\ 4]^T$.

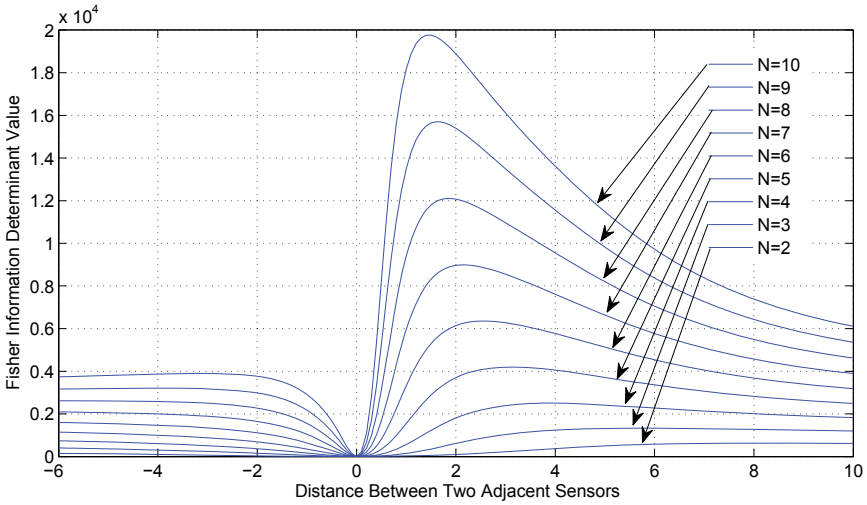

Figure 3.11: Variation of Fisher information determinant value with the distance between two adjacent sensors of ULA for di erent number of range sensors (One sensor xed).

Figure 3.11 shows the variation of Fisher information determinant value with the distance between the sensors for di erent number of sensors.

It can be seen from the gure that when the number of sensors are increased, the Fisher information determinant value increases and the distance between the sensors decreases for optimal localization while it is unique for a given number of sensors.

Two adjustable sensors

As depicted in Figure 3.4, sensors S_1 and S_2 are located anywhere on the x-axis. The target is at $P = [3\ 4]^T$. The variation of the Fisher information determinant value with the locations of the two sensors is depicted in Figure 3.12 and the corresponding contour plot in Figure 3.13. It can be seen that the Fisher information value maximizes when x_{s1} and x_{s2} satisfy (3.6.4)(Corollary 3.6.5).

ULA with multiple adjustable sensors

Consider a sensor-target geometry as illustrated in the Figure 3.5, where all the sensors are equally separated by x distance and the distance to the target from

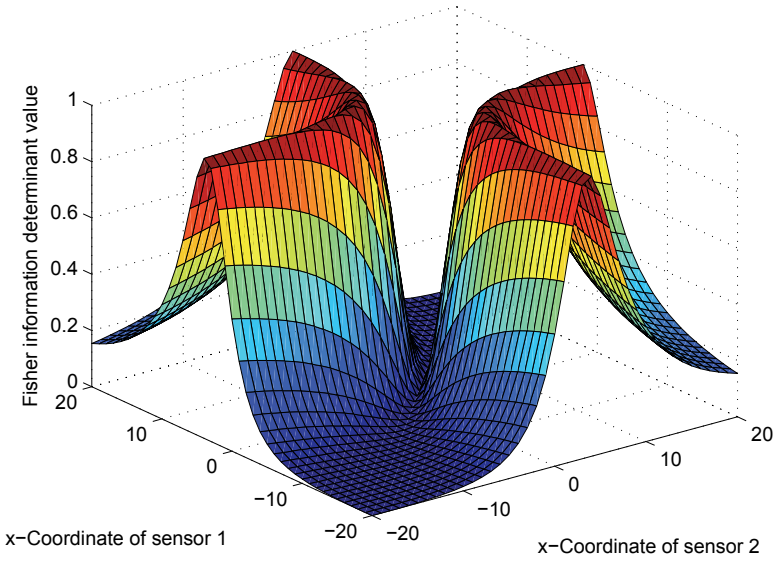

Figure 3.12: Variation of Fisher information determinant value with the range sensors positions.

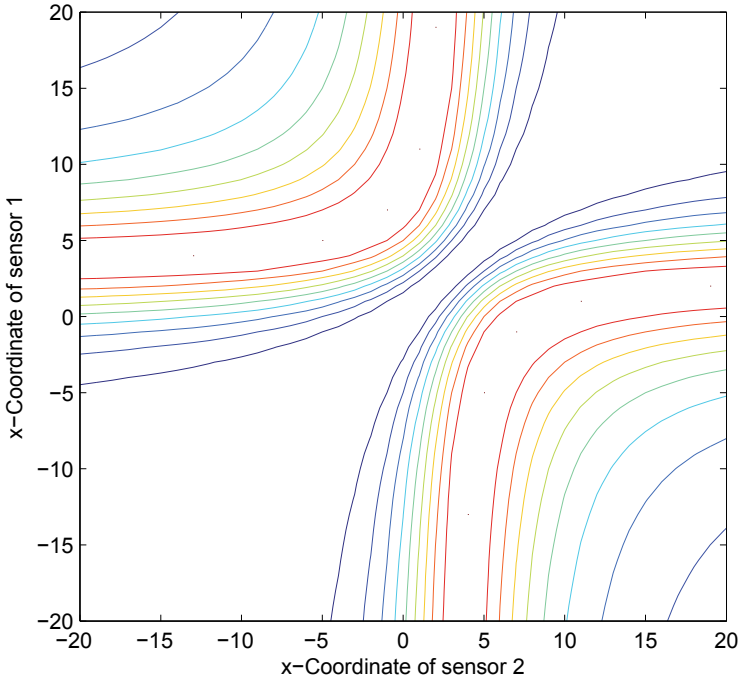

Figure 3.13: Variation of Fisher information determinant value with the range sensors positions(Contour plot).

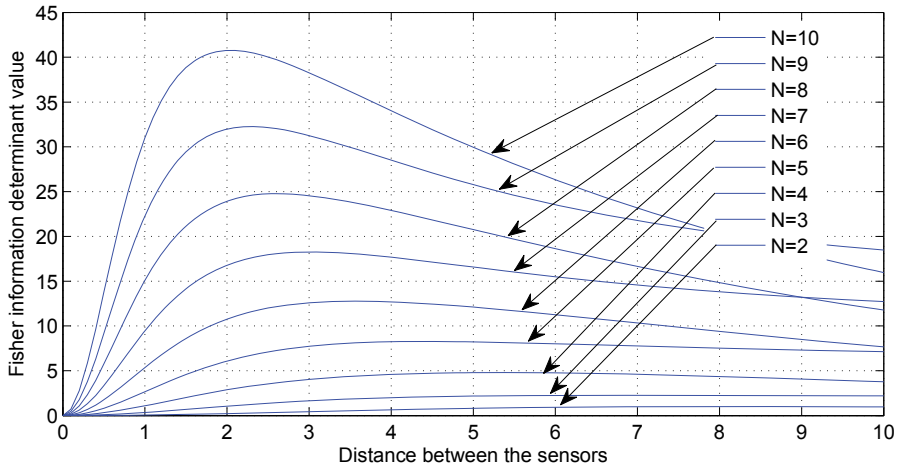

Figure 3.14: Variation of Fisher information determinant value with the distance between two adjacent sensors of ULA for di erent number of range sensors (All adjustable).

the line on which the sensors are placed is 4. Variation of the Fisher Information determinant value with respect to x is depicted in Figure 3.14 for di erent number of sensors.

It can be seen from the simulation that when the number of sensors increases, the Fisher information determinant value increases and the distance between the sensors decreases for optimal localization which is unique for a given number of sensors.

3.8 Summary

This chapter provides a characterization of optimal sensor-target geometry for linear arrays of AoA and range sensors in passive localization problems in R^2. The potential localization performance of unbiased and e cient estimator is used for these characterizations. The chosen measure of the localization performance (the area of the uncertainty ellipse) has an explicit and measurable connection between the sensor-target geometry. We have mainly discussed two generic problems of fully adjustable linear sensor arrays and the case of an array, where the sensors are

free to be moved with respect to a fixed sensor. Cramer-Rao lower bound and the corresponding Fisher information matrices are used to analyze the sensor target geometry for optimal localization.

By increasing the bias, the mean-squared error(or the variance) of an estimate can be reduced [127]. The relationship between the bias and the variance have been extensively studied in [125, 128, 129]. These works are helpful in understanding the bias-variance trade off. The results shown in these studies can be utilized to extend the results obtained in our study for more practical estimation algorithms such as maximum likelihood.

The results obtained in this chapter is useful in arranging the AoA or Range sensors in a manner which can significantly improve recursive localization performance. The analysis provided here is also related to optimal path planning and trajectory control of mobile sensors for localization, e.g see [15, 109, 111].

It should be noted that only the single target scenario is discussed in this chapter, but the multiple target localization can also be explored using the same concept presented.

The perfect knowledge of the emitter position should be available in the theoretical development for determining optimal sensor placement. Even though in practical applications this information is not available, a rough estimate of the likely region of the emitter is sufficient in determining the sensor positions to obtain improved localization results. In some practical applications, size of the sensor and the restrictions to the size of the array should be considered. Hence the results of this chapter can be utilized to establish guidelines for linear sensor placement leading to improved performance.

Chapter 4

Ghost Elimination in Time-Delay-of-Arrival and Time-of-Arrival Measurements

Data association problem or *ghost* formation is a phenomena which can be found in many multi target localization and tracking systems. When tracking multiple targets with relatively lesser number of sensors, the *ghost* formation occurs when incorrectly assigning *ghost* targets to real targets and vice versa. Limited number of spatially distributed sensors restrict the recovery of real target positions uniquely from the signals received at each sensor. At this instance, the number of combinations of the received measurements exceeds the number of real targets and some of these combinations refers to non existing targets. These particular virtual targets are denoted as *ghosts*. This chapter mainly discusses about the solution to the data association problem in TDoA and ToA based localization systems. It also addresses the unique solution region for minimal TDoA measurements.[1]

[1]Please note that some of the material presented in this chapter is accepted for publication in: S.C.K. Herath, P.N.Pathirana, B.T Champion and and S.W.Ekanayake, Localization with Ghost Elimination of Emitters Via Time-Delay-of-Arrival Measurements, IEEE 6th International Conference on Information and Automation for Sustainability (ICIAFS 2012)

Time-Delay-of-Arrival systems

Developing an accurate and e cient method to localize a signal sources has drawn signi cant attention in the recent past. Among numerous techniques, one very useful method of localization is based on measuring the di erence in the ranges from a particular emitter to sensors whose locations are known. In our approach, an array of sensors located at known positions in R^N are used to measure the signal arrival time transmitted from an emitter whose position is desired to be known. The time-delay-of-arrival (TDoA) of the received signal is calculated and converted to the corresponding range di erence by multiplying it by the velocity of signal propagation in the medium. However, in practical applications, the measurements are corrupted with noise and the sensor positions are often not precisely known. Localization based on TDoA technology is currently applicable in numerous applications including radar, sonar, navigation and sensor networks [112{115].

Generally in TDoA systems, the localization of an emitter is carried out by processing signal arrival-time measurements at three or more sensors in R^2 and four or more sensors in R^3. In the absence of noise and interference, the arrival-time measurements at two sensor positions are combined to produce a relative arrival time that, restrict the possible emitter location to a hyperbola in R^2 (Figure 2.3)and a hyperboloid in R^3, with the two sensor positions as foci. Position of the emitter is estimated from the intersections of two or more independently generated hyperbolas in R^2, and in R^3, from the intersections of three or more independently generated hyperboloids [26]. In these limited measurement cases, two hyperbolas or three hyperboloids can have either one or two points of intersection. In these instances there are some regions in the space which gives an unique solution to an emitter location [130]. The geometry of this space is related to the sensor geometry. This unique solution region gradually reduces with the increasing measurement error. Position estimation ambiguity occurred by two points of intersection may be

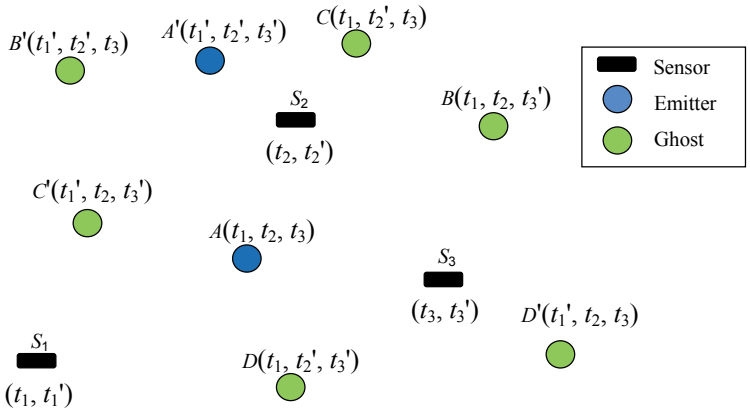

Figure 4.1: Ghost formation in TDOA measurements

resolved by using a priori information about the position or by using an additional sensor to construct a hyperbola/ hyperboloid.

The ghosts are formed when the time of arrival of two or more di erent emitters are used in combination to nd emitter locations. As depicted in Figure 4.1, for R^2, sensors S_1, S_2 and S_3 receive the time-of-arrival measurements $(t_i; t_i^0 : i\ 2\ 1;2;3)$ from emitters, A and A^0 respectively. Considering all the combinations of the measurements to localize the emitter positions, ghosts form at B, B^0, C, C^0, D and D^0.

Time-of-Arrival systems

Range from an emitter to a sensor can be measured form the time-of-arrival(ToA) of the signal [131{133]. Localization based on ToA technology is currently applicable in many applications including mobile cellular networks, intelligent transport system (ITS), electromagnetic radar and acoustic-based systems [131{146].

As the time-of arrival (ToA) can be measured accurately by using wide band or ultra wide band (UWB) signals and advanced signal processing technologies, a number of algorithms consider localization using distance measurements between each pair of neighboring sensors [92, 96, 98]. Time-of-arrival (ToA) systems, generally localize an emitter by processing signal arrival-time measurements at two or

more sensors in R^2 and three or more sensors in R^3. The arrival-time measurement at a sensor restricts the possible emitter location to a circle in R^2 and a sphere in R^3 with the sensor as the center. Position of the emitter is estimated from the intersections of two or more independently generated circles in R^2, and in R^3, from the intersections of three or more independently generated spheres.

Di erent types of data-association algorithms are provided for numerous measurement technologies for multi sensor-multi target scenario [72,75,147]. This chapter provide a discussion, which infers that the need for such elaborate techniques may not be necessary in many instances, including the simulation scenarios in [72] and [75]. Importantly, we show how the data-association problem can be removed through exhaustion.

Theoretical conditions are provided in this chapter for unique localization of emitters in the presence of the often overlooked ghost node problem that is found when attempting to nd the locations of multiple emitters in R^N using time-of-arrival measurements from multiple sensors located in R^N.

4.1 Time-Delay-of-Arrival systems

4.1.1 Localization of an emitter

Lets consider an emitter (T) in ND space, $N + 1$ number of sensors with $t_i + \frac{0}{i}$ denoting the signal arrival time at sensor i. Here, $\frac{0}{i}$. is the bound of the error. The arrival delay with respect to the reference sensor is $t_{i;0} = t_i \; t_0 + \frac{i}{c}$; $i = 1;2;:::;N$. Here $_i = {}^0_i \quad {}^0_0$ and $\frac{i}{c} \quad 2$. The corresponding range di erence is $d_i = c \; t_{i;0} = c(t_i \; t_0 + \frac{i}{c})$, where c is the velocity of signal propagation. Let the spatial coordinate vectors be: $x_0 = [x_0 \; y_0 \; z_0]^T = [0 \; 0 \; 0]^T$, $x_i = [x_i \; y_i \; z_i]^T$ and $x = [x_s \; y_s \; z_s]^T$, where x_0 is the reference sensor position, x_i is the i^{th} sensor position and the unknown emitter position is x. The range between the i^{th} sensor and the emitter can be written as, $R_{is} = kx_i \quad xk$. The distance between the reference

sensor and the emitter is $R_s = \|x\|$. Then the path difference can be written as, $d_i = R_{is} - R_s + \varepsilon_i$, which yields $x_i^T x + d_i R_s - R_{s\,i} = \frac{1}{2}\left(\|x_i\|^2 - (d_i^2 - \varepsilon_i)^2\right)$.

For a general case of $N + 1$ sensors, following matrices can be defined as $z = \frac{1}{2}[\|x_1\|^2 - (d_1^2 - \varepsilon_1)^2 : : \|x_N\|^2 - (d_N^2 - \varepsilon_N)^2]^T$, $S = [X_1 : : X_N]^T$, $d = [d_1 : : d_N]^T$ and $\varepsilon = [\varepsilon_1 : : \varepsilon_N]^T$ where, $X_i = [x_i - x_0]^T$. In matrix notation $Sx = z - (d - \varepsilon)R_s$ and solving for emitter position, $x = \left(S^T S\right)^{-1} S^T z - \left(S^T S\right)^{-1} S^T (d - \varepsilon) R_s$.

When not all range differences are measured to the same accuracy, a weighting matrix $R_{N\,N}$ is in order. Then,

$$\hat{x} = \left(S^T R^{-1} S\right)^{-1} S^T R^{-1} z - \left(S^T R^{-1} S\right)^{-1} S^T R^{-1} (d - \varepsilon) R_s: \tag{4.1.1}$$

Define the new vectors,

$$a = \left(S^T R^{-1} S\right)^{-1} S^T R^{-1} z = [a_1\ a_2\ a_3]^T \tag{4.1.2}$$

and

$$b = \left(S^T R^{-1} S\right)^{-1} S^T R^{-1} (d - \varepsilon) = [b_1\ b_2\ b_3]^T \tag{4.1.3}$$

Then, $\hat{x} = a - bR_s$ and the estimation for the source position $\hat{x}$ is obtained as

$$\hat{x} = \begin{bmatrix} x_s \\ y_s \\ z_s \end{bmatrix} = \begin{bmatrix} a_1 - b_1 R_s \\ a_2 - b_2 R_s \\ a_3 - b_3 R_s \end{bmatrix}: \tag{4.1.4}$$

Substituting x in $R_s = \|x\|$, the following quadratic equation can be obtained,

$$AR_s^2 + 2a^T b R_s + a^T a = 0 \tag{4.1.5}$$

where $A = b^T b - 1$.

4.1.2 Analysis on the solution area

In R^3 space, if at least four sensors are not coplanar and there is a subset of tree sensors which are not collinear, then the matrix S has full rank and it is possible to

solve the quadratic equation in (4.1.5). However, depending on the sensor-emitter con guration, (4.1.5) will lead to two possible solutions. It can be shown that (4.1.5) leads to an unique solution if $A<0$ and in R^2 plane and R^3 space, at least, 3 and 4 sensors are not collinear, respectively [130, 148]. Also, it can be shown that, generally, 3 and 4 non-collinear sensors are needed for unique localization of a target in R^2 plane and R^3 space, respectively, but an additional sensor is needed for both cases to resolve the ambiguity in some situations.

Theorem 4.1.1. The unique solution region for minimum number of TDoA measurements in R^N is given by,

$$\bigcap_{8\ ;k\ k_1<2}{}^{N} \tag{4.1.6}$$

where ^{N} is the N-dimensional region for $A<0$.

Proof. A in (4.1.5) can also be written as,

$$A = \quad S^T R^{\ 1} S^{\ 1} S^T R^{\ 1}(d \quad)^{\ T} \quad S^T R^{\ 1} S^{\ 1} S^T R^{\ 1}(d \quad) \quad 1:$$

If $C = \left[S^T R^{\ 1} S^{\ 1} S^T R^{\ 1} \right]^T \left[S^T R^{\ 1} S^{\ 1} S^T R^{\ 1} \right]$, further simpli cation will lead to

$$A = (d \quad)^T C (d \quad) \quad 1: \tag{4.1.7}$$

$A = 0$ is an equation of an ellipse in R^2 and ellipsoid in R^3 respectively. $A < 0$ is the region inside the ellipsoid which corresponds to the unique solution region in R^N. Region bounded by the intersection of all the ellipsoids $k \ k_1 < 2$ corresponds to the region in R^N which always guarantees a unique solution for the emitter position. Then it can be stated that for minimum number of TDoA measurements, the unique solution region in R^N is given by (4.1.6). □

4.1.3 Maximum bound for the error for a unique solution region

When the error bound increases the unique solution region given by (4.1.6) decreases. Then there is a maximum bound for the error ($_b$) before which, there is a unique solution region for an emitter for given sensor positions. $_b$ occurs at $k \ k_{min}$ for $\bigcap_{8\ ;k\ k_1<2}{}^{N} = f g$.

At this instant $d = [0;:::0]_{N\ 1}$. Hence (4.1.7) becomes

$$^{T}C \quad 1 = 0: \tag{4.1.8}$$

Since C is a symmetric matrix, using **eigen decomposition**,

$$y^{T}Q^{T}CQy \quad 1 = 0 \tag{4.1.9}$$

where Q is an orthogonal matrix with the columns which are eigen vectors of C and $y = Q^{1}$. Now (4.1.9) can be written as

$$y^{T}Dy \quad 1 = 0 \tag{4.1.10}$$

where

$$D = \begin{bmatrix} 1 & 0 & : & : & 0 \\ : & 2 & : & : & : \\ : & : & : & : & : \\ 0 & 0 & : & : & N \end{bmatrix}_{N\ N}$$

$_i; i\ 2\ f1;2;:::;Ng$ are the eigen values of C.

Above (4.1.10) refers to a rotated ellipsoid of (4.2.8) where the principal diagonals conside with the coordinate axes. Then the minimum distance between the origin and the ellipsoid is given by $\frac{1}{\sqrt{k\ k_1}}$. Hence, the at the minimum shift,

$$_{k\ k_{min}} = Q \quad 0 \ :::: \ \frac{1}{\sqrt{k\ k_1}} \ :::: \ 0 \quad ^{T}: \tag{4.1.11}$$

Then

$$_b = \frac{k\ k_{min} \quad 1}{2} \tag{4.1.12}$$

For a given sensor con guration if $< \ _b$, there is a region in which a unique solution can always be guaranteed.

The results obtained can be used to localize emitters in a given region with minimum number of sensors with known error bound.

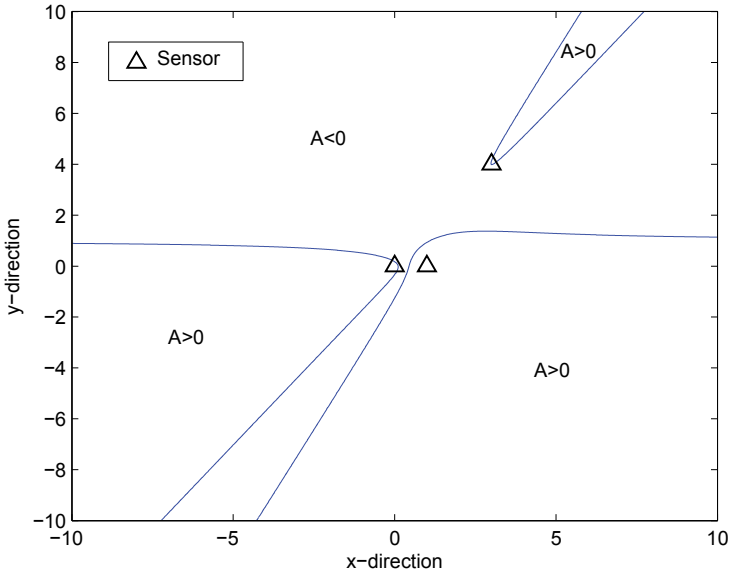

Figure 4.2: Unique solution area for R^2

Figure 4.2 depicts the unique solution area for three time-of-arrival sensors positioned in R^2 at $[0\ 0]^T; [1\ 0]^T$ and $[3\ 4]^T$. Figure 4.3 shows the corresponding transformed area, which is an ellipse.

A unique solution region for R^3 is shown in Figure 4.4, where the sensors are positioned at $[0\ 0\ 0]^T; [1\ 0\ 0]^T; [0\ 1\ 0]^T$ and $[1\ 1\ 1]^T$. The corresponding transformed region is depicted in Figure 4.5. In Figure 4.6, the unique solution regions for $= [\ 0{:}3251\ \ 0{:}3251\ 0{:}2380]^T$ and $= [0{:}3251\ 0{:}3251\ \ 0{:}2380]^T$ are shown. It can be seen that these two regions marginally touch each other at this error bound which agrees with our analysis.

4.1.4 Data association in TDoA measurements

Let us denote the following

p	number of emitters
T_j	jth emitter
$t_{i;j}$	time-of-arrival measurement at s_i from T_j
$t_{i;j;i^0;j^0}$	time di erence of arrival ($t_{i;j}$ - $t_{i^0;j^0}$)

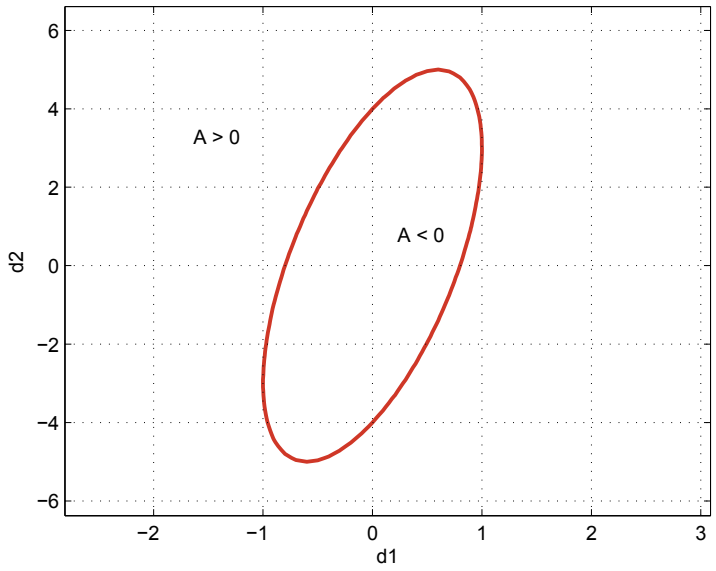

Figure 4.3: Transformed solution area for R^2

In this section, we consider the general problem involving $q+2$ or more sensors in q dimensions where $q = 2$ or $q = 3$. The emitters are assumed to be synchronized to send signals at the same time. Each sensor s_i, $i \in \{0;1;\ldots;N\}$ measures the time of signal arrival from each target T_j, $j \in \{1;\ldots;p\}$

For a given emitter, a system of $N \quad q + 1$ sensors provide N TDoA measurements that in the noiseless case are described by $t_{ij\,i^0j^0} = t_{i;j} \quad t_{i^0;j^0}$. True time difference for a particular emitter and two sensors occurs if and only if $j = j^0$. In all the other cases($j \neq j^0$), the time difference measurements will lead to ghosts or unrealistic emitter positions.

4.1.5 Ghost elimination

Definition 4.1.1. **Ghost**: A solution to (4.1.5) which is not overlapping with any real emitter.

Assumption 1. **Any combination of 4 sensors in the field is not collinear. This assures that the matrix S is full rank for all the combinations.**

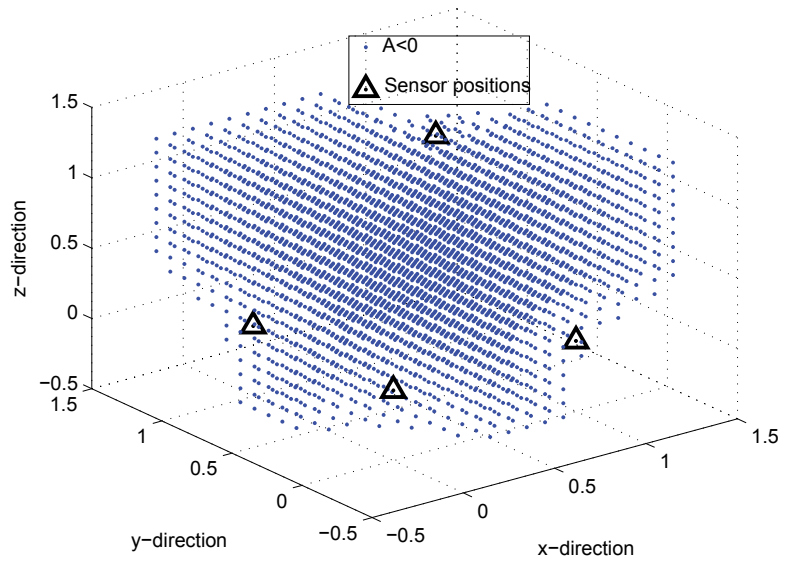

Figure 4.4: Unique solution region for R^3

Assumption 2. In (4.1.5), $A > 0$ for any combination of 4 sensors and any emitter. So, 5 sensors are needed for unique localization of any emitter.

Proposition 4.1.2. In R^3, if there are at least ve sensor measurements from a single emitter (T_j) in a measurement set, this will lead to the solution of that particular emitter (T_j) or to a ghost.

Proof. Lets consider a case where p number of emitters scattered over a R^3. N number of sensors are also placed over the same R^3 and the sensor-emitter geometry for each sensor is such that they need at least 5 sensors for unique localization.

Then with no loss of generality taking t_{01} as the reference measurement a general vector for d and z can be written as,

$$d = \begin{bmatrix} d_{1j_101} \\ d_{2j_201} \\ \vdots \\ d_{kj_k01} \\ \vdots \\ d_{Nj_N01} \end{bmatrix}; \tag{4.1.13}$$

$$z = \frac{1}{2}\begin{bmatrix} x_1^2 + y_1^2 + z_1^2 - d_{1j_101}^2 \\ x_2^2 + y_2^2 + z_2^2 - d_{2j_201}^2 \\ \vdots \\ x_k^2 + y_k^2 + z_k^2 - d_{kj_k01}^2 \\ \vdots \\ x_N^2 + y_N^2 + z_N^2 - d_{Nj_N01}^2 \end{bmatrix} \tag{4.1.14}$$

where $j_k \in (1;2;\dots;p)$.

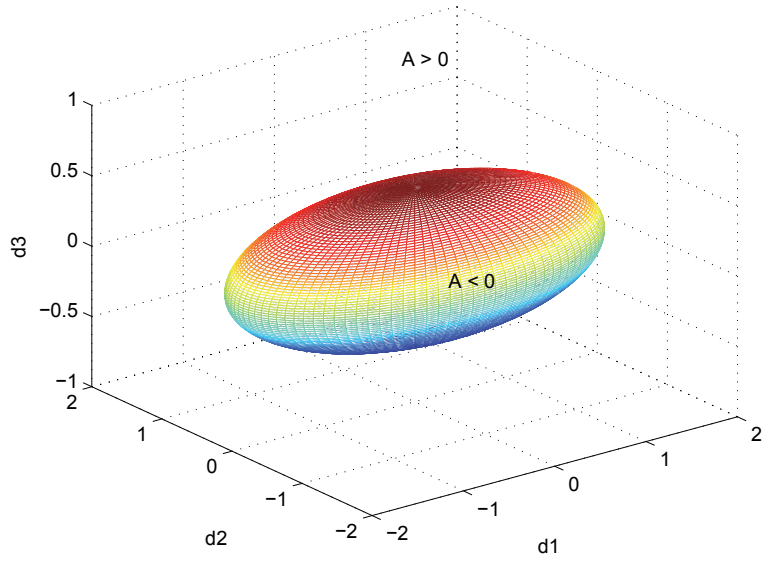

Figure 4.5: Transformed unique solution region for R^3

Lets consider a combination where subscripts $j_a = j_b = j_c = j_d = j_e$, and assume that all these refers to the T_j^{th} emitter. Now we select this subset and keeping T_{j_a} as the reference develop S^0, z^0 and d^0 matrices.

$$S^0 = \begin{bmatrix} x_b & y_b & z_b \\ x_c & y_c & z_c \\ x_d & y_d & z_d \\ x_e & y_e & z_e \end{bmatrix}; \tag{4.1.15}$$

$$z^0 = \frac{1}{2}\begin{bmatrix} x_b^2 + y_b^2 + z_b^2 - d_{bj_aj}^2 \\ x_c^2 + y_c^2 + z_c^2 - d_{cj_aj}^2 \\ x_d^2 + y_d^2 + z_d^2 - d_{dj_aj}^2 \\ x_e^2 + y_e^2 + z_e^2 - d_{ej_aj}^2 \end{bmatrix} \tag{4.1.16}$$

and

$$d^0 = \begin{bmatrix} d_{bj_aj} \\ d_{cj_aj} \\ d_{dj_aj} \\ d_{ej_aj} \end{bmatrix}. \tag{4.1.17}$$

This subset will lead to the unique position estimation of the T_j^{th} emitter. So the initial d and z vectors which contain this subset will yield the T_j^{th} emitter as the unique solution, if all the combinations are referring to the T_j^{th} emitter (subscripts $j_1 = j_2 = \cdots j_i = \cdots j_N$). If at least two subsets in a set lead to di erent solutions, the corresponding set will refer to a ghost or non-real solution, then the whole set can be discarded.

All the subsets in a set will lead to the same solution if and only if all of them are referring to a single real emitter. □

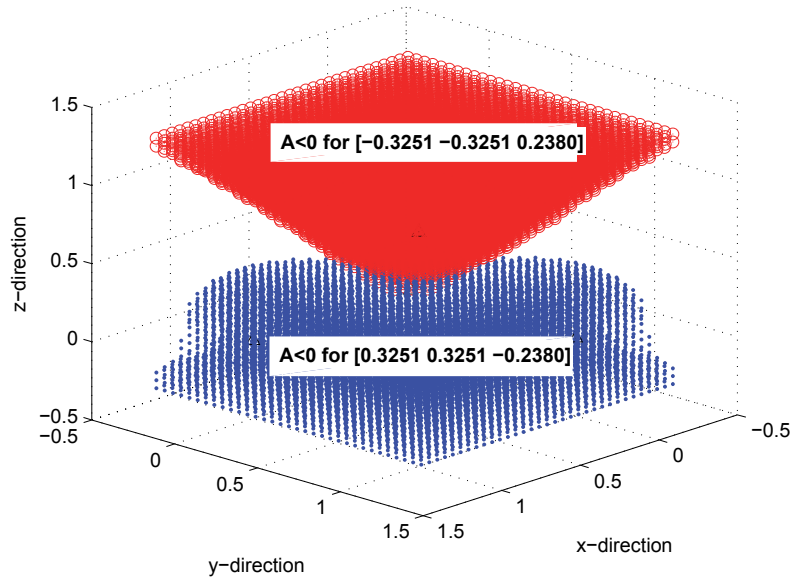

Figure 4.6: Unique solution region for R^3 with errors

Theorem 4.1.3. Assume that any combination of $q+1$ sensors in the field is not collinear. If the number of emitters in R^q is p, the minimum number of non-collinear sensors required for unique localization of all the targets is $(q+1)p+1$.

Proof. For R^q case , when $N = (q+1)p+1$ sensors are considered, for any combination of sensor measurement set, there is at least one combination which contains $(q+2)$ measurements from a single emitter. Using proposition 4.1.2, it can be shown that the measurement sets which have at least one measurement from a different emitter can be discarded. Hence, $N = (q+1)p+1$ number of non-collinear sensors will guarantee the elimination of all the ghosts. □

Let k be the number of sensor positions that are collinear with each other. Since the k collinear measurements provide no real additional information, they can be considered as null measurements. The minimum number of sensors, ignoring the null measurements, required to uniquely localize an emitter field of p emitters is $(q+1)p+k+1$.

4.1.6 Localization algorithm for TDoA measurements

In the unique localization of every emitter in the field, sensors must measure the time of arrival at spatially distinct positions and determine the locations of the

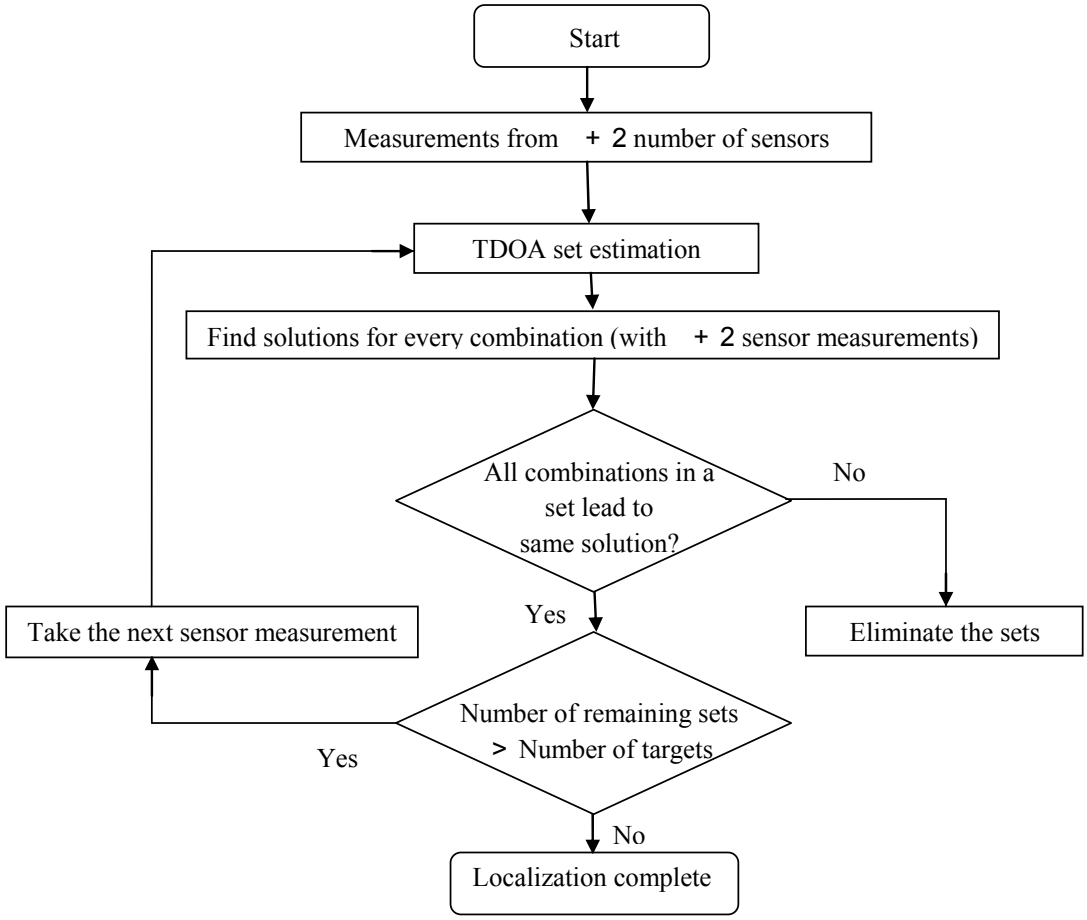

Figure 4.7: Algorithm owchart for unique localization in TDoA measurement technology

N-fold hyperbola/hyperboloid intersections at each measurement. The algorithm stops when the number of targets in the given area is equal to the detected N-fold hyperbola/hyperboloid intersections. If the number of emitters in the given area is not known, a statistical method can be used to estimate it. On the other hand, if the number of N-fold hyperbola/hyperboloid intersections remains the same over the consecutive measurements at some stage, one can infer that the intersections that were found correspond to the true emitter locations. In this case, it is assumed that the number of emitters is known. In a practical situation, the N-fold intersections will not perfectly overlap but should fall within some bounded region. The bounded region can be considered as a virtual point, if the measurements are noisy. Here, in

this analysis, we have assumed that the measurements are perfect.

The algorithm is brie y described in Figure 4.7.

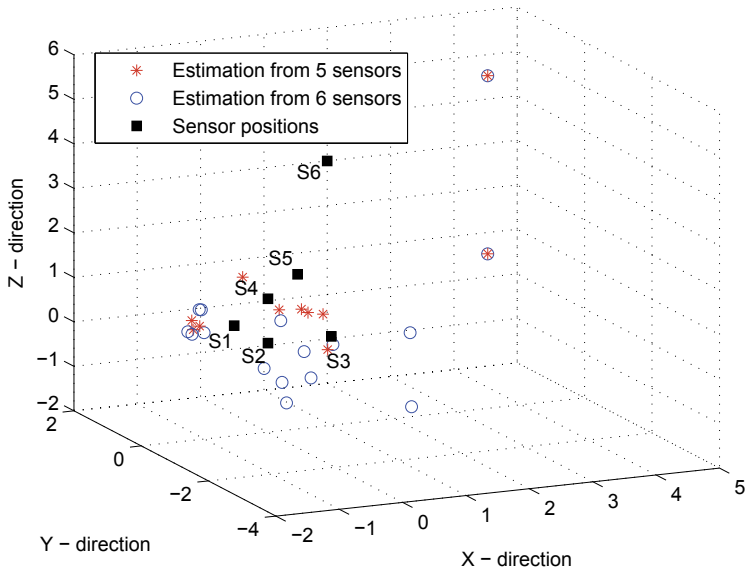

Figure 4.8: Estimation of emitters using ve and six sensors in R^3

For the simulations in R^3, six TDoA sensors were positioned at $(0;0;0)$, $(1;0;0)$, $(0;1;0)$, $(0;0;1)$, $(1;1;1)$ and $(2;2;3)$. Two emitters were located at $(4;1;1)$and $(4;1;5)$. First, from the measurements received at the sensors S_1,S_2,S_3,S_4 andS_5, target locations were estimated. Then the estimation was carried out using all the sensors (S_1, S_2, S_3, S_4, S_5 and S_6)(Figure 4.8). Finally, using our algorithm the real emitter locations were found(Figure 4.9).

The unique localization of two emitters require only six sensor measurements in R^3. It can be seen that the number of measurements does not go near the maximum bound (9 in R^3). The ghost problem will not necessarily disappear at these measurement as shown in the simulations. This is particularly true when the number of emitters is large and they are densely distributed in the eld.

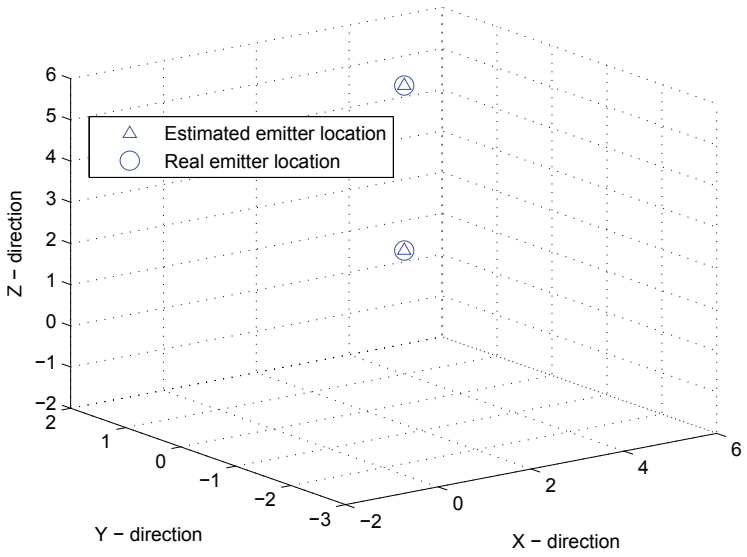

Figure 4.9: Final estimation of emitters in R^3

4.2 Time-of-Arrival systems

4.2.1 Localization of an emitter

Lets consider a radiating emitter T_j in R^3. In general, N number of sensors are employed to estimate the emitter position. The corresponding range between the s_i and the emitter can be written as $R_{ij} = ct_{ij}$ where c is the velocity of signal propagation. Let the spatial coordinate vectors be: $x_0 = [x_0\ y_0\ z_0]^T = [0\ 0\ 0]^T$, $x_i = [x_i\ y_i\ z_i]^T$ and $x = [x_s\ y_s\ z_s]^T$, where x_0 is the reference sensor position, x_i is the i^{th} sensor position and the unknown emitter position is x. The range between the i^{th} sensor and the emitter can be written as, $R_{is} = kx_i - xk$. The distance between the reference sensor and the emitter is $R_s = kxk$. Further expansion will yield $x_i^T x_j = \frac{1}{2}\ kx_i k^2 - R_{is}^2 + R_s^2$.

For a general case of N sensors, following matrices can be de ned:$z = \frac{1}{2}[kx_1k^2 - R_{1s}^2 : : kx_N k^2 - R_{1s}^2]^T$,$S = [X_1 : : X_N]^T$ and $d = [\frac{1}{2} : : \frac{1}{2}]^T$ where, $X_i = [x_i - x_0]^T$. In matrix notation $Sx = z + dR_s^2$. Solving for emitter position x, following preliminary position estimate can be obtained.

$$x = \left(S^T S\right)^{-1} S^T z + \left(S^T S\right)^{-1} S^T d R_s^2. \tag{4.2.1}$$

When not all range differences are measured to the same accuracy, a weighting matrix $R_{N\times N}$ is in order. Then the above (4.2.1) can be rewritten as

$$x = \left(S^T R^{-1} S\right)^{-1} S^T R^{-1} z + \left(S^T R^{-1} S\right)^{-1} S^T R^{-1} d R_s^2. \tag{4.2.2}$$

Defining the new vectors

$$a = \left(S^T R^{-1} S\right)^{-1} S^T R^{-1} z = [a_1\ a_2\ a_3]^T \tag{4.2.3}$$

and

$$b = \left(S^T R^{-1} S\right)^{-1} S^T R^{-1} d = [b_1\ b_2\ b_3]^T \tag{4.2.4}$$

(10) becomes

$$x = a + b R_s^2; \tag{4.2.5}$$

and the source position x is obtained as

$$x = \begin{bmatrix} x_s \\ y_s \\ z_s \end{bmatrix} = \begin{bmatrix} a_1 + b_1 R_s^2 \\ a_2 + b_2 R_s^2 \\ a_3 + b_3 R_s^2 \end{bmatrix}. \tag{4.2.6}$$

4.2.2 Data association in ToA measurements

Let us denote the following

p	number of emitters
N	number of time-of-arrival sensors
s_i	ith sensor
T_j	jth emitter
t_{ij}	time-of-arrival measurement at s_i from T_j

R_{ij} Range difference between s_i and T_j

In this section, we consider the general problem involving three or more sensors in two dimensions. The emitters are assumed to be synchronized to send signals at the same time. Each sensor s_i, $i \in \{0;1;\dots;N\}$ measures the time of signal arrival from each emitter T_j, $j \in \{1;\dots;p\}$

The measurements can be written in the matrix form,

$$M = \begin{bmatrix} t_{11} & \cdots & t_{N1} \\ \vdots & \vdots & \vdots \\ t_{1p} & \cdots & t_{Np} \end{bmatrix}; \tag{4.2.7}$$

where

$$t_{ij} = \frac{\|R_{ij}\|}{c}. \tag{4.2.8}$$

We assume that there are no measurement errors.

4.2.3 Ghost elimination

Definition 4.2.1. **Ghost**: A solution to (4.2.6) which is not overlapping with any real emitter.

Definition 4.2.2. **Measurement set**: Any combination of measurements selecting one element from each column of matrix M.

Assumption 3. Any combination of three sensors in the field are not collinear. This assures that the regressors matrix S is full rank for any combination.

Proposition 4.2.1. In R^3, if there are at least four sensor measurements from a single emitter (T_j) in a measurement set, this will lead to the solution of that particular emitter (T_j) or this set will lead to a ghost.

Proof. Lets consider a case where p number of emitters scattered over a R^3. N number of sensors are also placed over the same R^2.

Then a general vector for z can be written as,

$$z = \frac{1}{2}\begin{bmatrix} \|x_1\|^2 - R_{1j_1}^2 \\ \|x_2\|^2 - R_{2j_2}^2 \\ \vdots \\ \|x_k\|^2 - R_{kj_k}^2 \\ \vdots \\ \|x_N\|^2 - R_{Nj_N}^2 \end{bmatrix} \tag{4.2.9}$$

where $j_k \in (1; 2; \ldots; p)$.

Lets consider a combination in $S; z$ and d with subscripts $j_a = j_b = j_c = j_d$, and assume that all these refers to the T_j^{th} emitter. Now we select this subset and keeping $x_a = [x_a \; y_a \; z_a]^T$ as the reference sensor develop S^0 and z^0 matrices.

$$S^0 = \begin{bmatrix} x_b & y_b & z_b \\ x_c & y_c & z_c \\ x_d & y_d & z_d \end{bmatrix}; \tag{4.2.10}$$

and

$$z^0 = \frac{1}{2}\begin{bmatrix} \|x_b\|^2 - R_{bj_a}^2 \\ \|x_c\|^2 - R_{cj_a}^2 \\ \|x_d\|^2 - R_{dj_a}^2 \end{bmatrix}. \tag{4.2.11}$$

This subset will lead to the unique location estimation of the T_j^{th} emitter. So the initial z vector which contains this subset will yield the T_j^{th} emitter as the unique solution, if all the combinations are referring to the T_j^{th} emitter (subscripts $j_1 = j_2 = \ldots j_i = \ldots j_N$). If at least two subsets in a set lead to different solutions, the corresponding set will refer to a **ghost** or non-real solution, then the whole set can be discarded.

All the subsets in set will lead to the same solution if and only if all of them are referring to a single real emitter. □

Theorem 4.2.2. *Assume that the assumption 1 holds. If the number of emitters in R^q is p, the maximum number of sensors required for unique localization of all the emitters is $qp + 1$.*

Proof. When $N = qp + 1$ sensors are considered for any combination of sensor measurement set, there is at least one combination which contains $q + 1$ measurements from a single emitter. Using proposition 4.2.1, it can be shown that the measurement sets which have at least one measurement from a different emitter can be discarded. Hence, it can be concluded that $N = qp + 1$ number of non-collinear sensors will guarantee the elimination of all the ghosts.

□

Let k be the number of sensor positions that are collinear with each other. Since k collinear measurements provide no real additional information, they can be considered as null measurements. The maximum number of measurement positions,

ignoring the null measurements, required to uniquely localize an emitter field of p emitters is $qp + k + 1$.

4.2.4 Localization algorithm for ToA measurements

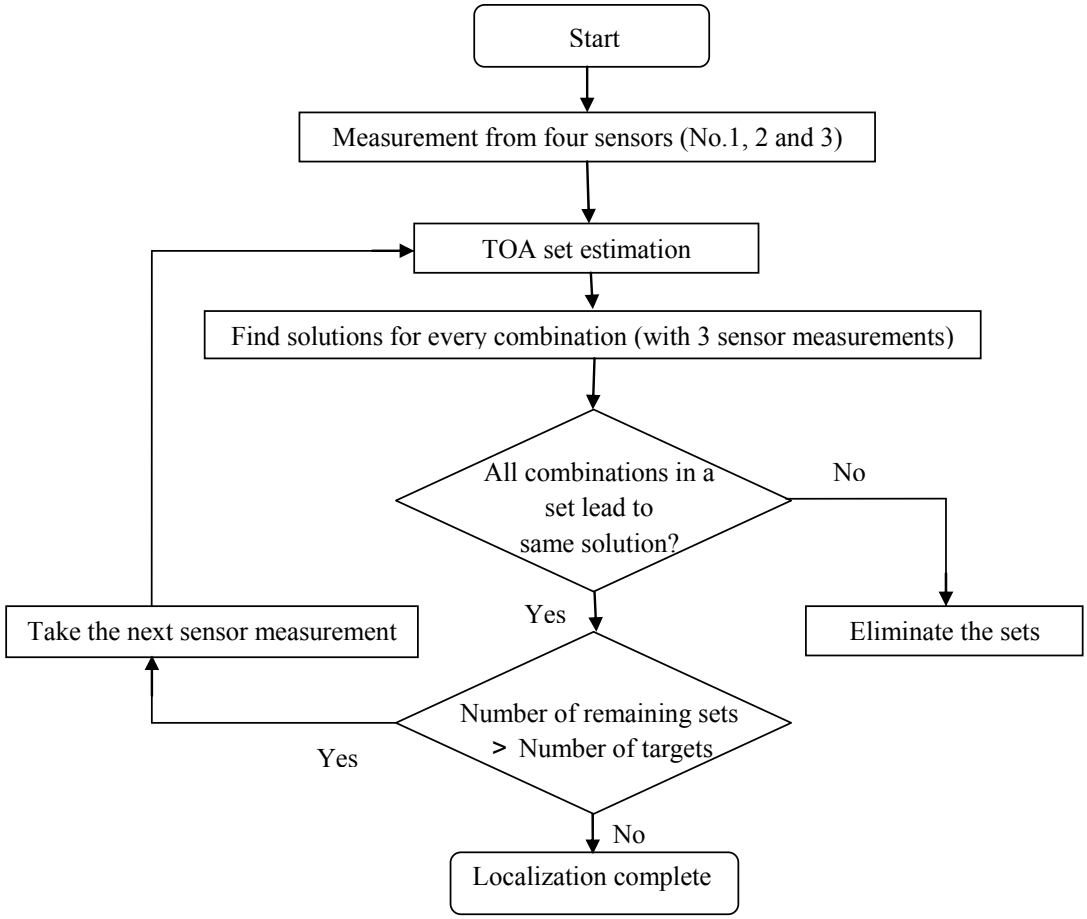

Figure 4.10: Algorithm flowchart for unique localization in ToA measurement technology

In uniquely estimating the position of every emitter in the field, ToA sensors must measure the time of arrival at spatially distinct locations and determine the position of each emitter. The algorithm stops when the number of remaining sets of measurements equals the number of target emitters in the field. It is assumed that the number of emitters is known or may be estimated using statistical methods. Also, if the number of remaining sets of measurements remains the same over

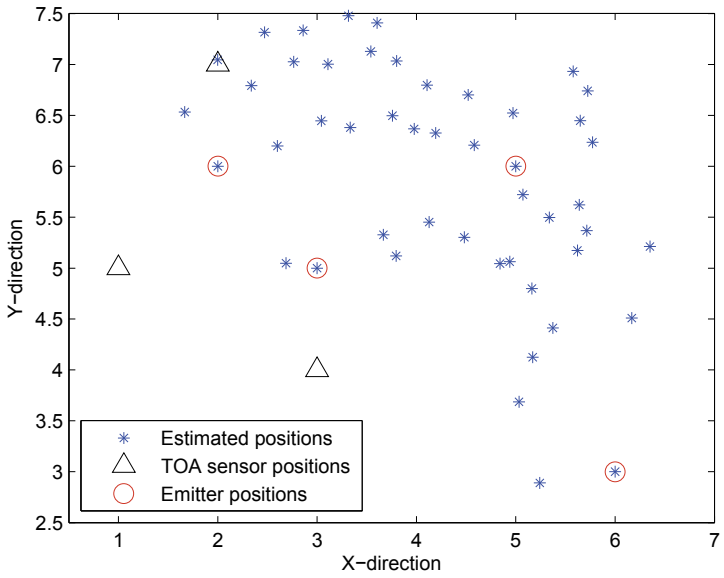

Figure 4.11: Estimation of emitter location for four emitters with three sensors

multiple measurements, then it can be inferred that the remaining sets correspond to the true emitter locations. In this case, it is assumed that the number of emitters are known. Also, this analysis has assumed perfect measurements (i.e noiseless).

The algorithm is brie y described in Figure 4.10.

To demonstrate the theoretical arguments proposed in this paper, a simulation was carried out with perfect measurements.

As shown in Figure 4.11, three ToA sensors were positioned at $(1;5)$,$(2;7)$ and $(3;4)$. Four emitters were located at $(3;5)$,$(5;6)$,$(6;3)$ and $(2;6)$. First, from the measurements received at the sensors, emitter locations were estimated. Then the fourth sensor is positioned at $(6;7)$ and the estimation was carried out using all the sensors. Finally, using our algorithm the real emitter locations were found(Figure 4.12).

In this simulation, unique localization of four emitters require only four sensor measurements in R^2 . It can be seen that the number of measurements does not go near the maximum bound (9 in R^2). The ghost problem will not necessarily disappear at these measurement as shown in the simulations. This is particularly

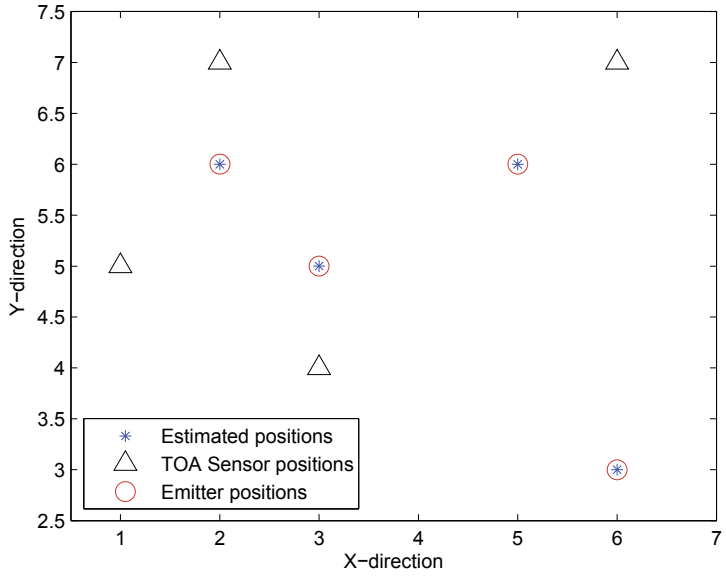

Figure 4.12: Final estimation of emitter locations for four emitters with four sensors true in a densely distributed eld, with large number of emitters to be localized.

4.3 Summary

A theoretical analysis has been provided in this chapter which is required for unique localization of an emitter using minimum number of TDoA measurements with bounded error. Error bounds have been found for both R^2 and R^3 after which, there is no existence of the unique solution region. More complex analysis can be carried out, specially in the geometry of the sensor positions for robust localizations based on this discussion.

Unique localization of multiple emitters using TDoA or ToA measurements is discussed in this chapter. Necessary fundamental requirements to solve the so-called ghost node problem associated with sensor arrays are speci cally examined. Importantly, a maximum bound on the required number of sensors to uniquely localize a given number of emitters in R^q was derived. The discussion provides the groundwork for further studies.

Chapter 5

Tracking with Doppler Radar

Localization and tracking of humans, vehicles or any other moving object is useful in many defense and commercial applications such as security surveillance, disaster search, rescue missions and urban warfare [3, 55, 56, 147, 149]. Until the recent pass, radar systems were primarily used for long range localization and tracking and those systems were very expensive and bulky in design. Due to the growth of the electronic engineering in recent decades, the cost and the physical size of Radio Frequency(RF) components have reduced dramatically. Therefore, many useful radar systems can now be realized with a reasonable cost and size; specially for indoor and commercial applications which were not prominent in the past. One of the close-range applications of radar known as Through-the-Wall Radar Imaging(TWRI) is a current research interest which has very useful applications in numerous situations [59{61, 150].

Among the other radar systems Continuous Wave (CW) radar systems have attracted signi cant attention due to its simplicity in design and implementation [151]. Single-frequency-Continuous-Wave (SFCW) radar can measure Doppler frequency shifts modulated from the moving targets to a higher accuracy. However, in target range measurements, relatively complex systems derived from CW radar

are currently being employed. These systems are expensive, and require sophisticated hardware systems for implementation. As an example, Frequency-Modulated-Continuous-Wave (FMCW) radar and pulsed Doppler radar both originated from the CW radar technique and they are capable of detecting range but poor in clutter mitigation. As opposed to those systems, CW radar is excellent in clutter suppression [3]; hence, it can be employed to localize moving targets as the Doppler shift in frequency provides a natural exclusion of clutter in the ltering [27].

Angle of arrival of a moving target can be measured using the phase di erence of waves arriving at two receiving antenna elements [3, 62]. In [55], tracking of moving targets is carried out by a two-frequency Doppler and AoA radar system where the velocity information of targets are unavailable. Even if the Doppler modulated signal is used in [56, 152] and [149], only the position information of the targets is obtained using the phase di erence of the Doppler shifted signal. In these studies, the distinctive frequencies are only utilized to identify the targets rather than using the Doppler shift to deduce their velocities. [66] [67] and [68] consider more complex pulsed radar system while correction of the received Doppler modulated signal under Gaussian assumptions is explored in [66]. Multi-target tracking through range and angle measurements are investigated in [67] and [68] providing comprehensive descriptions based on static optimization techniques.

The time derivatives of displacement is usually employed in systems which require velocity information of moving targets. This can potentially result in a time lag in velocity estimation. Specially, for more dynamic targets the accumulation of errors can be signi cant as the location estimation errors directly in uences the velocity estimations. As opposed to this method, the location and the velocity of the target can be estimated simultaneously by using CW radar with a dynamic system model for state estimation. Robustness to system uncertainties and measurement errors is another advantage of this particular approach. The Doppler frequency shift

due to the target motion is used in [69] to estimate the target velocity separately, providing a better estimate with additional measurements and the increased dimension of the measurement space. Further non-linearities are introduced in these type of measurement modeling. For the position measurement only case discussed in [3,55], converted measurement approach [70] has been employed to obtain a better linear formulation. Nevertheless, this has not been the case for Doppler radar and even in [69], the non-linear measurement equation is linearized with a first order approximation equivalent to Extended Kalman filtering in the estimation process. Specially in systems with large uncertainties, this type of linearizations are known for accumulation of errors and in some instances divergence can occur in the state estimation. Therefore, in this chapter a linear formulation for inherently non-linear Doppler measurements is used exploiting the strength in linear systems theory.

This study considers the case of tracking multiple mobile targets using the reflected Doppler modulated signals with two sets of receiver elements kept approximately half a wave length apart[1]. Notice that two element receiver combination is considered as a **sensor**. The sensors are positioned collinear to each other. The phase difference of the reflected waves within a single sensor can be used to measure the AoA of a target with respect to a particular set of elements. Once the AoAs are known triangulation can be used to find the target location while the target velocity can be deduced by measuring Doppler shifts due to the radial velocity component in the direction of the sensors . Hence, Doppler signal frequency and phase is **converted** into directional position and velocity **measurements** in order to be used in the linear form of a robust filter which provides estimates of the states (position,

[1]Please note that the material presented in this chapter was published as a journal paper : P.N. Pathirana , S.C.K. Herath, and A.V.Savkin , Multi-target tracking via space transformations using a single frequency continuous wave radar Accepted for publication in Transactions on Signal Processing in June 2012, and as a conference paper : S.C.K. Herath and P.N.Pathirana , Maximum likelihood approach for tracking multiple mobile agents with a moving Doppler radar system, in ISSNIP 2010 : Proceedings of the 6th International Conference on Intelligent Sensors, Sensor Networks and Information Processing, pp. 193-198, IEEE, United States

velocity and acceleration) of the targets recursively.

Maximum Likelihood approach for mobile target tracking with a moving sensor array

In the automobile industry, multiple mobile target tracking technology can be employed in a driver alerting systems to assist the driver with helpful information about the surrounding of the vehicle. Such improved safety functions are now being introduced to vehicles which reduce the risk of accidents.

Radar technology can be utilized in the context of sensing the surroundings in automobile safety applications [153{155]. In [154] use of ultra-wideband radar for short range vehicular applications is investigated while fusing the vision data with radar information to enhance the detection accuracy has been studied in [155]. [153] provides a novel Doppler sensor architecture for vehicular applications.

Technical organization

This chapter is organized as follows. First, the basic theory governing the Doppler radar based tracking is introduced in section 5.1. Two critical practical issues are discussed in section 5.2 - a formation of ghost targets due to Data association and a unique occurrence of missing information. These scenarios require special attention in multiple target tracking, since they can potentially lead to a large number of sensor elements in the linear receiver. A Theoretical justi cation is provided for the minimum number of sensor elements in the linear array to completely eliminate the issues mentioned above.

The solution to the above problems inevitably increases the number of sensor elements of the receiver array. As this is not desirable in most practical applications, minimum con guration array with two sensors is discussed when introducing our lter. Nearest neighbor type minimization is utilized to address the data association problem while solution to the missing information is provided by an extended version of the lter.

Doppler radar system with the linear sensor array and the dynamic modeling of the targets is presented in section 5.3. The Robust Linear Filter is introduced in section 5.4 as the main contribution of this chapter; for the minimal sensor array, the underlying non-linearly modeled measurements of Doppler radar(both angle and radial velocity) is addressed in a linear framework. The non-linear measurement model for the target is rst transformed into a linear separable form with bounded assumptions on the noise distribution. A model based estimation process is utilized to obtain the target states such as position, velocity and acceleration concurrently.

Computer simulations together with the hardware experimentation are provided in section 5.6 to prove the theoretical assertions outlined in this work.

Finally, in 5.7 of this chapter provides a method to track multiple mobile agents from an array of Doppler sensors mounted on a moving vehicle. Measurement technique used here is similar to the stationary case discussed earlier(frequency and corresponding phases of Doppler modulated signals from moving targets). The vehicle dynamics are taken into account and the maximum likelihood estimation is used to increase the accuracy in localization.

5.1 Basic theory

Figure 5.1 depicts two nearby scattered waves returning from a mobile target. The radial velocity of the target toward the sensor can be measured using equation 2.1.1. Due to the relative position of the agent, two antenna elements, Rx_1 and Rx_2 receive these two signals with a path di erence of y^0.

When d is the distance between the two antenna elements Rx_1 and Rx_2 , and ^{0} is the Angle-of-Arrival (A0A) of the mobile target,

$$y^0 = d \sin \; ^0. \tag{5.1.1}$$

Then the phase di erence of the two received waves , can be written as,

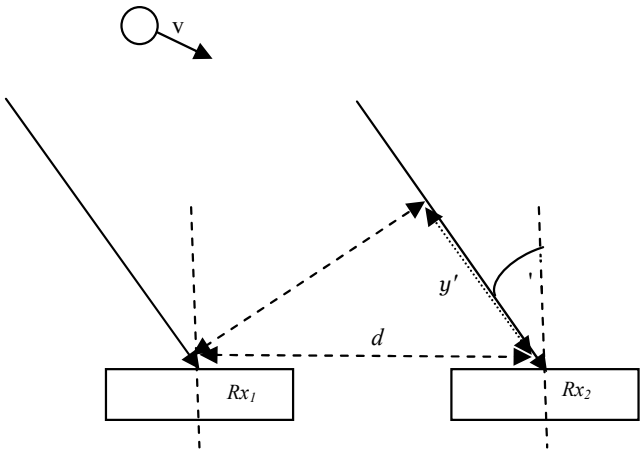

Figure 5.1: AoA using two receiving elements

$$= \frac{2\ y^{0}}{c} \tag{5.1.2}$$

where, $_c$ is the wave length of the carrier frequency. Then from (5.1.1) and (5.1.2), the AoA can be expressed as,

$$^{0} = \arcsin \frac{c}{2\ d} : \tag{5.1.3}$$

AoA of several mobile agents can be found by Doppler discrimination. As depicted in Figure 5.2, two mobile targets scatter Doppler modulated waves on four antenna elements. $x_1(t)$ and $x_2(t)$ are the receiving signals on antenna elements Rx_1 and Rx_2 after demodulation. Then,

$$x_1(t) = k_1 \sin(2\ f_{d1}t + \ _1) + k_2 \sin(2\ f_{d2}t + \ _2) \tag{5.1.4}$$

and,

$$x_2(t) = k_1 \sin(2\ f_{d1}t + \ _3) + k_2 \sin(2\ f_{d2}t + \ _4): \tag{5.1.5}$$

In (5.2.4) and (5.2.5), k_1 and k_2 are the amplitudes of the incoming waves and it can be assumed that they are constant for both waves due to a very small path di erence. f_{d1} and f_{d2} are the Doppler frequencies modulated by the two mobile

targets due to their relative velocity. $_1$, $_2$, $_3$ and $_4$ are the corresponding phases at the receiving elements.

Fast Fourier Transform (FFT) is performed on each of these signals. Hence, the frequency bins and the corresponding phases of each frequency bin is obtained. Phase di erence of a particular frequency bin $_1$, can be written as,

$$_1 = \ _1 \ \ _3: \tag{5.1.6}$$

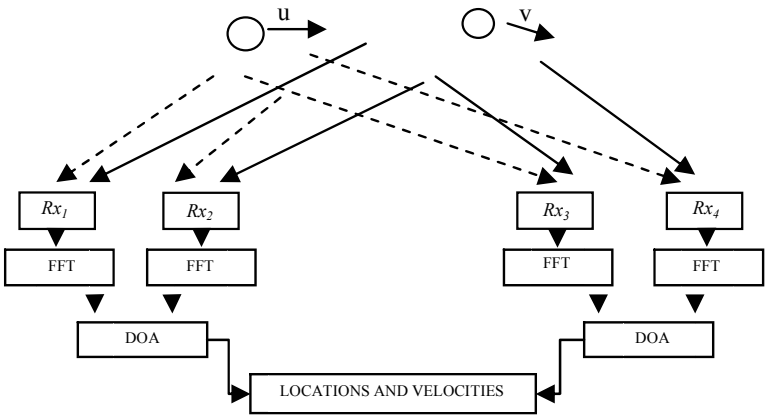

Figure 5.2: AoA using four receiving elements for multiple mobile agents

Then, the AoA of the mobile agent is,

$$^0_1 = \arcsin \ \frac{_1 \ c}{2 \ d} \ : \tag{5.1.7}$$

From this technique, AoA of multiple targets can be resolved, as long as they have considerable Doppler separation. AoA of any target i, can be expressed as,

$$^0_i = \arcsin \ \frac{_i \ c}{2 \ d} \ : \tag{5.1.8}$$

Let's consider two mobile targets having the same radial velocity toward a sensor, and for simplicity, assume that the distance to the target from the sensors is the same at a particular instance. Then, (8) can be rewritten as,

$$x_1(t) = k \sin(2 \ f_d t + \ _1) + k \sin(2 \ f_d t + \ _2):$$

$$x_1(t) = 2k \sin\ 2\ f_d t + \frac{_1 + \ _2}{2} \cos\ \frac{_1 \ \ _2}{2} :$$

$$x_1(t) = K\ \sin(2\ f_d t + \ ): \tag{5.1.9}$$

where,

$$K = 2k \cos\ \frac{_1 \ \ _2}{2}$$

and,

$$= \frac{_1 + \ _2}{2} :$$

It can be seen that the receiver is unable to distinguish between the two signals and it is perceived as a signal at the same frequency but in a phase, di erent to either phase of the two incoming signals preventing the AoA estimation using the phase of the incoming signals.

The optimal linear sensor separation in AoA measurement technique for improved localization of targets is discussed in Chapter 3 which can be integrated in this study. If the region in which the targets are moving is known, the results obtained in Chapter 3 can be utilized to position the sensors for better tracking accuracy. Also, if possible, the sensors can be dynamically adjusted for enhanced localization performance depending on the rough estimate of the target position.

5.2 Larger antenna array

Consider the situation where a single linear array of sensors are employed to track multiple targets. Here, a discussion is made on the two main issues that can adversely a ect tracking multiple targets with Doppler radar measurements.

1. Formation of ghost [156] targets: The problem of data association is created by the di erent Doppler shifts modulated by the targets on receiving elements. That is the problem of correctly assigning modulating frequency components and the associated phase di erences among sensors to the corresponding targets. Particularly when localization and tracking of relatively higher number

of targets with lesser number of sensors, the data association problem occurs on the incorrect assignments of **ghost** [156] targets to real targets and vice versa. Limited number of spatially dispersed sensors hinders the recovery of real target locations uniquely from the signals received at each sensor. In this case, the number of combinations of the received measurements exceeds the number of real targets and some of these combinations refers to non-existing targets. These virtual targets are denoted as **ghosts**. As shown in Figure 5.3 modulation of Doppler frequencies and corresponding bearing measurements in R^2 for the case of two mobile targets with two sensors in the linear array allows two **ghost** targets to exist.

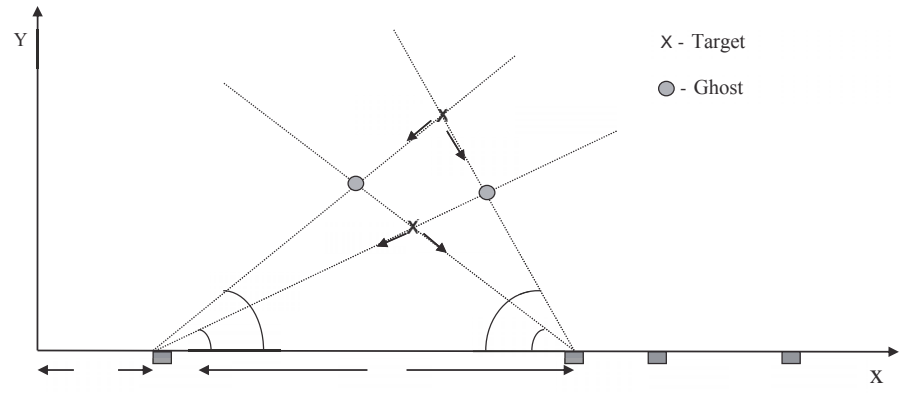

Figure 5.3: Angle of Arrival(AoA) and radial velocity measurements

2. Modulation of identical or indistinguishably close Doppler frequencies: Consider the two **Doppler bins** (collection of frequencies) at the two sensors depicted in Figure 5.4 modulated by four di erent mobile targets($A; B; C$ and D). Targets modulating frequencies $f_A^1; f_B^1; f_C^1$ and f_D^1 with the corresponding phases $\ ^1_A;\ ^1_B;\ ^1_C$ and $\ ^1_D$ in sensor 1, modulate frequencies $f_A^2; f_B^2; f_C^2$ and f_D^2 with corresponding phases $\ ^2_A;\ ^2_B;\ ^2_C$ and $\ ^2_D$ in sensor 2. The radial velocities of two or more distinct targets can potentially be very close to each other, hence, the respective Doppler frequencies from those targets modulate the same(or indistinguishably close) frequency in one sensor preventing the

resolution of the corresponding frequency and phase components as discussed in section 5.1. Then the sensor in concern perceived the two signals as a signal at the same frequency but in a phase di erent to either phase of the two incoming signals, so the AoA recovery using the phase of the incoming signals is not possible [19]. When this takes place, at least one Doppler bin contains number of frequencies which is less than N (number of targets). This can be considered as an *incomplete* information since the data from these sensors cannot be employed in the estimation process. As opposed to that, in *complete information* case, all the information is resolvable for all targets, i.e no overlapping of frequency in the Doppler bins during the entire tracking process. it should be emphasized that a fundamentally di erent case of *missing information* is considered here, compared to [157] where false alarm or clutter is characterized by a probabilistic distribution. Missing information case considered here is based on the target dynamics as this occurs when the same radial velocity from two or more distinct targets modulate the same Doppler frequency at the same sensor. The system detects this instance when the number of measurements is less than the number of targets and hence independent of any assertions based on probabilistic assumptions. Indeed the number of targets in the vicinity are assumed to be known in priori. This is the case with some practical indoor applications such as users connected to a wireless network or premises with monitored access etc. Evidently, if the number of targets is unknown, an upper bound for the number of targets can be used and as measurements are received on the sensors, the absent targets can be interpreted as *missing information* [158]. In this case, as the AoA measurements are not modeled with Doppler signals mathematically, an arbitrary values can be used for AoA measurements for the lter to work

properly. Subsequently, these estimations can be discarded as they are associated with missing information. Probabilistic assumptions such as false track discrimination procedures are employed in a more traditional target tracking context when the number of targets are unknown [159, 160]. These techniques are computationally taxing. The aggregation of data is eventually expected to ful ll the probabilistic assumptions, consequently enhancing the tracking process with an unknown number of targets.

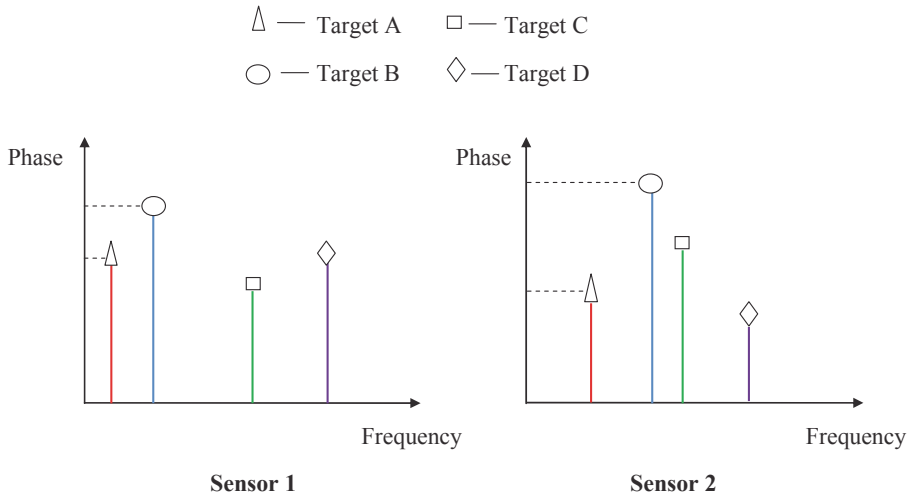

Figure 5.4: Instantaneous frequency and the phase distribution at the two sensors for four targets

Assumption 1. Following assumptions are made with respect to the target motion, in line with the de nition of the radar equation which uses the phase di erence of arriving signals:

1. Motion of the mobile targets are con ned to the positive Y half of the X Y plane.
2. At any given time targets are not collinear with the sensor array positioned along the positive X axis.

The proposition given below sates that two distinct targets can potentially modulate identical Doppler frequencies on maximum number of three sensors. Consider a set z of mobile targets moving only in the positive Y half of the X Y plane and a linear phase array with a set of distinct sensors positioned along the positive X

axis. Initially, consider two targets $A; B \in z$ with each modulating Doppler shifted frequencies $f_A^1; f_A^2; \quad f_A^{\langle i \rangle}$ and $f_B^1; f_B^2 \quad f_B^{\langle i \rangle}$ respectively due to their radial velocities and de ne, $_A = f_A^1 \quad f_A^{\langle i \rangle}$ and $_B = f_B^1 \quad f_B^{\langle i \rangle}$, where $\langle i \rangle$ denotes the cardinality of a set and $>$ the transposition.

Proposition 1. $\mathrm{Rank}[\mathrm{Diag}[\ _A \quad _B]] \quad \langle i \rangle \quad 3$

Proof. Here, **reductio ad absurdum** argumentation is utilized as an indirect proof to assert that if two mobile targets modulate the identical Doppler frequency in four distinct linear sensors, then the two targets are essentially the same - identical in position and velocity. Consider a linear array of four sensors S_i with $i \in \{1; 2; 3; 4\}$ with the i^{th} sensor at $d_i = (d_i; 0)$. T_1 and T_2 are two mobile targets with their locations $p; q \in R^2$ (in the positive Y half of the $X \quad Y$ plane) and the velocities $u; v \in R^2$ respectively. Hence, their respective radial velocities at the i^{th} sensor: v_1^i and v_2^i, are given by:

$$v_1^i = \frac{u^{>}(d_i \quad p)}{\|d_i \quad p\|}; \quad v_2^i = \frac{v^{>}(d_i \quad q)}{\|d_i \quad q\|} \quad i \in \{1; 2; 3; 4\}$$

respectively. Assume that these two mobile targets have identical radial velocities on each of the sensors corresponding to $i = 1; 2; 3; 4$. Then,

$$\frac{u^{>}(d_i \quad p)}{\|d_i \quad p\|} = \frac{v^{>}(d_i \quad q)}{\|d_i \quad q\|} \quad i \in \{1; 2; 3; 4\}: \tag{5.2.1}$$

In a situation where the target and the sensor array are collinear, the sensors receive the same radial velocity irrespective of the number of senors and with assumption 1, we avoid this occurrence. Let $r_{ijk} = v^{>}(d_i \quad q)(d_j \quad d_k)$, then the following system of constraints can be derived for the **cyclic** groups $S_1 = (1; 2; 3)$ and $S_2 = (1; 2; 4)$ respectively :

$$\sum_{\{i;j;k\} \in S_1} {}_i(d_j \quad d_k) = 0; \tag{5.2.2}$$

$$\sum_{\{i;j;k\} \in S_2} {}_i(d_j \quad d_k) = 0; \tag{5.2.3}$$

where, $_i = \frac{u^{>}(d_i \quad p)(\|d_i \quad q\|)}{\|d_i \quad p\|}$: Note that $\sum_{\{i;j;k\} \in S_1} r_{ijk} = 0$ and $\sum_{\{i;j;k\} \in S_2} r_{ijk} = 0$ are used in deducing the above constraints 5.2.2 and 5.2.3. Then taking $x_i = \frac{\|d_i \quad q\|}{\|d_i \quad p\|}$ and $q_{jk} = u^{>}(d_i \quad p)(d_j \quad d_k)$ for $\{i; j; k\} \in S_1 \quad S_2$ and noticing that

$$\sum_{\{i;j;k\} \in S_1} q_{jk} = \quad 0;$$

$$\sum_{\{i;j;k\} \in S_2} q_{jk} = \quad 0;$$

equation 5.2.2 and 5.2.3 can be written as

$$\sum_{\{i,j,k\} \in S_1} q_{jk} x_i = 0; \tag{5.2.4}$$

$$\sum_{\{i,j,k\} \in S_2} q_{jk} x_i = 0: \tag{5.2.5}$$

This result can be interpreted such that for an arbitrary constant p, all the possible variations of q. Two trajectories in two planes are given by above 5.2.4 and 5.2.5. x_is are independent variables of the planes. Since any two non parallel planes intersect in a straight line and as all the common points on the line $x_i = x_j \; 8i; j \in \{1; 2; 3; 4\}; i \neq j$ are on both planes, it can be inferred that the two planes intersect on this particular line. But taking in to account the de nition of x_i, only $x_i = 1; 8i \in \{1; 2; 3; 4\}$ point is valid(see Appendix I). This infers p = q and hence u = v. From equation 5.2.2 and 5.2.3 it can be shown that this holds only for four sensors and for one cyclic group there exists in nitely many solutions for q. □

Proposition 2. *The necessary and su cient condition for tracking z mobile targets using a linear array of sensors avoiding incomplete information and ghost elimination is* $hLi \quad 3^{\langle z \rangle} C_2 + \langle z \rangle + 1$.

Proof. Proposition 1 and the ghost elimination results given in [156] are used for the proof.

Typically, $\langle z \rangle$ number of frequencies are contained in each *Doppler bin* associated with the respective sensor. Using the rst proposition, considering the worst case scenario, a maximum of $3^{\langle z \rangle} C_2$ number of sensors should be discarded in order to guarantee that no remaining sensor receives the identical frequency due to two distinct targets. Moreover $\langle z \rangle + 1$ sensors are required to eliminate the ghost targets [156]. Therefore, the ghost formation problem is solved with $3^{\langle z \rangle} C_2 + \langle z \rangle + 1$ number of sensors in the linear array. This will ensure that there is no ambiguity in any of the mobile target localizations. □

Note that a comprehensive analysis on the similar type of *ghost elimination* for Time-Delay-of-Arrival (TDoA) and Time-of-Arrival (ToA) systems is provided in Chapter 4. Data association problem is solved using an exhaustion method in [156] similar to the approach provided in Chapter 4.

For numerous real world applications, enormous increase in the number of sensors and hence the physical size of the linear array for tracking multiple mobile targets posses practical limitations(146 sensors are required to track 10 targets and 591 to track 20 targets). The enlargement of the array is not desirable in close

range or indoor applications. On the other hand, aforementioned problems of *incomplete* information and *ghosting* will be prominent if the number of sensors are reduced. Therefore, in this chapter, a minimal array con guration of two sensors is considered for a multiple target tracking scenario addressing these underlying problems.

5.3 Targets and the receiver dynamic model

State space formulation can be used to depict a dynamic system with multiple mobile targets and two sensor receiver array. The dynamic system equation is linear in a Cartesian coordinate system for the kinematic modeling of targets and a sensor(linear array) [161]. Generally, the measurement models are non-linear in the state space formulations [54]. In this type of modeling, target kinematics are taken in to consideration but the mechanical dynamics are not accounted for each platform.i.e modeling parameters are not used to de ne rotational motion of either the targets or the receiver unlike in [162]. In [163], a data augmentation algorithm targeting at such target parameter estimation incorporating an interacting multiple model for kinematic state estimation is introduced for simultaneous implementation. A elaborate study of dual body kinematic modeling is given in [161] and a basic principal approach is proposed in [164] where they only consider the translational kinematics.

In this study, we consider a point target (or N number of feature points) that obey a linear dynamic model such as those studied in [54]. In this model, arbitrary number of point targets can be included and since each point is tracked independently,object rigidity is not required. However, the ghost formation problem (also known as the feature point association problem) [161] exists in practical applications for tracking multiple point targets which is described in section 5.5. Considering only the translational e ects is su cient for the case of radar based tracking with

a stationary receiver which employs a linear dynamic model.

Let $N = hz\,i$ and with respect to the phase array based coordinate system, the location, velocity and acceleration components in each $X;Y$ direction of the i^{th} target in each of the traditionally denoted $X;Y$ directions be $[x_1^i\ x_2^i]^{>} 2 R^2$,$[x_3^i\ x_4^i]^{>} 2 R^2$ and $[x_5^i; x_6^i]^{>} 2 R^2$ respectively.

Then we can de ne the state $x^i = [x_1^i\ x_2^i\ x_3^i\ x_4^i\ x_5^i\ x_6^i]^{>} 2 R^6$ and $x = [x^{1>} \quad x^{N>}]^{>} 2 R^{6N}$ such that it evolves according to

$$x(k) = Ax(k \quad 1) + Bw(k): \tag{5.3.1}$$

Here $k = 0;1;2;:::$, where A and B are suitably de ned system and noise transition matrices [161] respectively, which can be given as,

$$\begin{aligned} A &= \text{Diag}[\quad\quad]; \\ B &= \text{Diag}[\quad\quad]; \\ &= \begin{bmatrix} I_2 & k_s I_2 & \frac{k_s^2}{2} I_2 \\ O_2 & I_2 & k_s I_2 \\ O_2 & O_2 & I_2 \end{bmatrix}; \quad = \begin{bmatrix} \frac{k_s^2}{2} I_2 \\ k_s I_2 \\ I_2 \end{bmatrix}: \end{aligned} \tag{5.3.2}$$

Here, uncertain target maneuvers and additive system uncertainties are modeled by $w(k)\ 2\ R^{2N}$ while k_s denotes the sampling time. I_2 and O_2 indicate $2 \quad 2$ dimensional Identity and zero matrices respectively. Any a priori knowledge of target maneuvers is not assumed in this study and these are considered as system uncertainties while the full target state is estimated online. The derivation of estimation algorithm is quite general and it allows a large class of linear dynamic models to be included.

Remark 1. The coordinate basis is found rst by positioning sensor 1 at the origin, and sensor 2 a distance $d > 0$ apart from sensor 1(Figure 5.3)on the positive X axis. These two sensors de ne a horizontal axis from which the angle subtended by the target is measured for the AoA.

5.4 Linear robust filtering with nonlinear Doppler radar

The frequency and phase measurements of the Doppler signals that reflected back from the mobile targets are used to find the radial velocities and angle measurements in the underlying approach. While the frequency offset from the carrier frequency is directly proportional to the target radial velocity toward the sensor, the phase difference between the two elements in the sensor is used to find the AoA.

Consider the i^{th} target which modulates two frequencies f_1^d and f_2^d on each of the two sensors which correspond to radial velocities and AoA values given by $\hat{v}_1^i; \hat{v}_2^i$ and $\hat{\ }_1^i; \hat{\ }_2^i$ respectively. Next, the measurement model for the i^{th} target is outlined and the corresponding measurement conversion technique along with the robust linear filter which we derive as the state estimator are presented.

The corresponding measurement noise are given by $_i$ and $_i$ for $i = 1; 2$ and \ ^ " denotes the noisy measured variables. Then, considering the measurement for the i^{th} target,

$$\hat{y}^i(k) = \begin{bmatrix} \hat{v}_1^i(k) \\ \hat{v}_2^i(k) \\ \hat{\ }_1^i \\ \hat{\ }_2^i \end{bmatrix} = \begin{bmatrix} \sqrt{\frac{x_3^i x_1^i \ x_2^i x_4^i}{(x_1^i)^2 + (x_2^i)^2}} + {}_1 \\ \sqrt{\frac{x_3^i (d \ x_1^i) \ x_2^i x_4^i}{(d \ x_1^i)^2 + (x_2^i)^2}} + {}_2 \\ \arcsin \left(\frac{x_2^i}{\sqrt{(x_1^i)^2 + (x_2^i)^2}} \right) + {}_1 \\ \arcsin \left(\frac{x_2^i}{\sqrt{(d \ x_1^i)^2 + (x_2^i)^2}} \right) + {}_2 \end{bmatrix}; \tag{5.4.1}$$

with, $\hat{y} = \hat{y}^1 \quad \hat{y}^N >$ providing the true measurements for all N targets. Following converted measurement form can be used to write the noisy locations $(\hat{x}_1^i; \hat{x}_2^i)$ of $(x_1^i; x_2^i)$ and the noisy directional velocities $(\hat{x}_3^i; \hat{x}_4^i)$ of $(x_3^i; x_4^i)$:

$$\begin{bmatrix} \hat{x}_1^i \\ \hat{x}_2^i \\ \hat{x}_3^i \\ \hat{x}_4^i \end{bmatrix} = \begin{bmatrix} \frac{d\sin(\alpha_2^i+\beta_2)\cos(\alpha_1^i+\beta_1)}{\sin(\alpha_1^i-\alpha_2^i+\beta_1-\beta_2)} \\ \frac{d\sin(\alpha_1^i+\beta_1)\sin(\alpha_2^i+\beta_2)}{\sin(\alpha_1^i-\alpha_2^i+\beta_1-\beta_2)} \\ \frac{(v_1^i+\gamma_1)\sin(\alpha_2^i+\beta_2)+(v_2^i+\gamma_2)\sin(\alpha_1^i+\beta_1)}{\sin(\alpha_1^i-\alpha_2^i+\beta_1-\beta_2)} \\ \frac{(v_1^i+\gamma_1)\cos(\alpha_2^i+\beta_2)+(v_2^i+\gamma_2)\cos(\alpha_1^i+\beta_1)}{\sin(\alpha_1^i-\alpha_2^i+\beta_1-\beta_2)} \end{bmatrix}: \tag{5.4.2}$$

Here, as d is a known constant(distance between the sensors), we remove the bias such that $\hat{x}_1 = x_1(\text{noisy}) - d$ which will be added subsequent to the estimation process. Bounded errors assumed for the angle and velocity measurement . i.e $|\alpha_i| \le |\beta|$ for $i = 1;2$ and $|\gamma_j| \le |v_j^i|$ for $j = 1;2$ where $\beta \in [0;2\pi]$ and $0 < \rho < 1$ are given constants and $|\ |$ indicates absolute value operator. The fractional noise upper-bound is indicated by ρ. Then,

$$m^i, \begin{bmatrix} \hat{x}_1^i \\ \hat{x}_2^i \\ \hat{x}_3^i \\ \hat{x}_4^i \end{bmatrix} = \begin{bmatrix} d\frac{\omega_1\omega_2\sin(\alpha_2^i)\cos(\alpha_1^i)}{\omega_3\sin(\alpha_1^i-\alpha_2^i)} \\ d\frac{\omega_1\omega_2\sin(\alpha_1^i)\sin(\alpha_2^i)}{\omega_3\sin(\alpha_1^i-\alpha_2^i)} \\ \frac{(v_1^i+\gamma_1)\omega_2\sin(\alpha_1^i)+(v_2^i+\gamma_2)\omega_1\sin(\alpha_1^i)}{\omega_3\sin(\alpha_1^i-\alpha_2^i)} \\ \frac{(v_1^i+\gamma_1)\omega_2\cos(\alpha_1^i)+(v_2^i+\gamma_2)\omega_1\cos(\alpha_1^i)}{\omega_3\sin(\alpha_1^i-\alpha_2^i)} \end{bmatrix}; \tag{5.4.3}$$

with the following condition

$$\cos\omega_i \le \frac{1}{\cos\rho} = \begin{cases} 1 & i = 1;2 \\ 2 & i = 3 \end{cases} \tag{5.4.4}$$

is satis ed.

Remark 2. As the error variations are identical for both sin and cos terms, the same variable i.e ω_i is used for the representation (See the Appendix II).

For the case of N targets, taking $m = [m^1 \quad m^N]^\top \in R^{4N}$, a well-defined system of converted measurement equations comprising noise input processes is considered. Now assume that the target motion is given by (5.3.1) where the matrix A is non-singular. Let $0 < p_0 \quad 1$ be a given constant and the following assumptions are satisfied by the system initial condition $x(0)$, noise $w(k)$ and the actual measurement noise $_i$ and $_i$ $8i \in f1;2g$.

Assumption 2. The following inequalities with probability p_0 simultaneously hold:

$$j_i j \quad j j; \quad j_i j \quad jv_i^j j \; 8i \in f1;2g; j \in [1; \quad ;N] \tag{5.4.5}$$

$$(x(0) \quad x_0)^\top N(x(0) \quad x_0) + \sum_0^{1} w(k)^\top Q(k)w(k) \quad : \tag{5.4.6}$$

Here a given initial state estimate vector is denoted by x_0. $N = N^\top$ and $Q = Q^\top$ are given positive definite weighting matrices while > 0 is a given constant associated with the system. $T > 0$ denotes a given time.

The following Riccati difference equation [1, 165] is involved in underlying solution to the state estimation problem,

$$\begin{aligned} F(k+1) &= \hat{B}\left[\hat{B}^\top S(k)\hat{B} + Q\right]^{1}\hat{B}^\top S(k)\hat{A}; \\ S(k+1) &= \hat{A}^\top S(k)\left[\hat{A} \quad F(k+1)\right] + C^\top U(k+1)C \quad K^\top K; \\ S(0) &= N: \end{aligned} \tag{5.4.7}$$

where $\hat{A} \triangleq A^{-1}$ and $\hat{B} \triangleq A^{-1}B$. We also define

$$C \triangleq \begin{bmatrix} _1 & 0 & 0 & 0 & 0 & 0 \\ 0 & _2 & 0 & 0 & 0 & 0 \\ 0 & 0 & _3 & 0 & 0 & 0 \\ 0 & 0 & 0 & _4 & 0 & 0 \end{bmatrix}; \tag{5.4.8}$$

$$K \triangleq \begin{bmatrix} _1 & 0 & 0 & 0 & 0 & 0 \\ 0 & _2 & 0 & 0 & 0 & 0 \\ 0 & 0 & _3 & 0 & 0 & 0 \\ 0 & 0 & 0 & _4 & 0 & 0 \end{bmatrix}; \tag{5.4.9}$$

where,

$$\alpha_1 = \alpha_2 = \frac{\cos 2\theta\ (1+\cos^4\theta)}{2\cos^2\theta}; \quad \alpha_3 = \alpha_4 = \frac{(1+\cos^2\theta)}{2\cos 2\theta\ \cos\theta} + \frac{(1-\cos^2\theta)\cos\theta\ \cos 2\theta}{2};$$
$$\beta_1 = \beta_2 = \frac{\cos 2\theta\ (1-\cos^4\theta)}{2\cos^2\theta}; \quad \beta_3 = \beta_4 = \frac{(1+\cos^2\theta)}{2\cos 2\theta\ \cos\theta} - \frac{(1-\cos^2\theta)\cos\theta\ \cos 2\theta}{2}:$$

A set of state equations are considered as follows,

$$\begin{aligned}
\hat{x}(k+1) &= \left[\hat{A} - F(k+1)\right]\hat{x}(k) + C^{\top}V(k+1)m(k+1);\\
\hat{x}(0) &= Nx_0;\\
g(k+1) &= g(k) + m(k+1)^{\top}W(k+1)m(k+1)\\
&\quad \hat{x}(k)^{\top}\hat{B}\left[\hat{B}^{\top}S(k)\hat{B} + Q(k)^{-1}\right]\hat{B}^{\top}\hat{x}(k);\\
g(0) &= x_0^{\top}Nx_0:
\end{aligned} \tag{5.4.10}$$

Remark 3. Notice that the appropriately defined matrices U, V, W are utilized to account for the incomplete information case discussed in section 5.5.2. For the complete information case, the matrices are evaluated to identity matrices.

The state equation (5.4.10) and Riccati equation (5.4.7) can be regarded as a robust implementation of the standard linear Kalman Filter [166] for uncertainties which obey Assumption 2, e.g. see [51,165,166]. Now the main result of this section can be introduced.

Theorem 1. Let $0 < p_0 < 1$ be given, and suppose that Assumption 2 holds. Then the state x_T of the system (5.3.1) with probability $p > p_0$ belongs to the ellipsoid

$$E_T = \left\{ x_T \in R^{6N} : \left[\|S(T)^{\frac{1}{2}}x_T - S(T)^{-\frac{1}{2}}\rho(T)\|^2 - \rho^2\right]_+ \le \gamma \right\} \tag{5.4.11}$$

where

$$\rho = \rho(T)^{\top}S(T)^{-1}\rho(T) - g(T)$$

and the equations (5.4.10) define $\rho(T)$ and $g(T)$. Also, we require $\rho + \gamma > 0$.

Proof. It follows from (5.4.3) and (5.4.5) that,

$$\tilde{x}_i(k) = \alpha_i x_i(k) + n_i(k); \tag{5.4.12}$$

$\forall i \in \{1,\dots,4\}$ and $x_i(k)$ is the i^{th} component of the state vector $x(k)$ of the system (5.3.1) and the inequalities,

$$|n_i(k)| \le \sim_i |x_i(k)|; \tag{5.4.13}$$

hold together with (5.4.6) to a probability $p \quad p_0$. Hence, (5.4.13) suggest that

$$m(k) = Cx(k) + n(k); \tag{5.4.14}$$

where $n(k) \, , \, [n_1(k) \; n_2(k) \; n_3(k) \; n_4(k)]^{>}$ and the condition

$$kn(k)k^2 \quad k \, K_x k^2; \tag{5.4.15}$$

holds together with (5.4.6) to a probability $p \quad p_0$, where $k \; k$ indicates the vector norm. From (5.4.6) and (5.4.15) we obtain the following sum quadratic constraint that should be satis ed,

$$\begin{aligned} P \; & (x(0) \quad x_0)^{>} N(x(0) \quad x_0) + \\ & \sum_{0}^{T \; 1} w(k)^{>} Q(k) w(k) + kn(k+1)k^2 \\ & + \sum_{0}^{T \; 1} kK_x k^2; \end{aligned} \tag{5.4.16}$$

with probability $p \quad p_0$. Now it follows from Theorem 5.3.1 of [51], p. 75 (see also [165]) that the state $x(T)$ of the system (5.3.1), (5.4.14) belongs to the ellipsoid (5.4.11) with probability $p \quad p_0$. □

The centroid of the bounded ellipsoidal set which is given by $k = S(k)^{\; 1} \; (k)$ can be used to nd a point value state estimate. By diagonalizing matrices$(\; ; \;)$ as follows, the worst error in the estimates can be obtained:

$$\begin{aligned} k &= \quad ^{1} \quad ^{1} \quad ^{1} + p\frac{1}{+} \; S(k)^{\frac{1}{2}} \; (k) \; ; \\ S(k)^{\frac{1}{2}} &= \quad ^{1} \; ; \quad ^{1>} \quad ^{1} = \quad ^{>} \quad : \end{aligned} \tag{5.4.17}$$

Here, $= [0 \quad \sqrt{a_j} \quad 0]^{>} \; 2 \; R^N$ with $a_j = \max_{k=1}^{N} a_k$, where a_j is the spectral radius of ^{1}. and denote diagonal matrices of appropriate dimensions. The centroid (k, the state estimate) and the end points of the major axis(k) of the ellipsoid can be illustrated as in gure 5.5 for each iteration together with the corresponding uncertainty ellipse that provides the actual bounds of the uncertainty.

Therefore it can be proved that when the relevant uncertainties obey Assumption 1, the estimation errors are bounded in a probabilistic sense. A large class of non-linear and dynamic process noise characteristics can be accommodated in the sum quadratic constraint given in Assumption 1. As the Gaussian noise is bounded

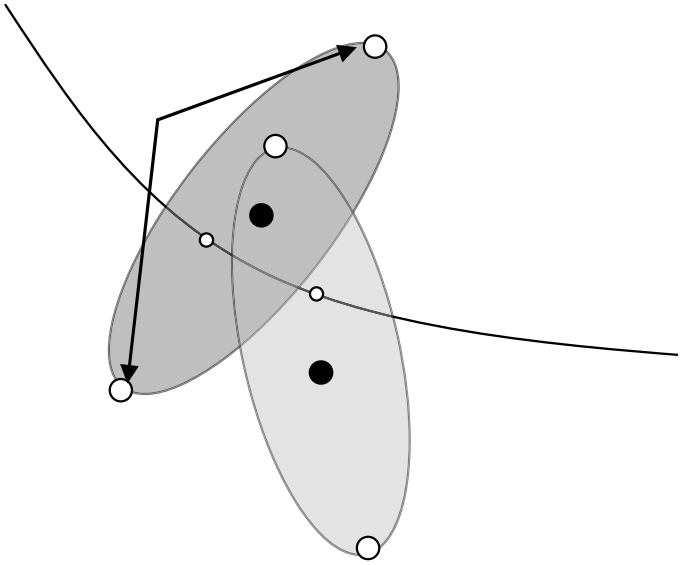

Figure 5.5: Uncertainty ellipse in RLF estimation

within the rst standard deviation to a probability of p_0 0:68 and within two standard deviations to a probability of p_0 0:95 etc, no generality is lost by considering uncertainties satisfying Assumption 2. That is, initial condition errors and Gaussian measurement process form a special case of Assumption 1 which belongs to a larger class of uncertainties. in this study, the Doppler radar problem is solved in the linear domain and the algorithm used permits very large potential initial errors. No such proofs available for the extended Kalman lter (EKF) or the majority of other approaches that utilizes some form of Taylor-series based approximations. The novel contribution in this study is that the fact that we can prove bounded tracking performance for Doppler radar based tracking with arbitrarily large initial condition errors.

5.5 Linear array with two Sensors

The number of sensors in the array a ects the physical size of the antenna which plays a crucial role in improving the practicality of the underlying approach, specially in close range applications. Data association problem occurs when the number

of sensors to obtain the minimum physical dimensions. Figure 5.6 depicts the AoA and radial velocity measurement scheme in a minimum physical dimension sensor array.

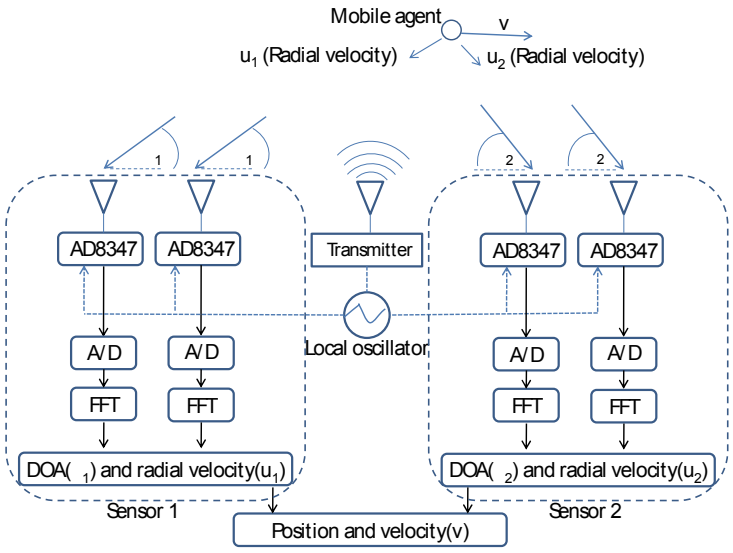

Figure 5.6: AoA and radial velocity measurement scheme in a Sensor array

5.5.1 Data association with complete information

In this complete information case an assumption is made that each sensor receives all the (N) measurements distinctively. During the entire tracking time the frequencies are easier to distinguish at each sensor as they are not very close to each other.

Doppler frequency at the receiver is directly related to the radial velocities and the corresponding AoA measurements of the targets. Let radial velocity and corresponding AoA measurement at sensor 1 and 2 be $L_1 = f(\hat{v}_1^1; \hat{\ }_1^1); \quad ;(\hat{v}_1^N; \hat{\ }_1^N)g$ and $L_2 = f(\hat{v}_2^1; \hat{\ }_2^1); \quad ;(\hat{v}_2^N; \hat{\ }_2^N)g$ respectively. Then the assignments should be made on each $(\ _1^i; \ _3^i) \ 2 \ L_1$ to $(\ _2^i; \ _4^i) \ 2 \ L_2$ so that these measurements correspond to the same target - data association problem.

Lets de ne the set $S = f \ = [\ _1^1 \ _2^1 \ _3^1 \ _4^1; \quad ; \ _1^i \ _2^i \ _3^i \ _4^i; \quad ; \ _1^N \ _2^N \ _3^N \ _4^N]^> :$ $(\ _1^i; \ _3^i) \ 2 \ L_1$ and $(\ _2^i; \ _4^i) \ 2 \ L_2; f \ _1^i \ _2^i \ _3^i \ _4^i g \ 6 = f \ _1^j \ _2^j \ _3^j \ _4^j g \ 8 i; j \ 2 [1; \quad ; N] g.$

Notice that the cardinality, $jSj = N!$. The actual physical distribution of the targets is given only by a one combination or only one element of S. The other combinations regarded as **ghosts**.

For $= [\ ^1_1\ ^1_2\ ^1_3\ ^1_4;\ \ldots;\ ^i_1\ ^i_2\ ^i_3\ ^i_4;\ \ldots;\ ^N_1\ ^N_2\ ^N_3\ ^N_4]^> 2 S$ and let $[Y^i_1\ Y^i_2\ Y^i_3\ Y^i_4]^> = f(\ ^i_1;\ ^i_2;\ ^i_3;\ ^i_4)$. Measurement conversion shown in equation 5.4.2 denoted as f.

Therefore $\$ Y = [Y^1_1\ Y^1_2\ Y^1_3\ Y^1_4 \quad Y^i_1\ Y^i_2\ Y^i_3\ Y^i_4 \quad Y^N_1\ Y^N_2\ Y^N_3\ Y^N_4]^>$ is a one-to-one mapping. Let

$$E^i = \begin{bmatrix} Y^i_1(k) \\ Y^i_2(k) \end{bmatrix} \begin{bmatrix} Y^i_1(k \quad 1) + k_s Y^i_3 \\ Y^i_2(k \quad 1) + k_s Y^i_4 \end{bmatrix}; \tag{5.5.1}$$

and then,

$$: \min_{2S} \sum_{i=1}^{N} kE^i k; \tag{5.5.2}$$

should correspond to the combination of the real target locations and hence eliminate all the **ghost** targets. That is; for the real targets, the two consecutive state estimates(converted measurements) are closer than the **ghost** targets. **ghost** targets do not behave according to the estimated measurements and dynamics considered; only the real targets.

In practical applications, maintaining the same order of measurements in the ltering process is crucial. This is illustrated graphically as given in gure 5.4. When the Doppler frequencies are not very close to each other, and maintained in that form, the ordering(of Y) is maintained and does not pose any complexities in the ltering process. If the modulated frequencies overlap, then the scenario described as **incomplete information** occurs (at least for a small duration) as the radial velocities of the targets and the corresponding angles are not resolvable at these particular instances. Obviously, the problem becomes challenging when the modulated frequencies cross each other due to the dynamics of the targets and

prevent keeping the order of the states corresponding to the relevant targets in the filtering process; but, the above minimization addresses this directly.

These searches are of $O(N)$ and for this particular 2D case, the solution is essentially in the nearest neighbor form for the linear case.

5.5.2 Data association with incomplete information

Multiple targets can provide the modulated frequency on any one of the two sensors. This results in inaccurate or irretrievable information and should be considered as missing information for that instant. That is $y(t)$ is incomplete or not available for that time interval t. Let $M(t) = [M^1(t)\ M^2(t) \quad M^{4N}(t)]^\top$ be a given vector for $t = 1; 2; \quad ; T$ such that $M^i \in \{0; 1\}$, for $i = 1; \quad ; 4N$. Then the matrix $M \triangleq [M(1) \quad M(T)]^\top$, is considered as the **incomplete** matrix. With M^i, let us define two sequences of matrices :

$$\begin{aligned} E(t) &= \text{Diag}[M^1(t)\ M^2(t) \quad M^{4N}(t)]; \\ \hat{E}(t) &= [\tilde{M}^1(t)\ \tilde{M}^2(t) \quad \tilde{M}^{4N}(t)]^\top; \end{aligned} \tag{5.5.3}$$

where $M^i(t) + \tilde{M}^i(t) = 1$.

$U; V$ and W are provided to account for the **incomplete information** in the Riccati equation 5.4.7 and 5.4.10, [51].

$$\begin{aligned} U &= \quad EWE; \\ V &= \quad EW; \\ W &= I \quad \hat{E}(\hat{E}^\top \hat{E})^{-1}\hat{E}^\top : \end{aligned} \tag{5.5.4}$$

Remark 4. For the case of complete information, $\hat{E}$ is the zero vector and E is the identity matrix. This ensures that $U; V$ and W are evaluated as identity matrices as stated in section 5.4.

In a practical application, the modulated velocities of two different agents are required to be close to the velocity resolution for this **incomplete information** to

occur. Using the standard Doppler shift equation ($f = \frac{"}{c} f_0$ where f is the frequency resolution, " is the velocity resolution, c denotes the speed of light and f_0 is the carrier frequency) " can be obtained. Actually, $j\hat{v}_1^i(k) \quad \hat{v}_2^i(k)j$ " distinguish distinct targets. Target dynamics which do not obey this expression should be regarded as missing information and this will be triggered by the absence of measurements.

5.6 Illustrative examples

The practical relevance of this approach is illustrated by a computer simulation and a hardware based experiment in an indoor setting.

5.6.1 Fictional simulation data

In the ctitious simulation scenario four mobile targets are tracked using Doppler radar measurements. Table 5.1 provide simulation parameters. Comparison between the Extended Kalman Filter(EKF) and the Robust Linear Filter(RLF) is made to show the strength of the underlying approach which is based on linear formulations. Both EKF and RLF are initialized using a Gaussian distribution with a mean at the ideal value and a standard deviation of 0.02 radians. The EKF is known to be diverging without correct initialization. The EKF parameters(Q_E and R_E) are tuned fairly accurately. Assuming the initial error statistics are known to the tracking system, the initial covariance of the EKF is also tuned . That is, for the EKF parameters, the perfect knowledge of all the relevant error statistics is assumed and tuned around these true values to get the best possible performance. In contrast, for the RLF the identity matrix for both the initial and process noise weightings is used. and are taken as two times the standard deviations of corresponding Gaussian measurement noise.

Actual and estimated trajectories of four maneuvering targets for the case of

Table 5.1: Simulation Parameters

Input	Value	Comments
w_1	$[0:03 \quad 0:07]^0$	Target 1 Accel. Input
w_2	$[0:01 \quad 0:08]^0$	Target 2 Accel. Input
w_3	$[0:15 \quad 0:01]^0$	Target 3 Accel. Input
w_4	$[0:15 \quad 0:01]^0$	Target 4 Accel. Input
$v_i, i \; 2 \; f1;2g$	$_{vi} = 0:5$	Gaussian Meas. Noise 1
$_i, i \; 2 \; f1;2g$	$_{vi} = 0:5$	Gaussian Meas. Noise 2
$[N_R; \; Q_R]$	$[10^{-4}I_6; \; 10^{-5}I_2] \; I$	Robust Filter Parameters
$[R_E; \; Q_E]$	$[10^{-8}I_2; \; 10^4] \; I$	EKF Uncertainty Weightings
$T \; @ \; t_s$	$10s \; @ \; 0:15s$	Track Duration and Periodicity

EKF and RLF are illustrated in Figure 5.7 and 5.8 respectively. Figure 5.9 depicts the actual velocity and the estimated velocity of the four targets for the case of RLF while the accelerations are given in gure 5.10. The tracking error($kb \quad xk$) for the robust linear lter and the EKF is illustrated in Figure 5.11 where the signi cance of the initial uncertainty for EKF is manifested. Due to the advantage in the underlying linear approach, the identical error in the initial condition(position and velocity) is instantly corrected by the RLF. The proposed linear robust lter basically utilizes the measurement conversion technique which is essentially a computation of 2D coordinates of a target in a closed-form manner. Actually, this robust estimator exhibits excellent performance. As opposed to the RLF, no computation of the 2D coordinates of the target is contained in the EKF and it is based on linearization and Taylor series type approximations. Specially in systems with large uncertainties, this type of linearizations causes accumulation of errors and in some instances divergence can occur in the state estimation.

As depicted in Figure 5.12, converted measurements provided in equation (5.4.2) are essentially ltered through the linear lter e ectively.

Some insight into the worst case measurement bounds is given by the end points of the major axis (kb shown in gure 5.5) of the uncertainty ellipse relevant to each

measurement generated for a target as shown in gure 5.13 in a 500 trial Monte Carlo simulation. In gure 5.14, the relationship between the system performance with the measurement noise intensity is depicted.

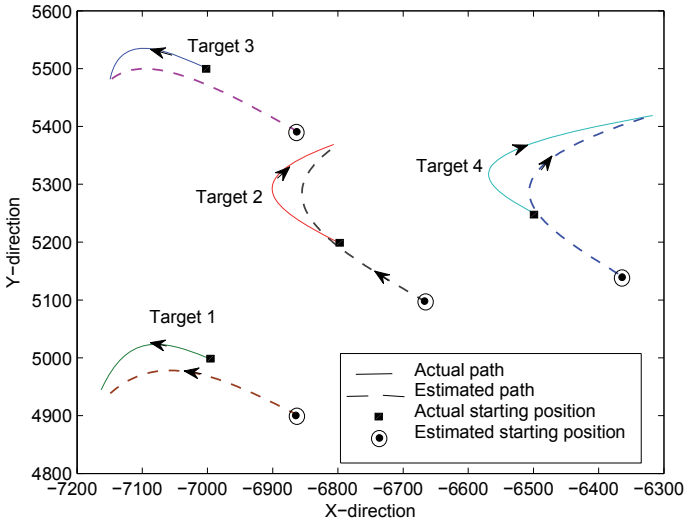

Figure 5.7: The actual and the EKF estimated trajectories of four targets.

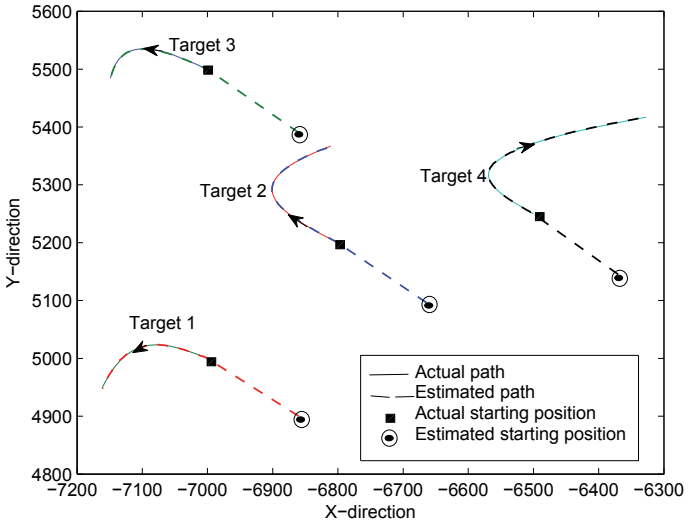

Figure 5.8: The actual and the RLF estimated trajectories of four targets

Figure 5.15 and 5.16 depicts the performance of the modi ed version of the

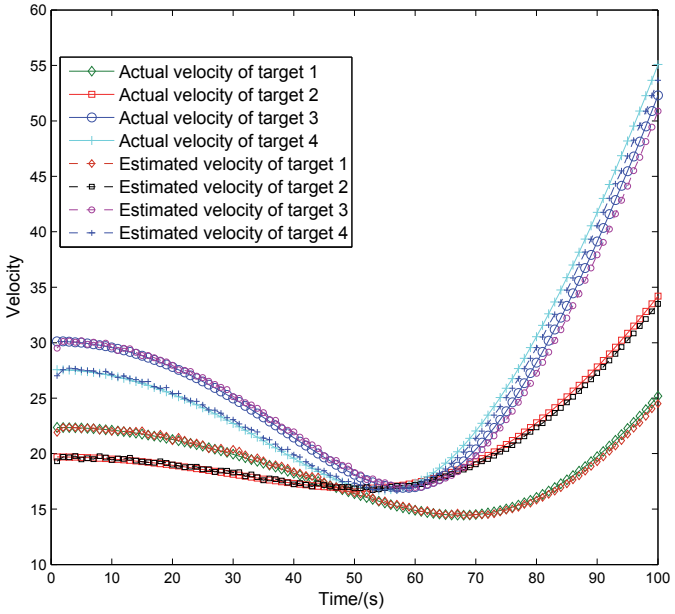

Figure 5.9: The actual and the RLF estimated velocities of four targets

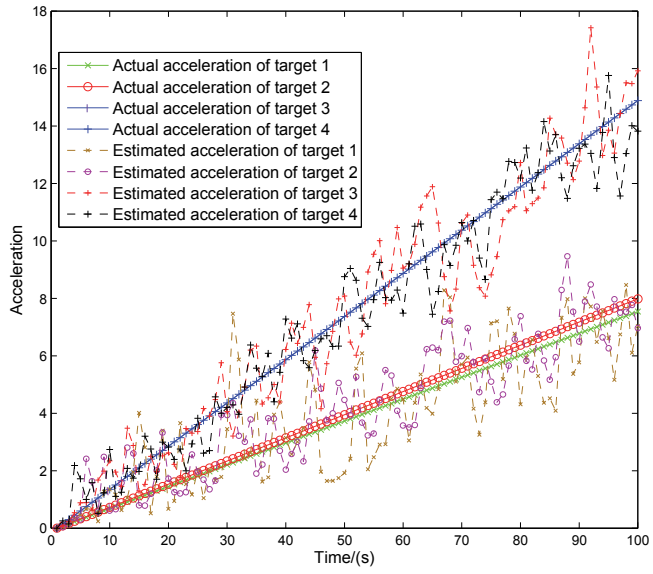

Figure 5.10: The actual and the RLF estimated accelerations of four targets

linear robust filter for the incomplete information scenario. Missing some measurements in the tracking interval can be a common occurrence in a practical multi-target Doppler radar application. This can be acute when the identical Doppler

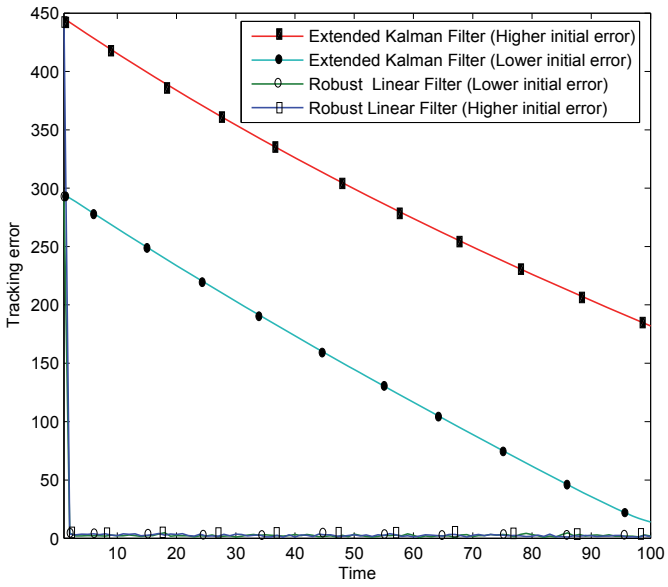

Figure 5.11: The complete state estimation error of the four targets using EKF and RLF

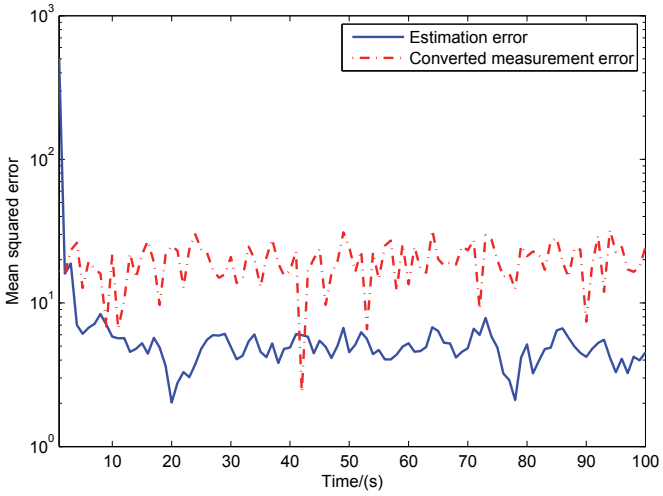

Figure 5.12: Converted measurements ltering in RLF

frequency(within the resolution) modulates at the same sensor from two distinct mobile targets. As illustrated in gure 5.15, the identical Doppler frequency is modulated by two targets at sensor 1. For this particular instant, modi ed version of the linear lter (equation 5.5.3 is used and 5.5.4) in comparison to the predicted velocity from the previous measurements for the missing instance. As evident in

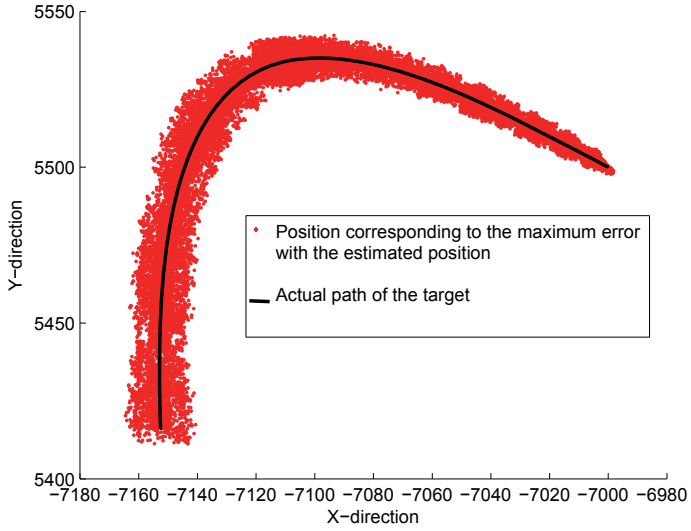

Figure 5.13: Error bounds for RLF location estimation

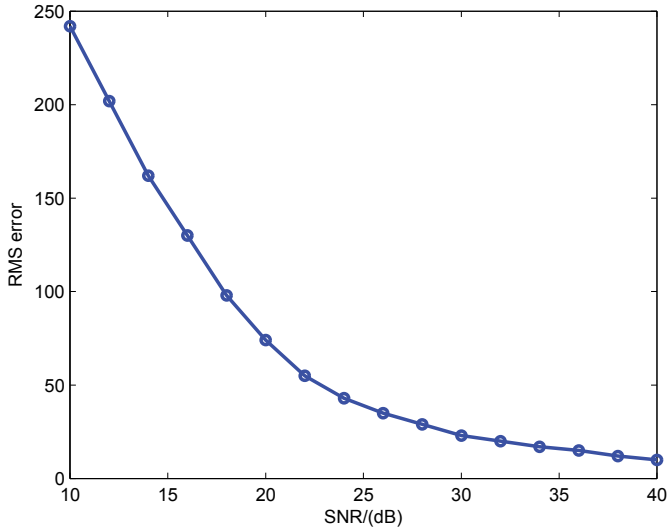

Figure 5.14: Measurement noise e ect on the performance

gure 5.16, a better estimation accuracy is produced by the modi ed version of the lter with incomplete information correction.

5.6.2 Real experimental data

A Doppler information acquisition system (gure 5.6) is set up to capture the re- ected Doppler signal from a person moving in a well de ned path in an indoor

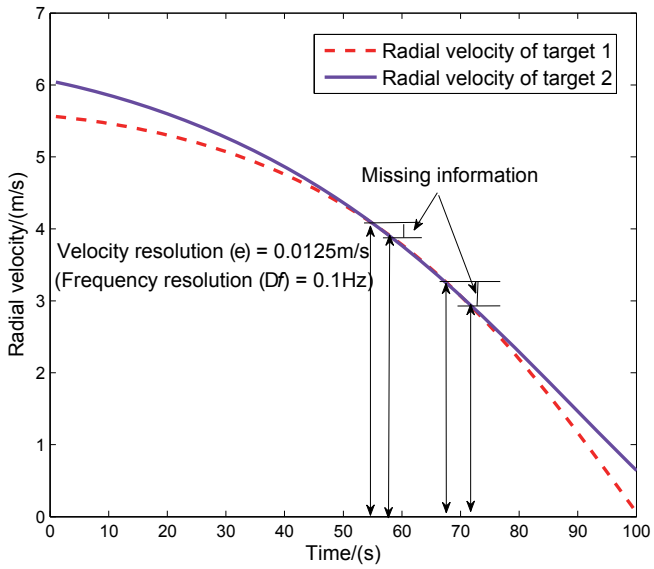

Figure 5.15: Radial velocity toward sensor 1 overlapping for two targets

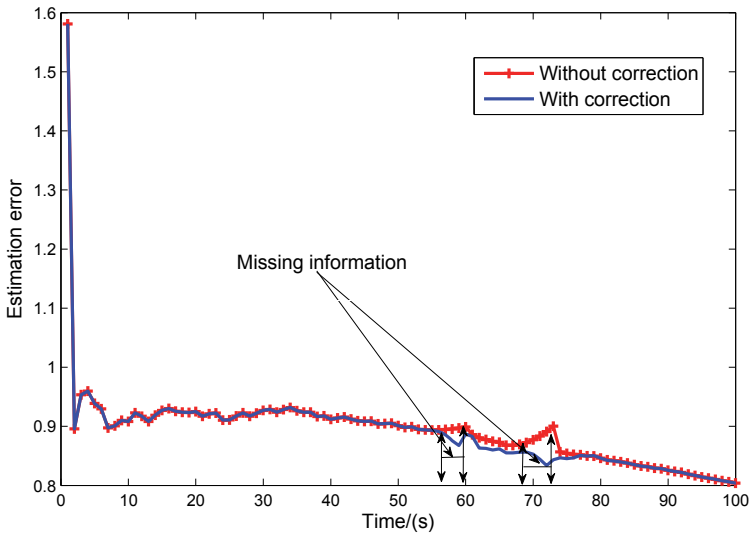

Figure 5.16: Linear Robust Filtering with incomplete information

setting. The receiving elements and sensors (one sensor is composed of two antennas elements) are positioned 6cm and 0.5m distance from the other similar device respectively along the X axis as depicted in the gure 5.18. 2.4GHz continuous wave RF at 12dBm is transmitted through the signal generator.

The re ected signals are captured by four low-cost, o -the-shelf integrated boards

(AD8347) which are quadrature (or I/Q) receivers. Each receiver comprises of low-noise amplifier (LNA), I/Q mixers, gain control, and baseband amplifications. Special analog filtering (as in the superheterodyne conversion) is not required as this chip allows a direct conversion from RF to baseband.

Then the 14-bit NI USB-6009 is used for analog to digital conversion. Next The digitized data is collected by the computer. DFT is performed on the data using Cooley-Turkey algorithm to find the Doppler frequencies and corresponding phase differences to measure the AoA of the object at each time step. 10^4 measurements are acquired for 200 point FFT with a succeeding frequency resolution of 0.1Hz and a calculated SNR of 34dB which is typical of a 2.4GHz band with surrounding IEEE 802.11 wireless LAN and personnel area networks employing Bluetooth enabled devices [167]. Indeed, the assumption on the noise model suits this type of noise and uncertainties which do not have a clear and elegant mathematical model [168].

In order to track a moving target the experimental setup depicted in figure 5.17 is used. The actual path and the estimated path of the person are shown in figure 5.18. The estimation error from the converted measurements and the estimation error for the filtered case is depicted in figure 5.19. A significant initial error is provided to demonstrate the effective convergence noticeable with the RLF.

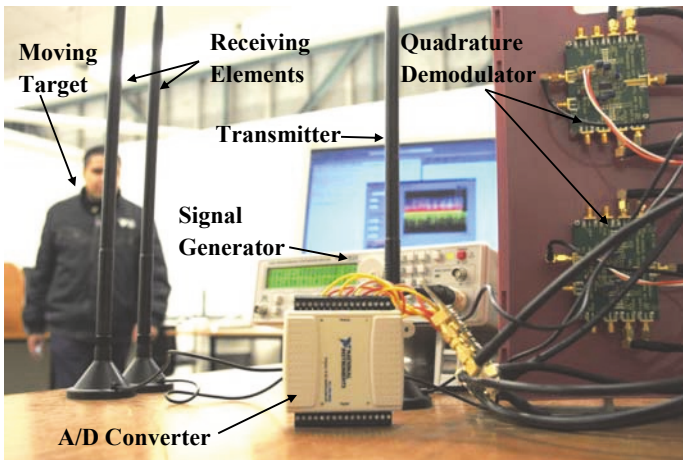

Figure 5.17: The experimental setup for tracking a person

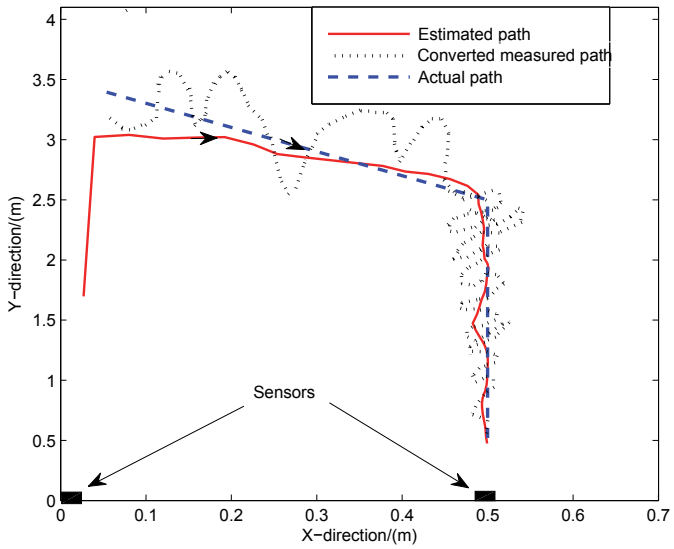

Figure 5.18: The estimated and actual path of the person

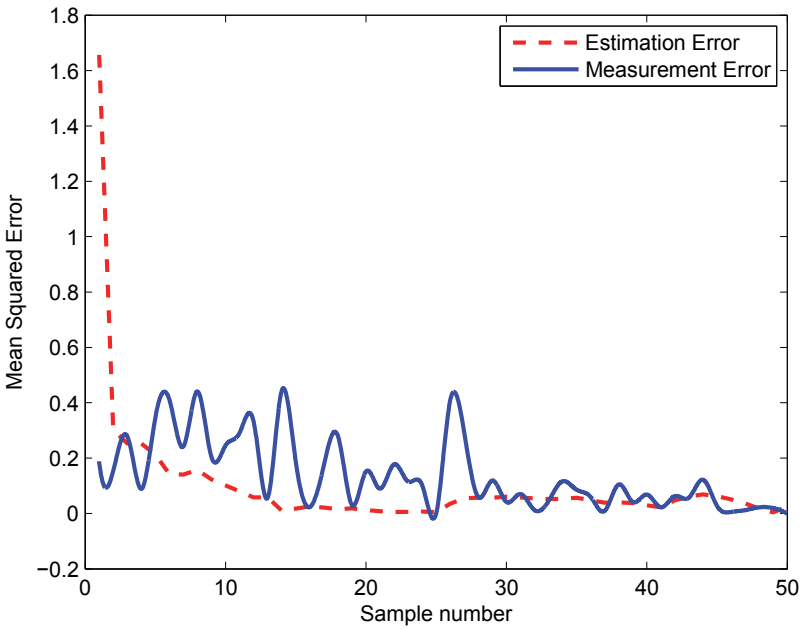

Figure 5.19: The estimation error of the four targets

5.7 Maximum Likelihood Estimation(MLE) based approach for moving sensor platform

In this section, we consider the case of tracking mobile targets with a linear sensor array mounted on a moving vehicle. The array is assumed to be placed at the

front bumper of the vehicle. The dynamics of the vehicle must be incorporated in accessing the state of the moving targets.

5.7.1 Vehicle dynamics

Lets consider the velocity pro le of the bumper of a vehicle when it is making a turn on a radius R [169]. As shown in Figure 5.20 , when the speed at the position P is U^0 and the angle it makes with a line drawn along the vehicle is $_{u^0}$, the velocity vector at that particular point is,

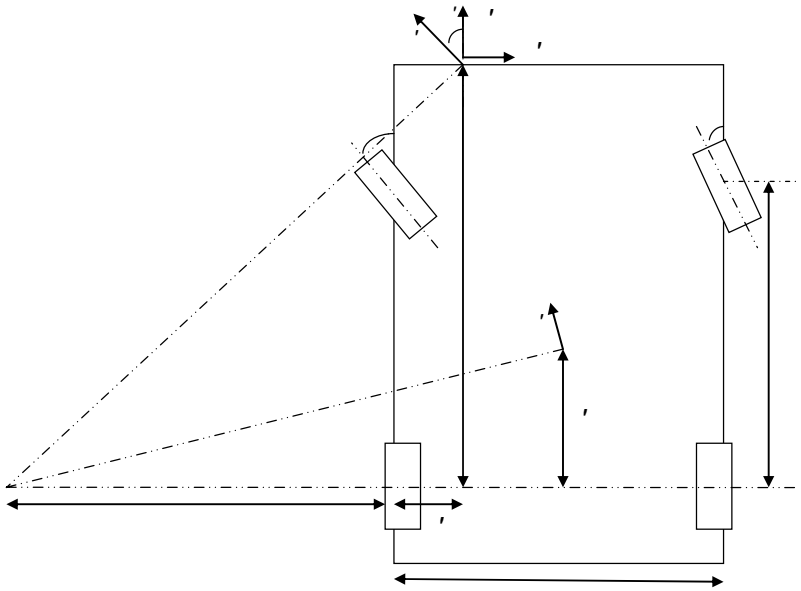

Figure 5.20: Steering dynamics

$$\begin{bmatrix} u_x^0 \\ u_y^0 \end{bmatrix} = \begin{bmatrix} U^0 \sin\ _{u^0} \\ U^0 \cos\ _{u^0} \end{bmatrix} \tag{5.7.1}$$

where,

$$U^0 = \frac{V^0 R_U}{R};$$

$$_{u^0} = \arctan\ \frac{b}{R_r + x^0}\ ;$$

$$= \arctan \frac{2}{\cot_{o} + \cot_{i}} ;$$

$$R = \sqrt{a^{2} + (l \cot)^{2}};$$

$$R_r = \frac{l}{\tan_{i}};$$

and,

$$R_u = \sqrt{(R_r + x^{0})^{2} + b^{2}}:$$

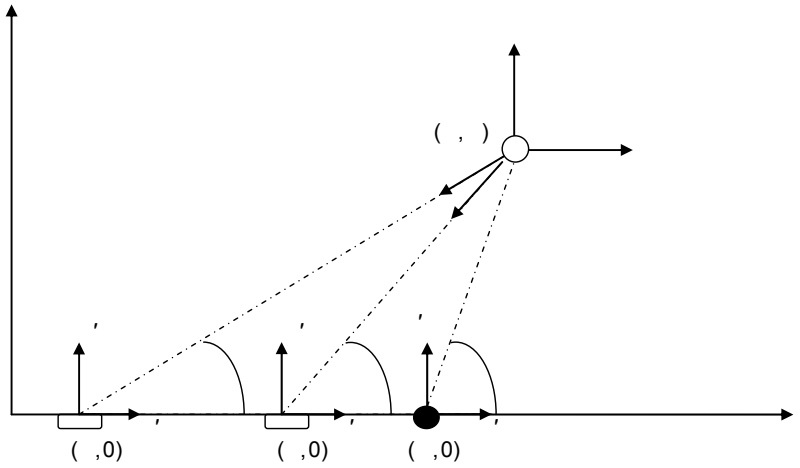

Figure 5.21: Tracking a target when the sensors are mounted on a moving vehicle

Consider the Figure 5.21. $u^{0}_{xA}; u^{0}_{xB}$ and u^{0}_{xG} are the velocity components at the points $A; B$ and G along x direction respectively. $u^{0}_{yA}; u^{0}_{yB}$ and u^{0}_{yG} are the velocity components at the points $A; B$ and G along y direction respectively. The signal generator is at $G(g; 0)$ and $_{G}$ is the bearing of agent with respect to G. For this dynamic case the state of the target without measurement errors can be written as,

$$\begin{bmatrix} x \\ y \\ u_x \\ u_y \end{bmatrix} = \begin{bmatrix} \frac{q\sin\ _B\cos\ _A - p\sin\ _A\cos\ _B}{\sin(\ _B - \ _A)} \\ \frac{(q-p)\sin\ _A\sin\ _B}{\sin(\ _B - \ _A)} \\ \frac{v_B^0\sin\ _A - v_A^0\sin\ _B}{\sin(\ _B - \ _A)} \\ \frac{v_A^0\cos\ _B - v_B^0\cos\ _A}{\sin(\ _B - \ _A)} \end{bmatrix} \tag{5.7.2}$$

where,

$$v_A^0 = v_A \quad (u_{xA}^0\cos\ _A + u_{yA}^0\sin\ _A + u_{xG}^0\cos\ _G + u_{yG}^0\sin\ _G)$$

and

$$v_B^0 = v_B \quad (u_{xB}^0\cos\ _B + u_{yB}^0\sin\ _B + u_{xG}^0\cos\ _G + u_{yG}^0\sin\ _G):$$

Now we consider the case where the angle measurements are corrupted with zero mean Gaussian noise, hence the Maximum likelihood based approach is provided to increase the localization accuracy.

5.7.2 Maximum likelihood for AoA-only location estimation

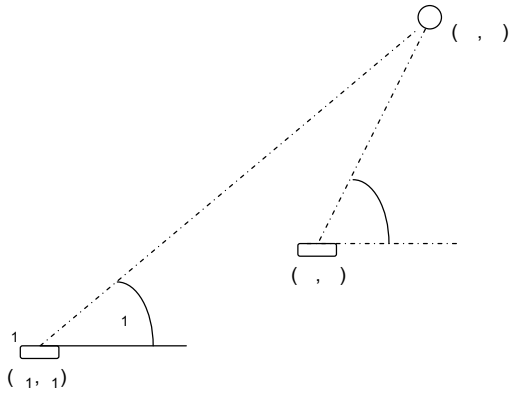

Figure 5.22: Sensor target locations and measurements

AoA-only localization problem can be formulated as follows in R^2. Let $x = (x_t; y_t)^T$ be the target position vector to be estimated from bearing measurements

$= (\ _1;\ _2;:::;\ _N)^T$, where $(:)^T$ denotes vector or matrix transposition. The target AoAs are measured from xed N number of sensors at known positions or from sensors xed to a moving platform where the trajectory of the platform is known. The sensor coordinates are denoted by $x_s = (x_s; y_s)$, which associate with the measurement $_s,(s\ 2\ 1;:::;N)$. The problem geometry is shown in Figure 5.22. The angle measurements consist of the true bearings $$, corrupted by additive noise $= (\ _1;\ _2;:::;\ _N)^T$, which is assumed to be zero mean Gaussian with N covariance matrix $S = diag(\ ^2_1;\ ^2_2;:::;\ ^2_N)$. Thus the problem is described by the nonlinear equation,

$$= g(x_t) + \quad : \tag{5.7.3}$$

where,

$$g(x_t) = (g_1(x_t);:::::;g_N(x_t))^T$$

and

$$g_n(x_t) = \arctan(\ _{yn} = \ _{xn});$$

$$_{xn} = x_t \quad x_n;$$

$$_{yn} = y_t \quad y_n; \quad n = 1;2;:::;N:$$

The Cramer-Rao Lower Bound on the covariance of any unbiased estimator for this problem is given by

$$C = (g_x^T S^{\ 1} g_x)^{\ 1}: \tag{5.7.4}$$

The derivative, $g_x = @g=@x$ evaluated at the true target position is then

$$g_x = \begin{pmatrix} \frac{y1}{r_1^2} & \frac{y2}{r_2^2} & :: & \frac{yk}{r_k^2} & :: & \frac{yN}{r_N^2} \\ \frac{x1}{r_1^2} & \frac{x2}{r_2^2} & :: & \frac{xk}{r_k^2} & :: & \frac{xN}{r_N^2} \end{pmatrix}^T$$

.

where,

$$r_k^2 = \quad {}^2_{xk} + \quad {}^2_{yk}; \; k = 1; :::; N:$$

N is the number of sensor positions.

The Maximum Likelihood estimator is useful due to its properties guaranteed by a well known theorem of estimation theory. The theorem states that, if the number of measurements is large enough, the ML estimator is unbiased and its covariance achieves the CRLB under mild regularity conditions. When the measurement noise is Gaussian with zero mean, the ML estimator of the target location x, is given by

$$\hat{x}_{ML} = \text{argmin}_x \, j F_{ML}(x; \;)j \tag{5.7.5}$$

where, the cost function, $F_{ML}(X; \;)$ has the form

$$F_{ML}(x; \;) = \frac{1}{2}(g(x) \quad)^T S^{\;1}(g(x) \quad):$$

Above (5.7.5) involves a nonlinear least-square minimization, which can be performed by the Newton-Gauss iterations:

$$\hat{x}_{i+1} = \hat{x}_i + (g_x^T S^{\;1} g_x)^{\;1} g_x^T S^{\;1}(\quad g(\hat{x}_i)); \quad i = 1; 2; :::: \tag{5.7.6}$$

An initial estimate, $\hat{x}_0$ is required for (5.7.6) which is close enough to the true minimum of the cost function. Such an initial estimate may be available from prior information. A simple (but suboptimal) procedure can also be used to obtain an initial estimate. The partial derivatives involved in (5.7.6) are evaluated at the current estimated position, $\hat{x}_i$. A number of 2-4 iterations are sufficient for convergence in real implementations.

Simulation result in Figure 5.23 shows the tracking of two mobile agents using three Doppler sensors mounted linearly on the bumper of a vehicle which are 0.5m apart. Figure 5.24 depicts the same dynamic system with four Doppler sensors mounted linearly. The mean squared error of the two systems are compared in the Figure 5.25 and it can be seen that the system with the four Doppler sensors performs better than the system with three sensors. The estimation accuracy will increase as the number of of sensors increases. This is due to the fact that, if the number of measurements is large enough, the ML estimator is unbiased and its covariance achieves the CRLB under mild regularity conditions.

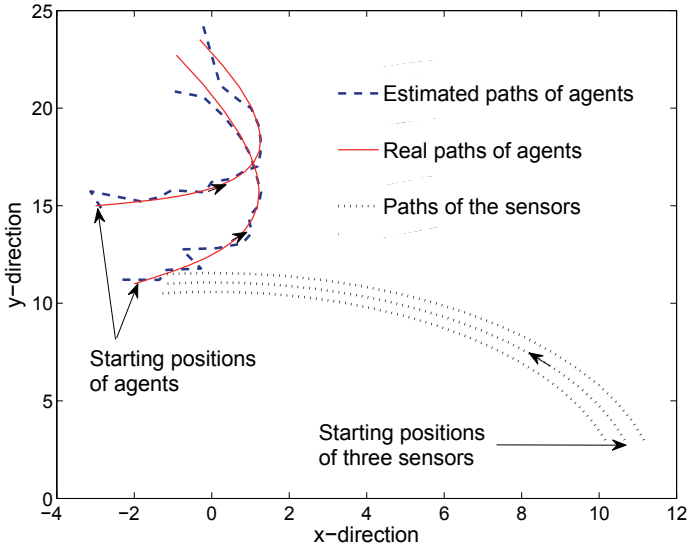

Figure 5.23: MLE for Doppler-radar tracking with three sensors

5.8 Summary

In this chapter a linear state estimator is derived with provable performance limits for radar based target tracking. Here, nonlinear Doppler frequency modulation and associated angle of arrivals are used as measurements. A completely linear algorithm is provided using a novel measurement conversion method that does not use Taylor-series type approximations. Mathematically rigorous proof of the

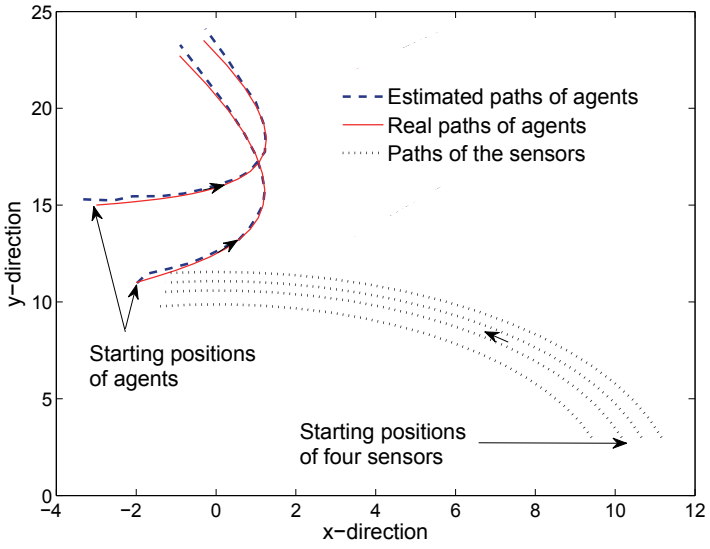

Figure 5.24: MLE for Doppler-radar tracking with four sensors

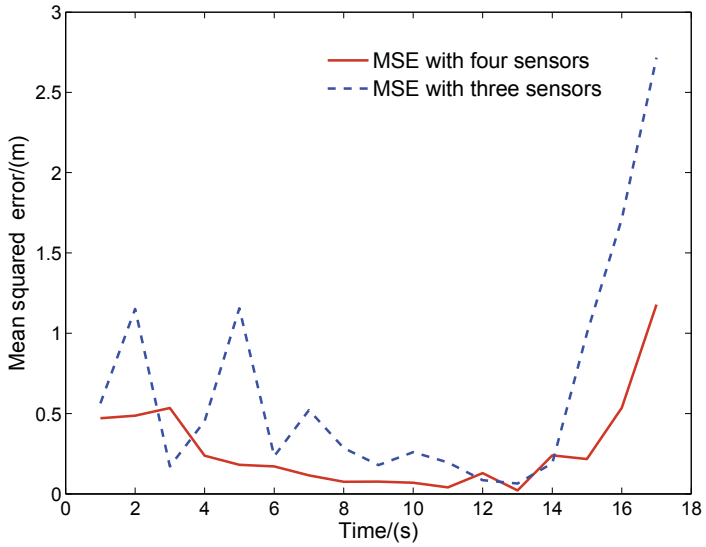

Figure 5.25: Variation of error with time for three and four sensors

boundedness of the ltering error is an important contribution of this technique. Extended Kalman lter does not provide such results.

A linear sensor array is considered here and the mathematically justi ed necessary and su cient condition in tracking multiple mobile targets is derived. The ghost formation problem is considered and removal of such targets is addressed

while restricting to the minimal con guration in the sensor array as an alternative to increasing the number of sensors in the array. The linear approach for the complete information case is also modi ed to account for the case of incomplete information. The theoretical assertions are veri ed via physical experimentation in addition to a ctitious simulation scenario.

Also, tracking multiple mobile targets with a Doppler radar sensor array mounted on a moving vehicle has been studied in this chapter. Similar to the stationary case, Doppler frequencies modulated from the mobile targets on the single-frequency-continuous-wave radar are captured by the linear sensor array and analyzed in order to estimate the positions and velocities of the targets. As the measurements corrupted by noise lead to poor localization, the maximum likelihood estimation (MLE) is employed to enhance the estimation accuracy. The theoretical derivations are veri ed using computer simulation.

For small number of samples maximum likelihood estimates can be heavily biased and the optimality properties may not apply. Also, the choice of starting values in uences the maximum likelihood estimation. Model based estimators, such as extended Kalman lter can be incorporated for better estimation in further studies.

Chapter 6

Concluding Remarks

This thesis has led to number of potential research directions in Doppler radar based tracking and sensor fusion in AoA, range,TDoA and ToA measurement techniques. Summary of the di erent research aspects studied in the dissertation is given in this chapter in the form of an application case study in close range tracking. The real world application value to the study is provided by linking it to the seemingly standalone research outcomes.

Through-Wall-Radar (TWR)

Through wall tracking of human activities is an emerging eld of interest due to the increasing demand in the applications of defense and commercial systems ranging from urban warfare to rescue operations. Tracking of human movements inside a building enhances the chance of successful law enforcements or military operations minimizing casualties. The radar system introduced in this thesis can be modi ed to track humans through the wall.

In such real world applications, the state of the target should be estimated robustly in real time. Ultra wide band (UWB) radar seems popular in these applications with resolution of the order of centimetres have been reported in [28{34]. The prominent disadvantage of these systems is the degradation of the accuracy in measurements due to the dispersion and signal loss as the waves are traveling through some wall materials such as concrete.

Human activity can be recognized by analysing the micro-Doppler e ects [35]. Micro-Dopplers are generated from non-rigid-body motions of human limbs and contain valuable information related to human gait recognition. Using a higher frequency the radar system discussed in our study can be modi ed to obtain the micro-Doppler e ects of moving limbs.

A coherent wave propagation model is needed in the context of Doppler-based continuous wave radar for through wall tracking. This model would address all the factors such as material type, thickness of the wall and homogeneity of the material and they should be included in the estimator so that more reliable readings can be obtained. The signal propagation patterns for di erent wall materials should be classi ed with their dispersion and loss e ects. Antenna arrays can be designed to capture the returning wave e ectively if the wave propagation model through the particular wall material is known. This radar system should have the capability to adjust in di erent circumstances, for example walls with di erent materials or thickness and also be portable and easy to handle by the operator.

As discussed in our study, robust linear ltering can be utilized to get a better approximation to the actual trajectories of the moving humans behind the wall since the waves contains some noise with the required information. Gait recognition can be carried out by further analysis of the micro-Doppler returns from the moving human body parts.

For automobile applications

Modern cars are equipped with reverse sensors, reverse cameras and blind-spot sensors for the safety of the vehicle and passengers. One of the main requirements in these designs is to identify the dynamic nature of the surroundings of the vehicle in real time. Camera systems are seemingly good candidate for this application but they inherently posses the following disadvantages,

Not reliable in rainy/ snowy conditions

Not reliable at night as sudden ashes of lights may cause fatal misjudgments

Not reliable when the clutter in the eld of view increases

As opposed to the camera systems, radar systems have advantages such as,

Can suppress the clutter when the correct type of Radar is used(As an example Doppler radar for moving target detection)

Environmental e ects such as rain and snow can be minimized signi cantly

Reliable at night or gloomy conditions

Not a ected by sudden light changes

Optimal sensor separation

In this thesis, optimal sensor separation for linear arrays employing AoA-only and range-only measurements is discussed. The Cramer-Rao lower bound for the unbiased estimators is utilized for the study and several important results have been derived. In practical applications, these results can only be used as a guide for sensor positioning as the estimation accuracy is a ected by the bias and e ciency characteristics of the employed estimator.

The bias and the variance (mean-squared error) has an inversely proportional relationship [127]. Extensive studies on this scenario are carried out in [125, 128, 129]. By incorporating the bias-variance trade o given in these studies, the results obtained in our study can be further extended for more practical estimation algorithms such as maximum likelihood.

The results obtained in Chapter 3 can be employed to arrange the AoA-only or Range-only sensors in a manner which signi cantly enhances recursive localization

performance. This analysis is also useful in practical applications such as optimal path planning and trajectory control of mobile sensors for localization [15,109,111].

For simplicity, single target scenario is analysed in this study. The same concept proposed here can be further extended for the multiple target localization. In general, overall optimal sensor placement for multiple targets will provide suboptimal positioning for individual targets.

The exact position of the target should be known in the theoretical analysis in determining the optimal sensor placement. Even though in practical situations this information is not readily available, a rough estimate of the likely region of the target is sufficient in finding the sensor positions to obtain enhanced localization results.

Time-Delay-of-Arrival and Time-of-Arrival systems

The unique localization of a target with minimum number of TDoA measurements is analysed in Chapter 4. The measurement error is assumed to be bounded. The limiting error bounds have been derived for both R^2 and R^3 after which, the unique solution region cease to exist. It has been shown that the sensor geometry influences the limiting error bound. This study can be further extended, specially in the geometry of the sensor positions for robust localizations.

When it comes to multiple target localization, the data association problem is prevalent. The study provides an analysis on unique localization of multiple emitters using TDoA or ToA measurements. For a given number of targets to be uniquely localized, the maximum bound on the required number of sensors in R^q is derived. This analysis provides the groundwork for further studies in TDoA and ToA based localization.

Final remark

Several application scenarios which use the aspects of this research is presented in the above section. However, there can be many other potential applications which could utilize the theories provided in this study either partially or completely. Although a major part of this thesis provides a solid foundation to a Doppler radar based close-range tracking using robust linear filtering, there exists many potential future work which will undoubtedly enhances the application value to the underlying work. Among them, real-world implementation of the though-wall tracking of humans with gate recognition is significant.

Appendix I

Consider arbitrary constants $x_i \in \mathbb{R}^2; i \in \{1,2,3\}; \in \mathbb{R}^+$, and $y_i \in \mathbb{R}^2$ arbitrary variables.

Proposition 3.

$$\frac{\|x_i - y_1\|}{\|x_i - y_2\|} = \quad \forall i \in \{1,2,3\} \text{ and } x_i \neq x_j; \text{ for } i \neq j \quad) \quad = 1$$

Proof.

$$\frac{\|x_i - y_1\|}{\|x_i - y_2\|} = \quad \forall i \in \{1,2,3\}:$$

This can be given as,

$$(1 \quad ^2)x_i^\top x_i \quad 2x_i^\top y_1 + 2 \quad ^2x_i^\top y_2 + y_1^\top y_1 \quad ^2y_1^\top y_1 = \quad 0 \quad \forall i \in \{1,2,3\}; \tag{6.0.1}$$

Considering, $i = 1;2$,

$$(1 \quad ^2)(x_1 + x_2) + 2 \quad ^2y_2 \quad 2y_1 = \quad 0; \tag{6.0.2}$$

and considering, $i = 1;3$,

$$(1 \quad ^2)(x_1 + x_3) + 2 \quad ^2y_2 \quad 2y_1 = \quad 0: \tag{6.0.3}$$

Hence, as y_1 is not a function of x_i and $x_2 \neq x_3$, $= 1$(only the positive sign is considered as per the de nition of the magnitude). □

.

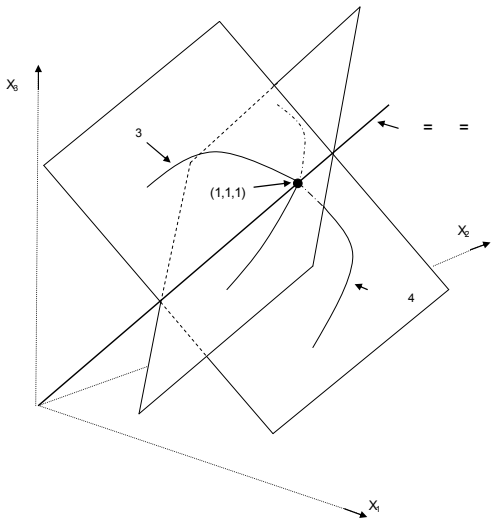

Figure 6.1: Trajectories of $x_i; i \in \{1;2;3;4\}$ as per equation 5.2.4 and 5.2.5

Appendix II

Consider the following two trigonometric equalities

$$\sin(\ + v) = \ ! \sin(\ ); \tag{6.0.4}$$

$$\cos(\ + v) = \ ! \cos(\ ); \tag{6.0.5}$$

with a given $\ > 0$.

Proposition 4. Then, $8 \ 2 [0; \ =2]$, and $v \quad jj \ 9 ! \ : \cos \quad ! \quad \frac{1}{\cos}$.

Proof. Writing the expressions 6.0.4 and 6.0.5 in the form of,

$$\sin(v) = \quad ! \sin \ \cos \quad \sin \ \sqrt{1 \ ! \ ^2 \sin^2 \ }; \tag{6.0.6}$$

$$\sin(v) = \quad ! \sin \ \cos \quad \cos \ \sqrt{1 \ ! \ ^2 \cos^2 \ }; \tag{6.0.7}$$

respectively. Consider the positive valued one as function f and the negative valued one as function g. If the maximum/minimum value of f and g denoted by $f_{max=min}(!\ )$ and $g_{max=min}$ respectively,

$$f_{max=min}(!\ ) = \begin{cases} \sqrt{1 \ \frac{1}{!^2}}; & \frac{1}{\cos} > ! > 1 \\ \sqrt{1 \ ! \ ^2}; & 1 > ! > \cos \ ; \end{cases}$$

$$g_{max=min}(!\ ) = \begin{cases} \sqrt{1 \ \frac{1}{!^2}}; & \frac{1}{\cos} < ! < \ 1 \\ \sqrt{1 \ ! \ ^2}; & 1 < ! < \cos \ : \end{cases}$$

Therefore the proof follows immediately. □

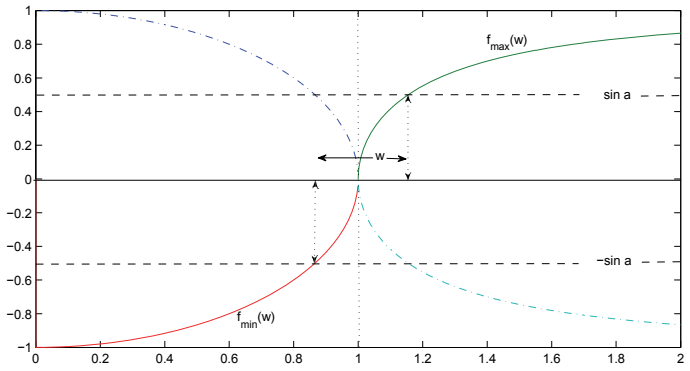

Figure 6.2: Error Variation of f with !

Due to the symmetric nature around the y axis, the corresponding expressions 6.0.6 and 6.0.7 represents identical error variation. The error variation of f for ! is illustrated in the gure 6.2.

Bibliography

[1] M. I. Skolnik, Introduction to Radar Systems. McGrawhill Book Company, 1962.

[2] H. E. Daniels, \The theory of position nding," Journal of the Royal Statistical Society, Series B (Methodological), vol. 13, no. 2, pp. 186{207, May 1951.

[3] A. Lin and H. Ling, \Doppler and Direction-of-Arrival (DDOA) Radar for Multiple Mover Sensing," IEEE Transactions on Aerospace and Electronic Systems, vol. 43, no. 4, pp. 1496{1509, 2007.

[4] | | , \Through-wall measurements of a Doppler and direction-of-arrival (DDOA) radar for tracking indoor movers," in Antennas and Propagation Society International Symposium, 2006, pp. 322{325.

[5] S. S. Ram and H. Ling, \Through-wall tracking of human movers using joint Doppler and array processing," Geoscience and Remote Sensing Letters, vol. 5, no. 3, pp. 537{541, 2008.

[6] J. Tsao and B. D. Steinberg, \Reduction of sidelobe and speckle artifacts in microwave imaging: The CLEAN technique," IEEE Transactions on Antennas Propagation, vol. 36, no. 4, pp. 543{556, 1988.

[7] J. Li and P. Stoica, \E cient mixed-spectrum estimation with applications to target feature extraction," IEEE Transactions of Signal Processing, vol. 44, no. 2, pp. 281{295, 1996.

[8] S. Nardone, A. Lindgren, and K. Gong, \Fundamental properties and performance of conventional bearing-only target motion analysis," IEEE Transactions on Automatic control, vol. 29, no. 9, pp. 775{787, September 1984.

[9] M. P. Wylie, S. Roy, and H. Messer, \Joint DOA estimation and phase calibration of linear equispaced (LES) arrays," , IEEE Transactions on Signal Processing, vol. 42, no. 12, pp. 3449 {3459, dec. 1994.

[10] A. Dempster, \Dilution of precision in angle-of-arrival positioning systems," Electronics Letters, vol. 42, no. 5, March 2006.

[11] A. N. Bishop, B. D. O. Fidan, B.and Anderson, K. Dogancay, and P. N. Pathirana, \Optimality analysis of sensor-target localization geometries," Automatica, vol. 46, no. 3, pp. 479{492, 2010.

[12] S. Martinez and F. Bullo, \Optimal sensor placement and motion coordination for target tracking," Automatica, vol. 42, no. 4, pp. 661{668, 2006.

[13] K. Dogancay and H. Hmam, \Optimal angular sensor separation for AOA localization," Signal Processing, vol. 88, no. 5, pp. 1248{1260, 2008.

[14] E. Fogel and M. Gavish, \Nth-order dynamics target observability from angle measurements," IEEE Transactions on Aerospace and Electronic Systems, vol. 24, no. 3, pp. 305{308, 1988.

[15] T. Song, \Observability of target tracking with bearings-only measurement," IEEE Transactions on Aerospace and Electronic Systems, vol. 32, no. 4, pp. 1468{1472, 1996.

[16] C. Jau ret and D. Pillon, \Observability in passive target motion analysis," IEEE Transactions on Aerospace and Electronic Systems, vol. 32, no. 4, pp. 1290{1300, 1996.

[17] D. Torrieri, \Statistical theory of passive location systems," IEEE Transactions on Aerospace and Electronic Systems, vol. 20, pp. 183{198, March 1984.

[18] Y. I. Abramovich, N. K. Spencer, and A. Gorokhov, \DOA estimation for noninteger linear antenna arrays with more uncorrelated sources than sensors," Signal Processing, IEEE Transactions on, vol. 48, no. 4, pp. 943 {955, 2000.

[19] S. C. K. Herath, C. V. D. Nagahawatte, and P. N. Pathirana, \Tracking multiple mobile agents with single frequency continuous wave radar," in Intelligent Sensors, Sensor Networks and Information Processing (ISSNIP), 2009 5th International Conference on, 2009, pp. 163 {167.

[20] M. Wylie, S. Roy, and R. Schmitt, \Self-calibration of linear equi-spaced (LES) arrays," in IEEE International Conference on Acoustics, Speech, and Signal Processing, 1993. ICASSP-93., 1993, pp. 281 {284.

[21] J. R. Irons, B. L. Johnson, and G. H. Linebaugh, \Multiple-angle observations of re ectance anisotropy from an airborne linear array sensor," IEEE Transactions on Geoscience and Remote Sensing, vol. GE-25, no. 3, pp. 372 {383, may. 1987.

[22] Y. I. Abramovich, N. K. Spencer, and A. Y. Gorokhov, \Detection-estimation of more uncorrelated gaussian sources than sensors in nonuniform linear antenna arrays - part iii: detection-estimation nonidenti ability," IEEE Transactions on Signal Processing, vol. 51, no. 10, pp. 2483 { 2494, oct. 2003.

[23] | | , \Detection-estimation of more uncorrelated gaussian sources than sensors in nonuniform linear antenna arrays. ii. partially augmentable arrays," IEEE Transactions on Signal Processing, vol. 51, no. 6, pp. 1492 { 1507, jun. 2003.

[24] Y. Bresler and A. Macovski, \On the number of signals resolvable by a uniform linear array," IEEE Transactions on Acoustics, Speech and Signal Processing, vol. 34, no. 6, pp. 1361 { 1375, dec. 1986.

[25] Y. Abramovich, N. Spencer, and A. Gorokhov, \Resolving manifold ambiguities in direction-of-arrival estimation for nonuniform linear antenna arrays," IEEE Transactions on Signal Processing, vol. 47, no. 10, pp. 2629 {2643, oct. 1999.

[26] D. Torrieri, \Statistical theory of passive location systems," IEEE Transactions on Aerospace and Electronic Systems, vol. 20, pp. 183{198, March 1984.

[27] G. W. Stimson, Introduction to Airborne Radar. SCITECH Publishing, Inc, 1998.

[28] G. Franceschetti, J. Tatoian, D. Giri, and G. Gibbs, \Timed arrays and their application to impulse sar for through-the-wall imaging," in IEEE Antennas Propag. Soc. Int. Symp. Dig, vol. 3, June 2004, p. 30673070.

[29] S. Nag, M. Barnes, T. Payment, and G. Holladay, \Ultrawideband through-wall radar for detecting the motion of people in real time," SPIERadar Sensor Technology and Data Visualization, vol. 4744, p. 4857, July 2002.

[30] A. Attiya, A. Bayram, A. Safaai-Jazi, and S. Raid, \Uwb applications for through wall detection," in IEEE Antennas Propag.Soc. Int. Symp. Dig, vol. 3, June 2004, p. 30793082.

[31] Y. Yang and A. Fathy, \See-through-wall imaging using ultra-wideband short-pulse radar system," in IEEE Antennas Propag. Soc. Int.Symp. Dig, vol. 3B, July 2005, p. 334337.

[32] P. van Dorp and F. Groen, \Human walking estimation with radar," Inst. Electr. Eng.Radar, Sonar Navigl, vol. 150, no. 5, p. 356365, October 2003.

[33] A. Hunt, \A wideband imaging radar for through-the-wall surveillance," SPIESensors, and Command, Control, Communications,and Intelligence (C3I) Technologies, vol. 5403, p. 590596, September 2004.

[34] C. Lai and N. R.M., \Through-wall imaging and characterization of human activity using ultrawideband (uwb) random noise radar," SPIESensors and C3I Technologies for Homeland Security andHomeland Defense, vol. 5778, p. 186195, May 2005.

[35] J. Geisheimer, E. Greneker, and W. Marshall, \High-resolution doppler model of the human gait," SPIERadar Sensor Technology and Data Visualization, vol. 4744, p. 818, Jul. 2002.

[36] M. Otero, \Application of a continuous wave radar for human gait recognition," SPIE Signal Process., Sensor Fusion, Target Recog, vol. 5809, p. 538548, May 2005.

[37] T. Thayaparan, S. Abrol, E. Riseborough, L. Stankovic, D. Lamothe, and G. Du , \Analysis of radar micro-doppler signatures from experimental helicopter and human data," IET Radar, Sonar Navig, vol. 1, no. 4, p. 289299, Aug. 2007.

[38] P. Setlur, M. Amin, and F. Ahmad, \Urban target classi cations using time-frequency micro-doppler signatures," in 9th Int. Symp. Signal Process. Appl, Feb. 2007, p. 14.

[39] A. Stove and S. Sykes, \A doppler-based automatic target classi er for a battle eld surveillance radar," in IEEE Radar Conf., Oct. 2002, Oct. 2002, p. 419423.

[40] G. Smith, K. Woodbridge, and C. Baker, \Navebayesian radar micro-doppler recognition," in Int. Conf. Radar, Sep. 2008, p. 111116.

[41] I. Bilik, J. Tabrikian, and A. Cohen, \Gmm-based target classi cation for ground surveillance doppler radar," IEEE Transactions on Aerospace and Electronic Systems, vol. 42, no. 1, p. 267278, January 2006.

[42] K. Youngwook and L. Hao, \Human activity classi cation based on micro-doppler signatures using a support vector machine," IEEE Transactions on Geoscience and Remote Sensing, vol. 47, p. 1328 1337, May 2009.

[43] S. M. Kay, Fundamentals of Statistical Signal Processing. Prentice Hall PTR, Upper Saddle River, New Jersey, 1993.

[44] X. R. Li and V. P. Jilko, \Survay of maneuvering target tracking part iii: Measurement models," in In Proceeding of the SPIE Conference on Siganl and Data Processing of Small Targets, San Diego, USA, July-August 2001, pp. 423{446.

[45] | | , \Survay of maneuvering target tracking part iii: Dynamic models," IEEE Transactions on Aerospace and Electronic Systems, vol. 39, no. 4, pp. 1333{1364, October 2003.

[46] D. Lerro and Y. Bar-Shalom, \Tracking with debiased consistent converted measurements verses ekf," IEEE Transactions on Aerospace and Electronic Systems, vol. 29, no. 3, pp. 1015{1022, July 1993.

[47] J. Hightower and Borriello, \Location systems of ubiquitous computing," IEEE Computer, vol. 34, no. 8, pp. 57{66, August 2001.

[48] M. Schlosser, \Limitations in tracking with extended Kalman lters," IEEE Transactions on Aerospace and Electronic Systems, vol. 40, no. 4, pp. 1351{1359, October 2004.

[49] Z. Zhao, X. R. Li, and V. P. Jilko, \Best linear unbiased ltering with nonlinear measurements for target tracking," IEEE Transactions on Aerospace and Electronic Systems, vol. 40, no. 4, pp. 1324{1336, October 2005.

[50] S. julier and J. Uhlman, \Unscented ltering and nonlinear estimation," Proceedings of the IEEE, vol. 92, no. 3, pp. 401{422, Marchr 2004.

[51] I. Petersen and A. V. Savkin, Robust Kalman Filtering for Signals and Systems with Large Uncertainities. Birkhauser, Boston 1999.

[52] S. julier, J. Uhlman, and H. Dhurrant-whyte, \A new method for the nonlinear transformation of means and covariances in lters and estimators," IEEE Transactions on Automatic Control, vol. 45, no. 3, pp. 477{482, March 2000.

[53] M. S. Arulampalam, S. Maskel, N. Gordon, and T. Clapp, \A tutorial on particle lters for online nonlinear/non-Gaussian Bayesian tracking," IEEE Transactions on Signal Processing, vol. 50, no. 2, pp. 174{187, February 2002.

[54] F. Gustafsson, F. Gunnarsson, N. Bergman, U. Forssell, J. Jansson, R. Karlsson, and P. Nordlund, \Particla lters for position, navigation and tracking," IEEE Transactions on Signal Processing, vol. 50, no. 2, pp. 425{437, February 2000.

[55] A. Lin and H. Ling, \Location tracking of indoor movers using a two-frequency doppler and direction-of-arrival (DDOA) radar," in IEEE Antennas and Propagation Society International Symposium 2006, 2006, pp. 1125{1128.

[56] | | , \Two-dimensional human tracking using a three-element Doppler and direction-of-arrival (DDOA) radar," 2006 IEEE Conference on Radar, p. 4pp, 2006.

[57] A. Yasotharan and T. Thayaparan, \Strengths and limitations of the Fourier method for detectingaccelerating targets by pulse Doppler radar," IEE Proceedings - Radar, Sonar and Navigation,, vol. 149, no. 2, pp. 83{88, 2002.

[58] P. Heide, V. Magori, and R. Schwarte, \Coded 24 GHz Doppler radar sensors: a new approach tohigh-precision vehicle position and ground-speed sensing in railway and automobile applications," in Microwave Systems Conference, 1995. Conference Proceedings., IEEE NTC, 1995, pp. 101{104.

[59] C. Bodenstein, W. Venter, and G. Kahl, \A Doppler radar for multiple targets," IEEE Transactions on Instrumentation and Measurement,, vol. 43, no. 5, pp. 706{710, 1994.

[60] F. Vincent and O. Besson, \Estimating time-varying DOA and Doppler shift in radar array processing," IEE Proceedings on Radar, Sonar and Navigation, vol. 147, no. 6, pp. 285{290, 2000.

[61] S. Ram, Y. Li, A. Lin, and H. Ling, \Human Tracking Using Doppler Processing and Spatial Beamforming," in Radar Conference IEEE 2007, 2007, pp. 546{551.

[62] V. Cevher and J. McClellan, \General direction-of-arrival tracking with acoustic nodes," IEEE Transactions on Signal Processing, vol. 53, no. 1, pp. 1 {12, 2005.

[63] W. Foy, \Position-location solutions by Taylor-series estimation," IEEE Transactions on Aerospace and Electronic Systems, vol. 12, no. 2, pp. 187{194, 1976.

[64] | | , \Position-location solutions by Taylor series estimation," IEEE Transactions on Aerospace and Electronic Systems, vol. 12, no. 2, pp. 187{194, March 1976.

[65] S. Kay, \Fundamentals of statistical signal processing: Estimation theory," Prentice-Hall, vol. Upper Saddle River, 1993.

[66] D.Orlando and G. Ricci, \Adaptive radar detection and localization of a point-like target," IEEE Transactions on Signal Processing, vol. 59, no. 9, pp. 4086{4096, September 2011.

[67] X.Zhang, P.K.Willett, and Y.Bar-Shalom, \Monopulse radar detection and localization of multiple unresolved targets via joint bin processing," IEEE Transactions on Signal Processing, vol. 53, no. 4, pp. 1225{1236, April 2005.

[68] | | , \Detection and localization of multiple unresolved extended targets via monopulse radar signal processing," IEEE Transactions on Aerospace and Electronic Systems, vol. 45, no. 2, pp. 455{472, April 2009.

[69] X. Wang, D. Musicki, R. Ellem, and F. Fletcher, \E cient and enhanced multi-target tracking with doppler measurements," IEEE Transactions on Aerospace and Electronic Systems, vol. 45, no. 4, pp. 1400 {1417, 2009.

[70] L. Mo, X. Song, K. Sun, Z, and Y. Bar-Shalom, \Unbiased converted measurements for tracking," IEEE Trasactions on Aerospace and Electronic Systems, vol. 34, no. 3, pp. 1023{1027, July 1998.

[71] Y. Bar-Shalom and T. Fortman, Tracking and data association. Academic Press, San Diego, CA, 1987.

[72] S. Deb, M. Yeddanapudi, K. Pattipati, and Y. Bar-Shalom, \A generalized S-D assignment algorithm for multisensor-multitarget state estimation," IEEE

Transactions on Aerospace and Electronic Systems, vol. 33, no. 2, pp. 523{538, April 1997.

[73] H. Naus and C. Van Wijk, \Simultaneous localization of multiple emitters," in IEEE Proceedings on Radar, Sonar and Navigation, April 2004, pp. 65{70.

[74] K. Pattipati, S. Deb, Y. Bar-Shalom, and R. Washburn Jr, \A newrelaxation algorithm and passive sensor data association," IEEE Transactions on Automatic Control, vol. 37, no. 2, pp. 198{213, February 1992.

[75] R. Popp, K. Pattipati, and Y. Bar-Shalom, \m-Best S-D assignment algorithm with applications to mutitarget tracking," IEEE Transactions on Aerospace and Electronic Systems, vol. 37, no. 1, pp. 22{39, January 2011.

[76] B. Vo and W. K. Ma, \The Gaussian mixture probability hypothesis density lter,"IEEE Transactions on Signal Processing, vol. 54, no. 1, pp. 4091{4104, November 2006.

[77] B. Vo, S. Singh, and A. Doucet, \Sequential Monte Carlo methods for Bayesian multitarget ltering with random nite sets," IEEE Transactions on Aerospace and Electronic Systems, vol. 41, no. 4, pp. 1224{1245, October 2005.

[78] A. Barabell, \Improving the resolution performance of eigenstructure-based direction nding algorithms," in In proceedings of the IEEE International Conference on Acoustic, Speech and Signal Processing, Boston, MA, April 1983, pp. 336{339.

[79] R. Bhaskar and K. Hari, \Perfoormance analysis on root-music," IEEE Transactions on Acoustic, Speech and Signal Processing, vol. 37, no. 12, pp. 1939{1949, 1989.

[80] R. Roy and T. Kailath, \ESPIRIT- estimation of signal parameters via rotational invariance techniques," IEEE Transactions on Acoustic, Speech and Signal Processing, vol. 37, no. 7, pp. 984{995, July 1989.

[81] R. Schmidt, \Multiple emitter location and signal parameter estimation," IEEE Transactions on Antennas and Propagation, vol. 34, no. 3, pp. 276{280, March 1986.

[82] P. Stoica and A. Nehorai, \MUSIC, maximum likelihood and Cramer-Rao lower bound," IEEE Transactions on Acoustic, Speech and Signal Processing, vol. 37, no. 5, pp. 720{741, May 1989.

[83] | | , \MUSIC, maximum likelihood and Cramer-Rao lower bound:Further results and comparisons," IEEE Transactions on Acoustic, Speech and Signal Processing, vol. 38, no. 12, pp. 2140{2150, December 1990.

[84] P. Stoica and K. Sharman, \maximum likelihood methods for direction of arrival estimation," IEEE Transactions on Acoustic, Speech and Signal Processing, vol. 38, no. 7, pp. 1132{1143, July 1990.

[85] L. Ta , \Target localization of bearing only localization," IEEE Transactions on Aerospace and Electronic Systems, vol. 33, no. 1, pp. 2{10, January 1997.

[86] R. Stans eld, \Statistical theory of DX xing," Journal pf IEE, vol. 94, no. 15, pp. 762{770, October 1947.

[87] M. Gavish and A. Weiss, \Performance analysis of bearing-only target location algorithms," IEEE Transactions on Aerospace and Electronic Systems, vol. 28, no. 3, pp. 817{828, 1992.

[88] R. Iltis and K. Anderson, \A consistent estimation criterion for mutisensor bearing only tracking," IEEE Transactions on Aerospace and Electronic Systems, vol. 32, no. 1, pp. 108{120, January 1996.

[89] J. Le Cadre and C. Jau ret, \On the convergence of iterative methods for bearing only tracking," IEEE Transactions on Aerospace and Electronic Systems, vol. 35, no. 3, pp. 801{818, July 1999.

[90] E. Olson, J. J. Leonard, and S. Teller, \Robust range-only beacon localization," Oceanic Engineering, IEEE Journal of, vol. 31, no. 4, pp. 949 {958, oct. 2006.

[91] K. C. Ho and M. Sun, \An accurate algebraic closed-form solution for energy-based source localization," IEEE Transactions on Audio, Speech, and Language Processing, vol. 15, no. 8, pp. 2542 {2550, nov. 2007.

[92] D. Jourdan, D. Dardari, and M. Win, \Position error bound for uwb localization in dense cluttered environments," IEEE Transactions on Aerospace and Electronic Systems, vol. 44, no. 2, pp. 613 {628, april 2008.

[93] Z. Ma, W. Chen, K. Letaief, and Z. Cao, \A semi range-based iterative localization algorithm for cognitive radio networks," IEEE Transactions on Vehicular Technology, vol. 59, no. 2, pp. 704 {717, feb. 2010.

[94] K. Lui and H. So, \Range-based source localisation with pure re ector in presence of multipath propagation," Electronics Letters, vol. 46, no. 13, pp. 957 {958, 24 2010.

[95] J. Koo and H. Cha, \Localizing wi access points using signal strength," Communications Letters, IEEE, vol. 15, no. 2, pp. 187 {189, february 2011.

[96] F. Chan and H. So, \Accurate distributed range-based positioning algorithm for wireless sensor networks," IEEE Transactions on Signal Processing, vol. 57, no. 10, pp. 4100 {4105, oct. 2009.

[97] F. Chan, H. So, and W.-K. Ma, \A novel subspace approach for cooperative localization in wireless sensor networks using range measurements," Signal Processing, IEEE Transactions on, vol. 57, no. 1, pp. 260 {269, jan. 2009.

[98] S. Zhu and Z. Ding, \A simple approach of range-based positioning with low computational complexity," IEEE Transactions on Wireless Communications, vol. 8, no. 12, pp. 5832 {5836, december 2009.

[99] Y. H. Hu and D. Li, \Energy based collaborative source localization using acoustic micro-sensor array," in 2002 IEEE Workshop on Multimedia Signal Processing, dec. 2002, pp. 371 { 375.

[100] D. Li and Y. H. Hu, \Least square solutions of energy based acoustic source localization problems," in 2004 International Conference on Parallel Processing Workshops, 2004. ICPP 2004 Workshops. Proceedings., aug. 2004, pp. 443 { 446.

[101] J. Smith and J. Abel, \Closed-form least-square source location estimation from range-di erence measurements," IEEE Transactions on Acoustic, Speech and Signal Processing, vol. 35, no. 12, pp. 1661{1669, December 1987.

[102] S. Birch eld and R. Gangishetty, \Acoustic localization by interaural level di erence," in IEEE International Conference on Acoustics, Speech, and Signal Processing, 2005. Proceedings. (ICASSP '05)., vol. 4, march 2005, pp. 1109 {1112.

[103] X. Sheng and Y.-H. Hu, \Maximum likelihood multiple-source localization using acoustic energy measurements with wireless sensor networks," IEEE Transactions on Signal Processing, vol. 53, no. 1, pp. 44 { 53, jan. 2005.

[104] D. Blatt and A. Hero, \Energy-based sensor network source localization via projection onto convex sets," IEEE Transactions on Signal Processing, vol. 54, no. 9, pp. 3614 {3619, sept. 2006.

[105] S. Nardone, A. Lindgren, and K. Gong, \Fundamental properties and performance of conventional bearings-only target motion analysis," IEEE Trans. Automatic Control, vol. 29, no. 9, pp. 775{787, 1984.

[106] B. A. N., \On the geometry of localization, tracking and navigation," Submitted in ful lment of the rerements for the degree of Doctor of Philosophy, Deakin University, January 2008.

[107] K. Dogancay, \Online optimization of receiver trajectories for scan based emmiter location," IEEE Transactions on Aerospace and Electronic Systems, vol. 43, no. 3, pp. 1117{1125, 2007.

[108] A. N. Bishop and P. N. Pathirana, \Optimal trajectories for homing navigation with bearing measurements," in Proceedings of the International Federation of Automatic Control World Congress,Seoul,Korea, July 2008.

[109] K. Dogancay, \Optimaized path planning for UAVs with AOA/scan based sensors," in Proceedings of the 15th Europian Signal Processing Conference(EUSIPCO),Poznan,Poland, September 2007.

[110] A. Farina, \Target tracking with bearing-Only measurements," Signal Processing, vol. 78, pp. 61{78, 1999.

[111] Y. Oshman and P. Davidson, \Optimization of observer trajectories for bearings-only target localization," IEEE Transactions on Aerospace and Electronic Systems, vol. 35, no. 3, pp. 892{902, 1999.

[112] K. Yang, J. An, X. Bu, and G. Sun, "Constrained total least-squares location algorithm using time-difference-of-arrival measurements," IEEE Transactions on Vehicular Technology, vol. 59, no. 3, pp. 1558 {1562, march 2010.

[113] M. Gillette and H. Silverman, "A linear closed-form algorithm for source localization from time-difference of arrival," Signal Processing Letters, IEEE, vol. 15, pp. 1 {4, 2008.

[114] N. Liu, Z. Xu, and B. Sadler, "Low-complexity hyperbolic source localization with a linear sensor array," Signal Processing Letters, IEEE, vol. 15, pp. 865 {868, 2008.

[115] D. Musicki, R. Kaune, and W. Koch, "Mobile emitter geolocation and tracking using TDOA and FDOA measurements," IEEE Transactions on Signal Processing, vol. 58, no. 3, pp. 1863 {1874, 2010.

[116] J. Collins and P. Grant, "A review of current andfuture components for electronic warfare receivers," IEEE Transactions on Sonics and Ultrasonic, vol. 28, no. 3, pp. 117{125, Ma 1981.

[117] A. Spezio, "Electronic warfare systems," IEEE Transactions on Microwave Theory and Techniques, vol. 50, no. 3, pp. 633{644, March 2002.

[118] I. Getting, "The global positioning system," IEEE Spectrum, vol. 30, no. 12, pp. 36{38, December 1993.

[119] H. Schau and A. Robinson, "Passive source localization employing intersecting spherical surfaces from time-of-arrival differences," IEEE Transactions on Acoustic, Speech and Signal Processing, vol. 35, no. 8, pp. 1223{1225, August 1987.

[120] R. Schmidt, \A new approach to geometry of range di erence localization," IEEE Transactions on Aerospace and Electronic Systems, vol. 8, no. 6, pp. 821{835, November 1972.

[121] K. Dogancay, \Emitter localization using clustering-based bearing association," IEEE Transactions on Aerospace and Electronic Systems, vol. 41, no. 2, pp. 525{536, April 2005.

[122] H. Cramer, \Mathematical Methods of Statistics," Princeton University Press, Princeton,NJ, 1946.

[123] C. Rao, Linear Statistical Inference and its Apllications. John Wiley and Sons, New York,NY, 1973, vol. 2nd edition.

[124] P. Stocia and T. L. Marezetta, \Parameter estimation problem with singular estimation matrices," IEEE Transactions on Siganl Processing, vol. 49, no. 1, pp. 87{90, 2001.

[125] H. L. Van Trees, \Detection Estimation and Modulation Theory," John Wiley and Sons, New York,NY, 1968.

[126] S. C. K. Herath and P. N. Pathirana, \Optimal sensor separation for aoa based localization via linear sensor array," in Intelligent Sensors, Sensor Networks and Information Processing (ISSNIP), 2010 6th International Conference on, 2010, pp. 187{192.

[127] Y. C. Elda, \Uniformly improving the Cramer-Rao lower bound and maximum-likelihood estimation," IEEE Transactions on Signal Processing, vol. 54, no. 8, pp. 2943{2956, August 2006.

[128] | | , \Minimum variance in biased estimation: Bounds and asmptotically optimal estimators," IEEE Transactions on Signal Processing, vol. 52, no. 7, pp. 1915{1930, July 2004.

[129] A. O. Hero, J. A. Fessler, and U. Usman, \Exploring estimator biase-variance trade o s using the uniform CR bounds," IEEE Transactions on Signal Processing, vol. 44, no. 8, pp. 2026{2041, August 1996.

[130] S. Beladi and P. N. Pathirana, \TDOA based transmitter localization with minimum number of receivers and power measurements," in 10th International Conference on Control, Automation, Robotics and Vision, 2008. ICARCV 2008., 2008, pp. 1259 {1264.

[131] X. Wang, Z. Wang, and B. O'Dea, \A TOA-based location algorithm reducing the errors due to non-line-of-sight (NLOS) propagation," IEEE Transactions on Vehicular Technology, vol. 52, no. 1, pp. 112 { 116, jan 2003.

[132] A. Hernandez, R. Badorrey, J. Choliz, I. Alastruey, and A. Valdovinos, \Accurate indoor wireless location with IR UWB systems a performance evaluation of joint receiver structures and toa based mechanism," IEEE Transactions on Consumer Electronics, vol. 54, no. 2, pp. 381 {389, may 2008.

[133] S. Gezici, Z. Tian, G. B. Giannakis, H. Kobayashi, A. F. Molisch, H. V. Poor, and Z. Sahinoglu, \Localization via ultra-wideband radios: a look at positioning aspects for future sensor networks," IEEE Signal Processing Magazine, vol. 22, no. 4, pp. 70 { 84, july 2005.

[134] T. Jia and R. Buehrer, \On the optimal performance of collaborative position location," IEEE Transactions on Wireless Communications, vol. 9, no. 1, pp. 374 {383, january 2010.

[135] K. Yu, Y. J. Guo, and M. Hedley, \TOA-based distributed localisation with unknown internal delays and clock frequency o sets in wireless sensor networks," IET Signal Processing, vol. 3, no. 2, pp. 106 {118, march 2009.

[136] T. Wang, G. Leus, and L. Huang, "Ranging energy optimization for robust sensor positioning based on semide nite programming," IEEE Transactions on Signal Processing, vol. 57, no. 12, pp. 4777 {4787, dec. 2009.

[137] I. Guvenc and C.-C. Chong, "A survey on TOA based wireless localization and NLOS mitigation techniques," IEEE Communications Surveys Tutorials, vol. 11, no. 3, pp. 107 {124, quarter 2009.

[138] B. Alavi and K. Pahlavan, "Modeling of the TOA-based distance measurement error using uwb indoor radio measurements," IEEE Communications Letters, vol. 10, no. 4, pp. 275 { 277, apr 2006.

[139] K. W. K. Lui, H. C. So, and W. K. Ma, "Maximum a posteriori approach to time-of-arrival-based localization in non-line-of-sight environment," IEEE Transactions on Vehicular Technology, vol. 59, no. 3, pp. 1517 {1523, march 2010.

[140] E. Xu, Z. Ding, and S. Dasgupta, "Source localization in wireless sensor networks from signal time-of-arrival measurements," IEEE Transactions on Signal Processing, vol. 59, no. 6, pp. 2887 {2897, june 2011.

[141] H. Schau and A. Robinson, "Passive source localization employing intersecting spherical surfaces from time-of-arrival di erences," IEEE Transactions on Acoustics, Speech and Signal Processing, vol. 35, no. 8, pp. 1223 { 1225, aug 1987.

[142] F. K. W. Chan, H. C. So, J. Zheng, and K. . W. K. Lui, "Best linear unbiased estimator approach for time-of-arrival based localisation," IET Signal Processing, vol. 2, no. 2, pp. 156 {162, june 2008.

[143] C. K. Seow and S. Y. Tan, \Non-line-of-sight localization in multipath environments," IEEE Transactions on Mobile Computing, vol. 7, no. 5, pp. 647 {660, may 2008.

[144] N. Patwari, J. N. Ash, S. Kyperountas, A. O. Hero, R. L. Moses, and N. S. Correal, \Locating the nodes: cooperative localization in wireless sensor networks," IEEE Signal Processing Magazine, vol. 22, no. 4, pp. 54 { 69, july 2005.

[145] H. C. So and F. K. W. Chan, \A generalized subspace approach for mobile positioning with time-of-arrival measurements," IEEE Transactions on Signal Processing, vol. 55, no. 10, pp. 5103 {5107, oct. 2007.

[146] K. W. Cheung, H. C. So, W. K. Ma, and Y. T. Chan, \Least squares algorithms for time-of-arrival-based mobile location," IEEE Transactions on Signal Processing, vol. 52, no. 4, pp. 1121 { 1130, april 2004.

[147] A. N.Bishop and P. N. Pathirana, \Localization of Emitters via the Intersection of Bearing Lines: A Ghost Elemination Approach," IEEE Transaction on Vehicular Technology, vol. 56, no. 5,part 2, pp. 3106{3110, 2007.

[148] I. Mellen, G., M. Pachter, and J. Raquet, \Closed-form solution for determining emitter location using time di erence of arrival measurements," IEEE Transactions on Aerospace and Electronic Systems, vol. 39, no. 3, pp. 1056 { 1058, 2003.

[149] A. Lin and H. Ling, \Three-dimensional tracking of humans using very low-complexity radar," Electronics Letters, vol. 42, no. 18, pp. 1062{1063, 2006.

[150] Y. Zhang, M. Amin, and F. Ahmad, \A Novel Approach for Multiple Moving Target Localization Using Dual-Frequency Radars and time-frequency

distributions," Conference Record of the Forty-First Asilomar Conference on Signals, Systems and Computers, ACSSC 2007., pp. 1817{1821, 2007.

[151] J. Pinezich, J. Heller, and T. Lu, \Ballistic projectile tracking using CW Doppler radar," IEEE Trasactions on Aerospace and Electronic Systems, vol. 46, no. 3, pp. 1302{1311, July 2010.

[152] Y. Yang, J. Lei, W. Zhang, and C. Lu, \Target Classication and Pattern Recognition Using Micro-Doppler Radar Signatures," in Seventh ACIS International Conference on Software Engineering, Arti cial Intelligence, Networking, and Parallel/Distributed Computing, 2006. SNPD 2006, 2006, pp. 213{217.

[153] T.-H. Ho and S.-J. Chung, \Design and measurement of a doppler radar with new quadrature hybrid mixer for vehicle applications," IEEE Transactions on Microwave Theory and Techniques, vol. 58, no. 1, pp. 1{8, 2010.

[154] I. Gresham, A. Jenkins, R. Egri, C. Eswarappa, N. Kinayaman, N. Jain, R. Anderson, F. Kolak, R. Wohlert, S. P.Bawell, J. Bennett, and J.-P. Lanteri, \Ultra wideband radar sensors for short-range vehicular applications," IEEE Transactions on Microwave Theory and Techniques, vol. 52, no. 9, pp. 2105{2122, 2004.

[155] G. Alessanddretti, A. Broggi, and P. Cerri, \Vehicle and guard rail detection using radar and vision data fusion," IEEE Transactions on Intelligent Transportation Systems, vol. 58, no. 1, pp. 1{8, 2010.

[156] A. Bishop and P. N. Pathirana, \Localization of Emitters via the Intersection of Bearing Lines: A Ghost Elemination Approach," IEEE Transaction on Vehicular Technology, vol. 56, no. 5,part 2, pp. 3106{3110, 2007.

[157] Y. Bar-Shalom and E. Tse, "Tracking in a cluttered environment with probabilistic data association," *Automatica*, vol. 11, no. 5, pp. 451–460, 1975.

[158] A. Savkin and I. R. Petersen, "Robust filtering with missing data and a determinstic description of noise and uncertanity," *International Journal of System Science*, vol. 28, no. 4, pp. 373–378, 1997.

[159] D. Reid, "An algorithm for tracking multiple targets," *IEEE Transactions on Automatic Control*, vol. 24, no. 6, pp. 843–854, 1979.

[160] D. Musicki, "Multi target tracking using multiple passive bearing-only asynchronouse sensors," *IEEE Transactions on Aerospace and Electronic Systems*, vol. 44, no. 3, pp. 1151–1160, 2008.

[161] Y. Bar-Shalom and X. Li, *Estimation and Tracking Principles, Techniques and Software*. Norwood, MA: Artech, 1993.

[162] J. Clark, S. Robbiati, and R. Vinter, "The shifted rayleigh mixture filter for bearings-only tracking of maneuvering targets," *IEEE Transactions on Signal Processing*, vol. 55, no. 7, pp. 3218–3226, 2007.

[163] D. Angelova and L. Mihaylova, "Extended object tracking using monte carlo methods," *IEEE Transactions on Signal Processing*, vol. 56, no. 2, pp. 825–832, 2008.

[164] A. Savkin, P. Pathirana, and F. Faruqi, "The problem of precision missile guidance : LQR and H^1 control framework." *IEEE Transactions on Aerospace and Electronic Systems*, vol. 39, no. 3, pp. 901 – 910, 2003.

[165] A. V. Savkin and I. R. Petersen, "Robust state estimation and model validation for discrete-time uncertain systems with a deterministic description of noise and uncertainty," *Automatica*, vol. 34, no. 2, pp. 271–274, 1998.

[166] B. Anderson and J. Moore, Optimal Filtering. Englewood Cli s, N.J.: Prentice Hall, 1979.

[167] T. Wysocki and H. Zepernick, \Characterization of the indoor radio propagation channel at 2.4 ghz," Journal of Telecommunications and Information Technology, vol. 1, no. 3-4, pp. 84{90, 2000.

[168] H. Lee, A. Cerpa, and P. Levis, \Improving wireless simulation through noise modelling," Information Processing in Sensor Networks (ISPN), 2007.

[169] R. N. Jazar, \Vehicle dynamics : theory and applications," Springer, c2008.